AD 273 672

REPORT NO. 1
JANUARY 12, 1962

(9)

MECHANICAL

THE EFFECT OF SPECIMEN GEOMETRY ON FRACTURE TOUGHNESS OF HIGH - STRENGTH SHEET STEEL - PART I

THE EFFECT OF TEMPERING TEMPERATURE, GRAIN SIZE AND TEST TEMPERATURE ON FRACTURE TOUGHNESS OF HIGH - STRENGTH SHEET STEEL - PART II

AUBURN RESEARCH FOUNDATION
AUBURN UNIVERSITY

INVESTIGATION OF MECHANISM OF FAILURE OF HIGH-STRENGTH MATERIALS

CONTRACT DAI-01-009-ORD-889

Part I

THE EFFECT OF SPECIMEN GEOMETRY ON FRACTURE TOUGHNESS OF HIGH-STRENGTH SHEET STEEL

Part II

THE EFFECT OF TEMPERING TEMPERATURE, GRAIN SIZE AND TEST TEMPERATURE ON FRACTURE TOUGHNESS OF HIGH-STRENGTH SHEET STEEL

by

Hal W. Maynor, Jr.
Richard E. Mueller
Edward O. Jones, Jr.*

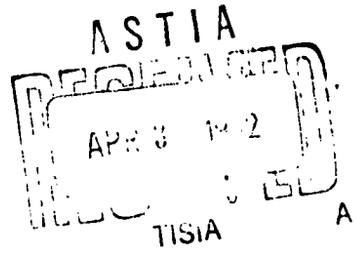

*Dr. Maynor is Professor, Mr. Mueller is Instructor, and Mr. Jones is Associate Professor, Department of Mechanical Engineering, Auburn University, Auburn, Alabama. This work was sponsored by the Army Rocket and Guided Missile Agency, U. S. Army, Under Contract Number DAI-01-009-ORD-889, and administered by the Auburn Research Foundation of Auburn University.

January 12, 1962

TABLE OF CONTENTS

PART ONE

PART TWO

APPENDIXES

3. TABLE 1 Fracture Toughness Data For X-200 (Group 1-3)

TABLE 2 Fracture Toughness Data For H-11 (Group 1-3)

LIST OF FIGURES

PART ONE

PART TWO

THE EFFECT OF SPECIMEN GEOMETRY ON FRACTURE TOUGHNESS OF HIGH-STRENGTH SHEET STEEL

A number of failures of solid propellant rocket motor cases have been attributed to brittle fracture. These cases, fabricated from sheet steels having yield strengths greater than 200,000 psi, often failed as a result of brittle fracture at stresses well below design stresses. The latter usually were based on the yield strength of the material. The occurrence of such failures at stress levels below the design stress indicated a need for brittle fracture studies of various high-strength sheet steels.

In 1959 the American Society for Testing Materials organized an ad hoc committee to study and recommend test methods for evaluating the resistance of high-strength sheet steel to brittle fracture.[1] The committee encouraged additional investigation of the test methods which it eventually proposed on the basis of the study.

Accordingly, it appeared appropriate to investigate the fracture toughness characteristics of a high-strength sheet steel by employing the two methods which were suggested by the committee. Specifically, the objectives of the work reported herein were as follows:

(1) To determine the magnitude of critical fracture toughness (K_c) for specimens having various crack-length to specimen-width ratios ($2a_o/W$).

(2) To determine the magnitude of K_c for specimens having various width-to-thickness ratios $(\frac{W}{B})$.

(3) To investigate the variation of K_c for specimens having various $\frac{2a_o}{W}$ ratios.

(4) To investigate the variation of K_c for specimens having various $\frac{W}{B}$ ratios.

(5) To compare the relative merits of the staining method and the fracture toughness method, both of which are used in the determination of fracture toughness values.

The parameter K_c represents the intensity of local tensile stress necessary for unstable crack propagation. For the determination of this parameter, the use of either edge-notched specimens or centrally-notched specimens was, at one time, recommended. It was believed that these two types of specimens represented a reasonable compromise between ideal and practically obtainable conditions for fracture-toughness evaluation.[1] However, edge-notched specimens are now considered appropriate for screening purposes only.[2] Also recommended is the use of fracture-toughness specimens having width-to-thickness ratios $\frac{W}{B}$ ranging from 16 to 45 and $\frac{2a_o}{W}$ ratios ranging from 0.3 to 0.4.

In the present investigation, specimens were used which had $\frac{W}{B}$ ratios of 12 to 47 and $\frac{2a_o}{W}$ ratios of 0.1 to 0.6. It should be noted that these ratios include the recommended ratios shown above.

APPARATUS AND PROCEDURE

Fracture toughness specimens used during this investigation were sheared from a sheet of X-200 steel, the average thickness of which was 0.080 inch. The sheet was received in the spheroidized-annealed condition. Specimens were sheared from the sheet in such a manner that the longitudinal axis of each corresponded to the rolling direction of the sheet. The longitudinal edges were milled to the dimensions shown in Figure 1. Holes for the pin-supported specimens were provided by drilling to 1/64 inch undersize and boring to the final dimension. The remaining machining operation consisted of drilling a 0.046 inch diameter hole located at the geometric center of the specimen. Eighty-four test specimens, consisting of 42 pairs, were used for the investigation in order that two sets of data could be obtained for each type specimen. A description of the test specimens is given in Figure 1. This table indicates that specimen geometries reflect seven different widths and six different crack lengths per specimen width.

A jeweler's saw, the blade of which was 0.005 inch thick, was used to cut a center slot ($2a_s$) in each specimen. Center slots ($2a_s$) subsequently were extended to predetermined lengths ($2a_o$) by means of fatigue stressing.

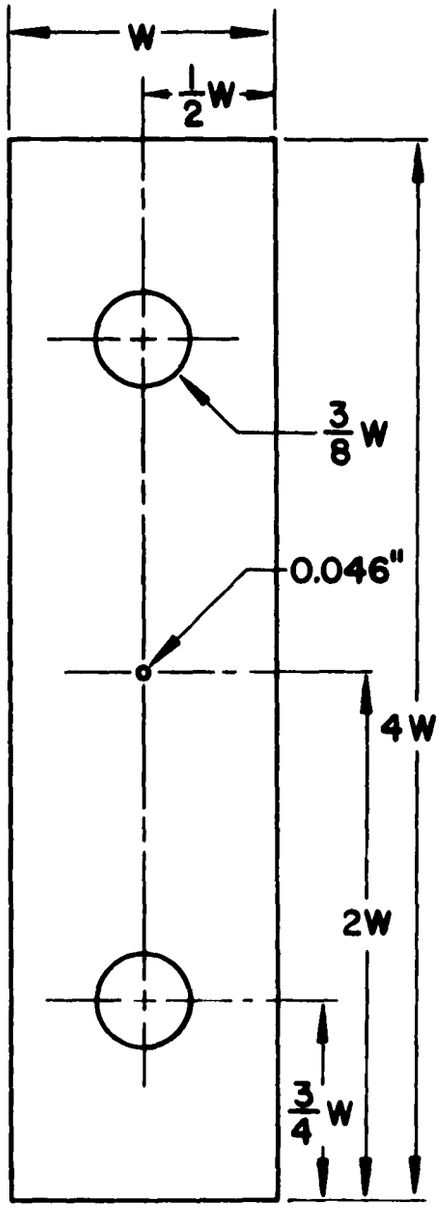

WIDTH W (IN.)	LENGTH (IN.)	PIN HOLE DIA. (IN.)
1.000	4.000	0.375
1.500	6.000	0.562
2.000	8.000	0.750
2.500	10.000	0.937
3.000	12.000	1.125
3.500	14.000	1.312
4.000	16.000	1.500

NOTE:

1. TOLERANCE ON ALL DIMENSIONS EXCEPT THAT OF PIN HOLES (SEE NOTE 2) ± 0.001 IN.
2. PIN HOLE TOLERANCE $\frac{+0.0005}{-0.0000}$

Figure 1. Fracture Toughness Specimen

The specimens then were buffed with a wire wheel in the vicinity of the center slot until the surface was comparatively smooth and bright. Two applications of layout dye then were made to the buffed surface. This type surface was helpful to the investigators in following the progress of extension of the center slot to the desired dimension during the subsequent fatigue stressing.

Each test specimen, in turn, was mounted in a fatigue machine, shown in Figure 2, which was regulated to produce a maximum tensile load and a minimum tensile load. These maximum and minimum loads were of such magnitudes that the corresponding net-section stresses in each specimen were 50% and 15% respectively, of the yield strength (0.2% offset) of the material. These fatigue-cracking data are shown in Table 1. A floodlight and a 3X magnifying glass were used to follow the crack growth to the length $2a_o$.

At the conclusion of the fatigue-cracking operation, the specimens were heat treated to an ultimate tensile strength of approximately 300,000 psi. The heat treating operation was performed in an endothermic atmosphere having a dew-point temperature of 25°F. The specimens were austenitized at 1750°F for 30 minutes and then quenched in oil. Immediately afterwards, they were tempered for one hour at 500°F. After air cooling to room temperature, a second tempering treatment was performed under the same conditions as the first. The specimens

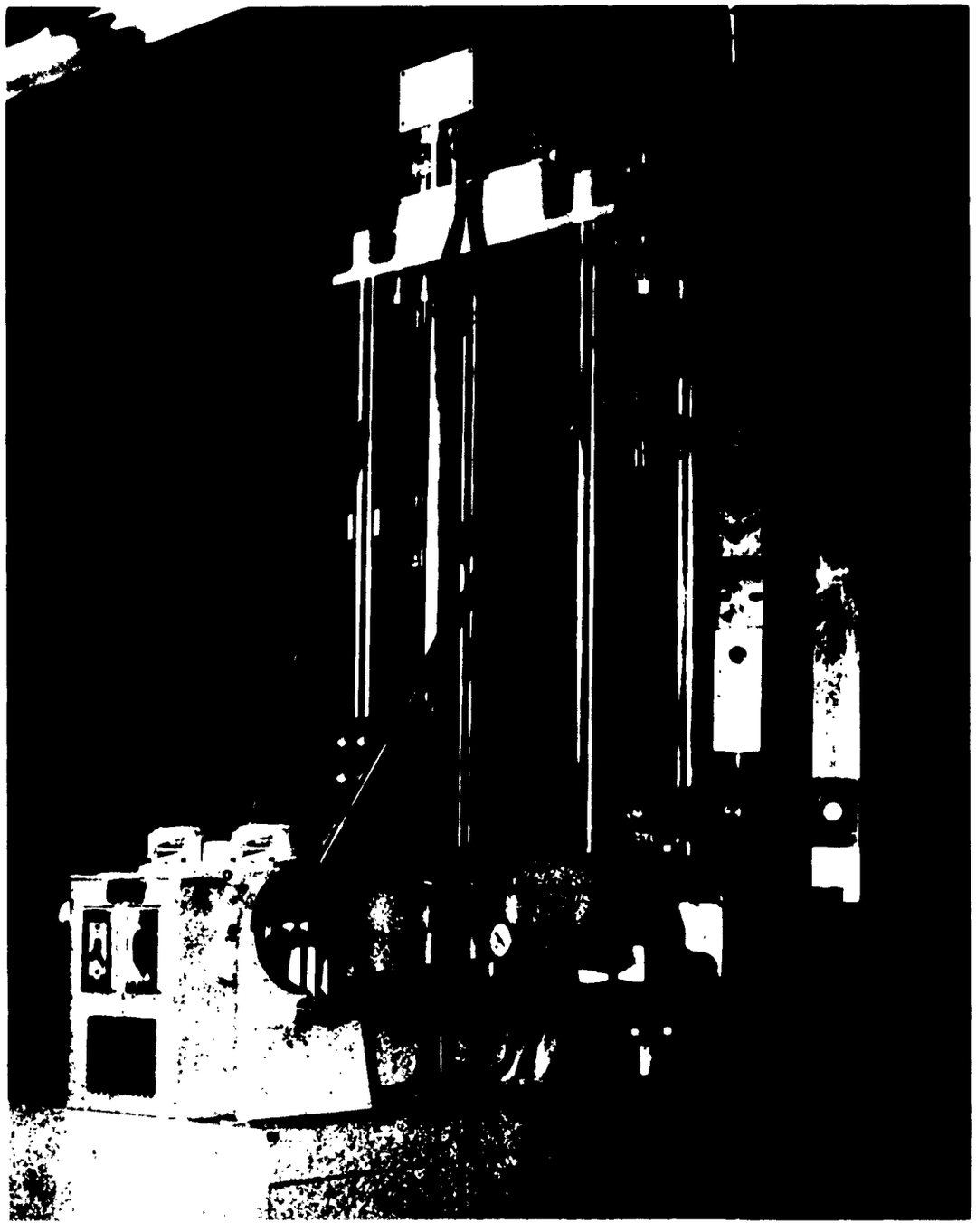

Figure 2. Fatigue Machine (Showing Positioning of Fracture Toughness Specimen)

then were cleaned with acetone in order to remove residual quantities of oil remaining from the quenching operation.

No attempt was made to effect controlled decarburization of specimen surfaces. Rather, decarburization (as well as carburization) was avoided intentionally. Small quantities of X-200 steel were heat treated coincidentally with the test specimens in order to provide an indication of surface condition. Conclusions regarding surface condition were based on metallographic and hardness determinations. No evidence of decarburization was observed in any instance.

Two standard tensile specimens were sheared from the same sheet of X-200 steel that was used for the fracture-toughness test specimens. The longitudinal axes of the two specimens were oriented in a direction parallel to the rolling direction of the sheet. The dimensions of the standard tensile-test specimens are indicated in Figure 3. These specimens were heat treated under the same conditions as described for the fracture toughness specimens.

A universal testing machine, shown in Figure 4, was used in performing a stress-strain test on each of the standard tensile specimens. A mechanical extensometer was used in the determination of the strain values. Stress-strain curves were plotted for each standard tensile specimen in order to determine the yield strength (0.2% offset). The average yield strength of the two standard tensile specimens was taken as representative of this property.

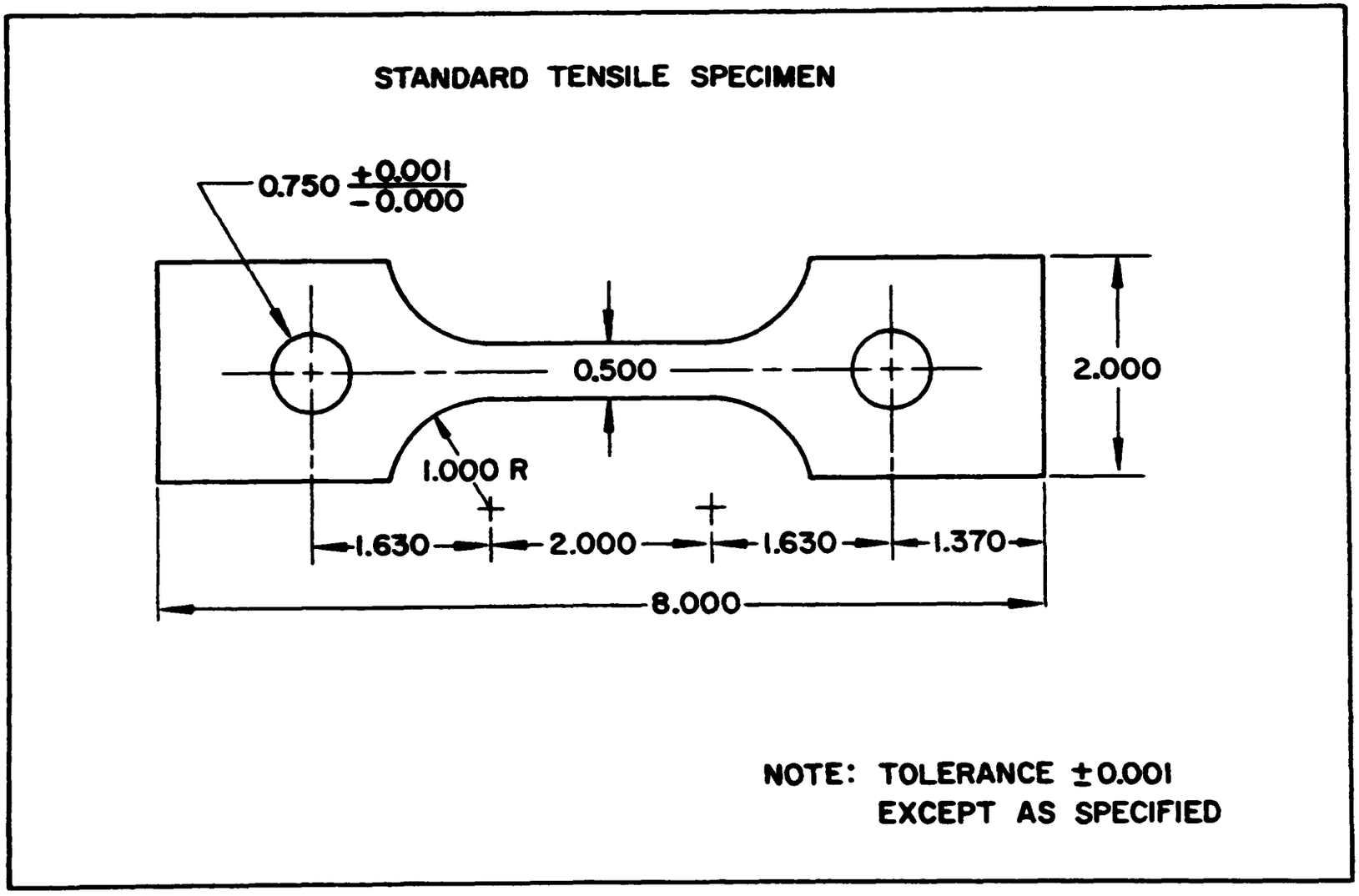

Figure 3. Standard Tensile Specimen

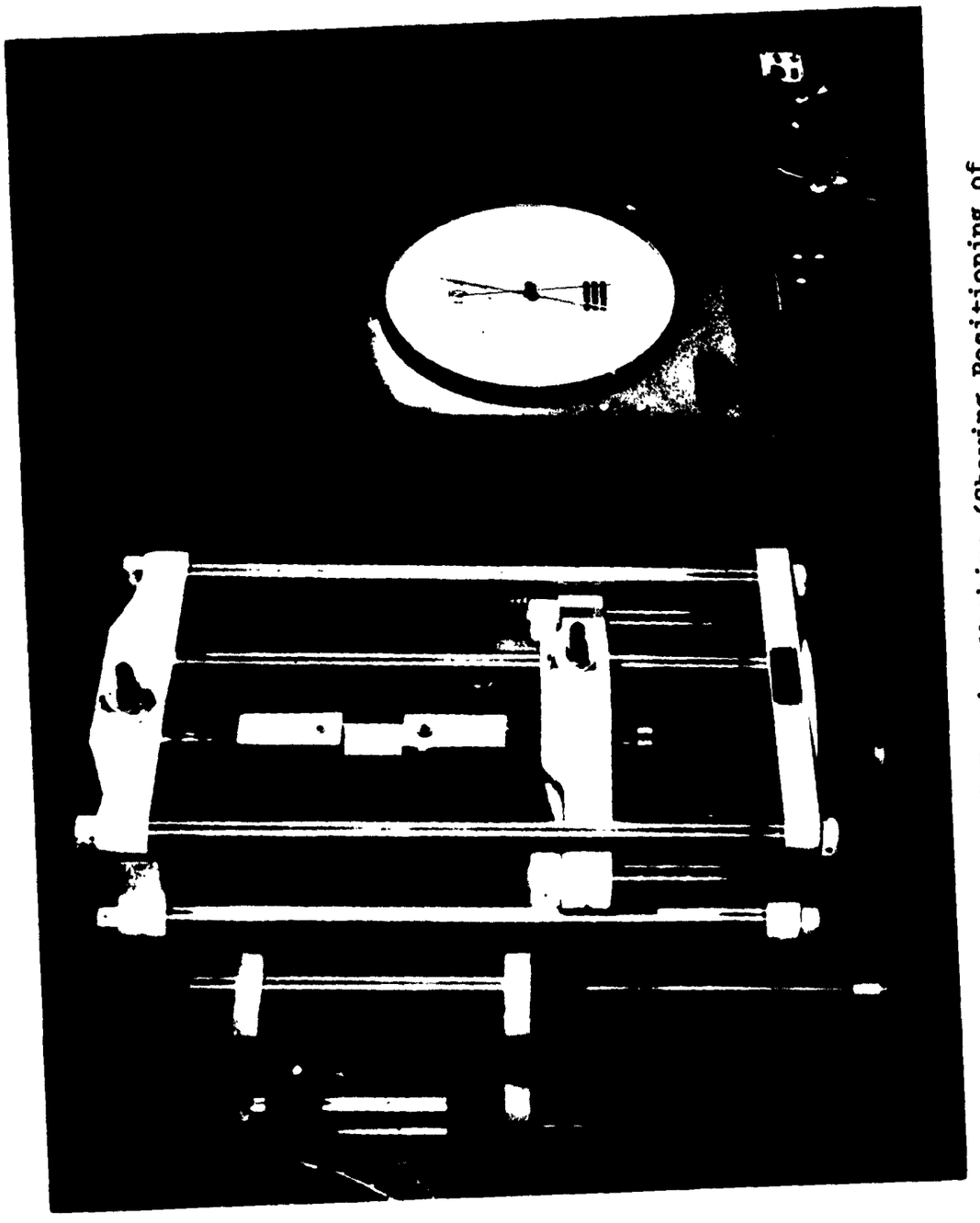

Figure 4. Universal Testing Machine (Showing Positioning of Fracture Toughness Specimen)

A universal testing machine was used to determine the maximum tensile load for each specimen. Fracture toughness has been found to be sensitive to loading rates; therefore, a variable load pacer was used to maintain a constant loading for each specimen.[1]

Before specimens were loaded, a small amount of red India ink was placed in the center slot. Specimens were loaded at a rate of 3500 pounds per minute. As the center crack began to grow, the ink flowed into the crack. Slow crack growth continued until the onset of rapid crack propagation, the latter phenomenon being ultimately responsible for the failure of the specimen. The flow of ink ceased with the beginning of rapid crack propagation. Maximum load (P_M) and room temperature (T_r) values were observed in each instance.

The stained areas of fractured specimens were examined at magnifications up to 60X. The termination of the stained area marked the extent of the slow growth (2a). The leading edge of the slow-growth area usually was curved, as shown in Figure 5. For the measurement of 2a, reference was made to a line that equally divided the stained area ahead from the unstained area behind.[1] The line was contained in the fracture surface. The actual measurement of 2a was made with a pair of vernier calipers which could be read to 0.001 inch. A schematic illustration of the fracture surface used in the determination of 2a is shown in Figure 5.

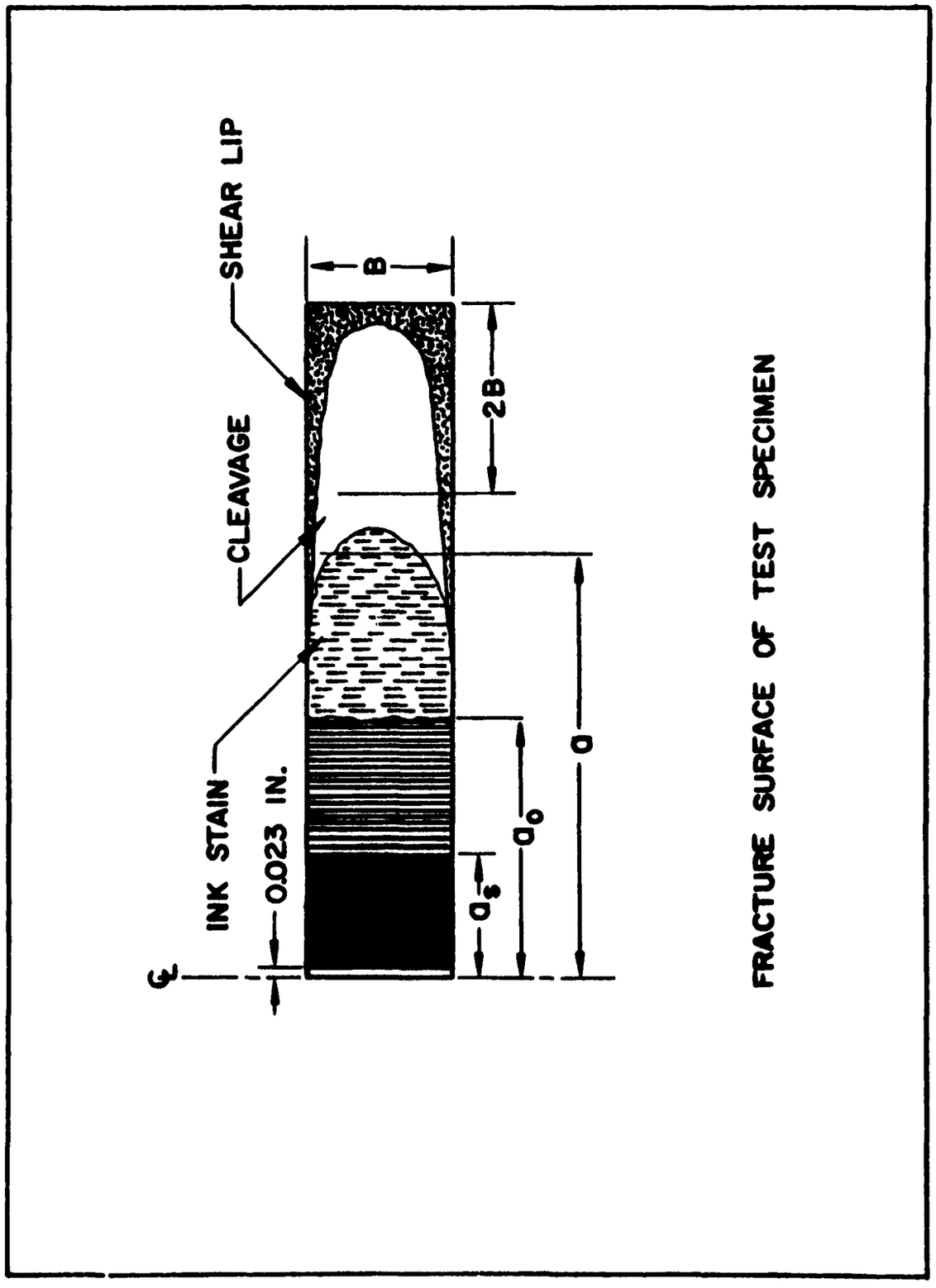

Figure 5. Fracture Surface of Test Specimen

All equations shown were taken from a report of a special ASTM Committee.[1]

A value of K_c was calculated for each test specimen by using the following equation:

(1) $K_{c1} = \sigma_M (q_{c1} W)^{\frac{1}{2}}$

in which $\sigma_M = \frac{P_M}{WB}$

and q_{c1} = stress distribution factor.

The value of q_{c1} was determined by using the following equations:

(2) $q_{c1} = \tan u$

(3) in which $u = \frac{\pi a}{W} + \frac{1}{2} \left(\frac{\sigma_M}{\sigma_{YS}}\right)^2 q_{c1}$

(4) hence $\frac{\pi a}{W} = \tan^{-1} q_{c1} - \frac{1}{2} q_{c1} \left(\frac{\sigma_M}{\sigma_{YS}}\right)^2$

The tabulated values of K_{c1} are shown in Table 2.

It is apparent that equation (4) is the equation for a straight line having a negative slope of $\frac{1}{2} q_{c1}$ and an ordinate intercept of $\tan^{-1} q_{c1}$. A number of straight lines were plotted using equation (4), which would include the range of $\frac{\pi a}{W}$ and $\left(\frac{\sigma_M}{\sigma_{YS}}\right)^2$ values determined in this investigation. The values of q_{c1} were determined by simply entering the $\frac{\pi a}{W}$ value and corresponding $\left(\frac{\sigma_M}{\sigma_{YS}}\right)^2$ value into the plot and reading the corresponding q_{c1} value.

Another method, referred to as the fracture appearance or percent shear method, was also used in the evaluation of a second set of K_c values. These values K_{c3} are shown in Table 3. This method does not require a stain to be used during the tensile test. However, the test specimens which were used in the determination of the initial K_c values also were used in evaluating the second set of K_c values. Each fracture surface of the test specimens consisted of a generally flat cleavage surface bordered by a shear lip. The fracture appearance method consists of measuring the shear lip, as shown in Figure 5, and expressing the shear lip distance as a percentage of the total specimen width. The shear-lip measurement was made at a distance of twice the specimen width from the extreme specimen edge. The measurement was made by using a 60X stereoscope microscope equipped with a calibrated reticle which could be read to 0.001 inch.

The shear values then were used in the determination of q_{c3} values in order that the values of K_c could be evaluated from the following equation:

$$(5) \quad K_{c3} = \sigma_M (q_{c3} W)^{\frac{1}{2}}$$

in which $\sigma_M = \frac{P_M}{WB}$

and q_{c3} = stress distribution factor.

The value of q_{c3} was determined by using the following equations:

$$(6)\quad 2\tan^{-1} q_{c3} - \frac{q_{c3}}{1 + q_{c3}^2} = \frac{2\pi a_o}{W} + 2C + \frac{1}{2}\left(\frac{\sigma_M}{\sigma_{YS}}\right)^2 q_{c3}$$

which can be expressed in the following form:

$$\frac{\pi a_o}{W} + C = \tan^{-1} q_{c3} - \frac{0.5 q_{c3}}{1 + q_{c3}^2} - \frac{1}{4} q_{c3} \left(\frac{\sigma_M}{\sigma_{YS}}\right)^2$$

It is apparent that this latter form of equation 6 is the equation of a straight line having a negative slope of $\frac{1}{4} q_{c3}$ and an ordinate intercept of $(\tan^{-1} q_{c3} - \frac{0.5 q_{c3}}{1 + q_{c3}^2})$.

The term C in equation 6 is an empirical correction term based on the running crack shear-lip fraction (P) and is determined from the following equation:

$$(7)\quad C = 4.7(P - 0.43)\frac{B}{W}$$

A number of straight lines were plotted using equation 6 which would include the range of $(\frac{\pi a_o}{W} + C)$ and $(\frac{\sigma_M}{\sigma_{YS}})^2$ values determined during the investigation. The values of q_{c3} were determined in a manner similar to that employed for the determination of q_{c1} values.

Each P value was substituted into equation 7 in order to determine, ultimately, the value of the ordinate, y. The equation for y is shown as follows:

$$y = \frac{\pi a_o}{W} + C$$

DISCUSSION OF RESULTS

Reduction of Data

The scales employed in the graphical representation of K_c values are consistent with the estimated accuracy involved in the accumulation of the corresponding data. Each point of the several graphs reflecting W, for example, represents six different crack lengths (0.1 - 0.6 in.). Since duplicate specimens were employed, any particular value of W represents 12 experimental determinations. Similarly, each point reflecting crack length represents the product of seven different values of W (1 - 4 in., in $\frac{1}{2}$ in. increments) and two (duplicate) specimens or 14 experimental determinations.

Curve fitting was effected by employing the method of least squares.

The data were expressed in terms of the parameter K_c rather than in terms of the parameter G_c because:

1. The test procedures employed in the present study were based upon "Fracture Testing of High-Strength Sheet Materials": A report of a Special ASTM Committee.[1] This report presents the development of an experimental means of evaluating fracture toughness in terms of the parameter K_c.

2. The q_c term of the K_c equation may be derived relatively simply from graphical relationships presented in the above mentioned report.

3. In addition to what has been said, once knowing K_c the value of G_c may be established from the relationship:

$$K_c^2 = EG_c$$

Center-cracked (by fatigue) specimens were employed because of indications that this type specimen is preferred by the ASTM Committee for the determination of K_c.[2]

Critical Fracture Toughness (K_{c3}) as a Function of Specimen Width

The observed relationship for K_{c3} and W, shown in Figure 6b, indicates the former to be essentially independent of the latter within the range W = 2.0 to W = 3.0. For values of W lying outside this range, K_{c3} may or may not be independent of W, but definitely is of rather considerably different magnitude. Within the range W = 3.5 to W = 4.0, K_{c3} corresponds to 98,000 psi, whereas, within the ragne W = 1.0 to W = 1.5, K_{c3} corresponds to 69,500 psi. A comparison of these latter values of K_{c3} with the value of K_{c3} (85,000 psi) corresponding to the range W = 2.0 to W = 3.0 indicates a rather symmetrical distribution of K_{c3} (W = 1.0 - 1.5) and K_{c3} (W = 3.5 - 4.0) values about that of K_{c3} (W = 2.0 - 3.0).

Significantly, perhaps, the lowest values of K_{c3} fall either outside or just inside the lower end of the recommended $\frac{W}{B}$ range. Similarly, the highest values of K_{c3} fall either outside or just inside the higher end of the recommended $\frac{W}{B}$ range. Reasons for the two types of behavior have been advanced elsewhere.[1] With reference to the value W = 4.0 ($\frac{W}{B}$ = 50), the $\frac{W}{B}$ ratio beyond this value at which the corresponding K_{c3} value would undergo a marked decrease in magnitude

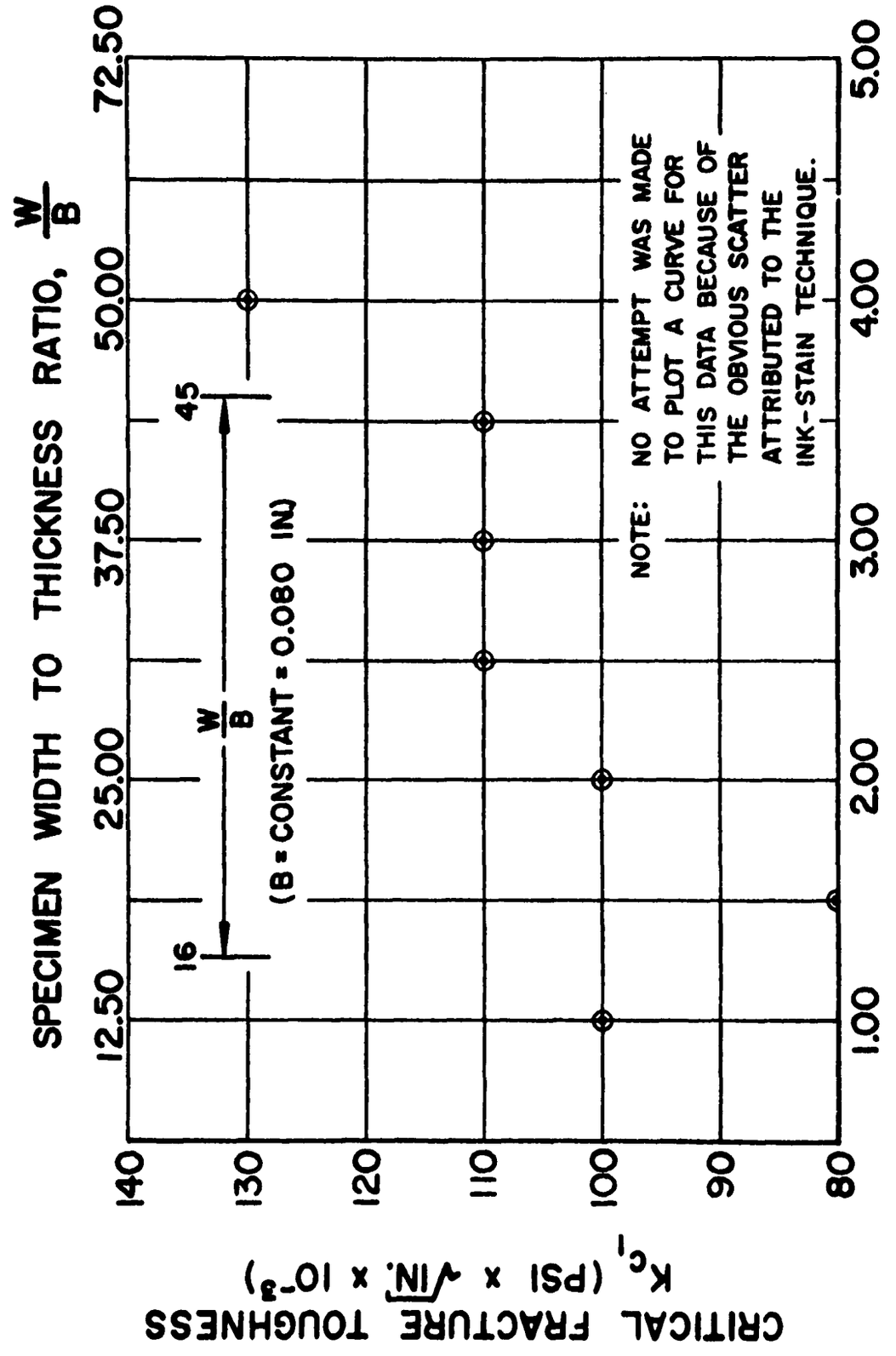

Figure 6a. Critical Fracture Toughness (K_{c1}) as a Function of Specimen Width (W)

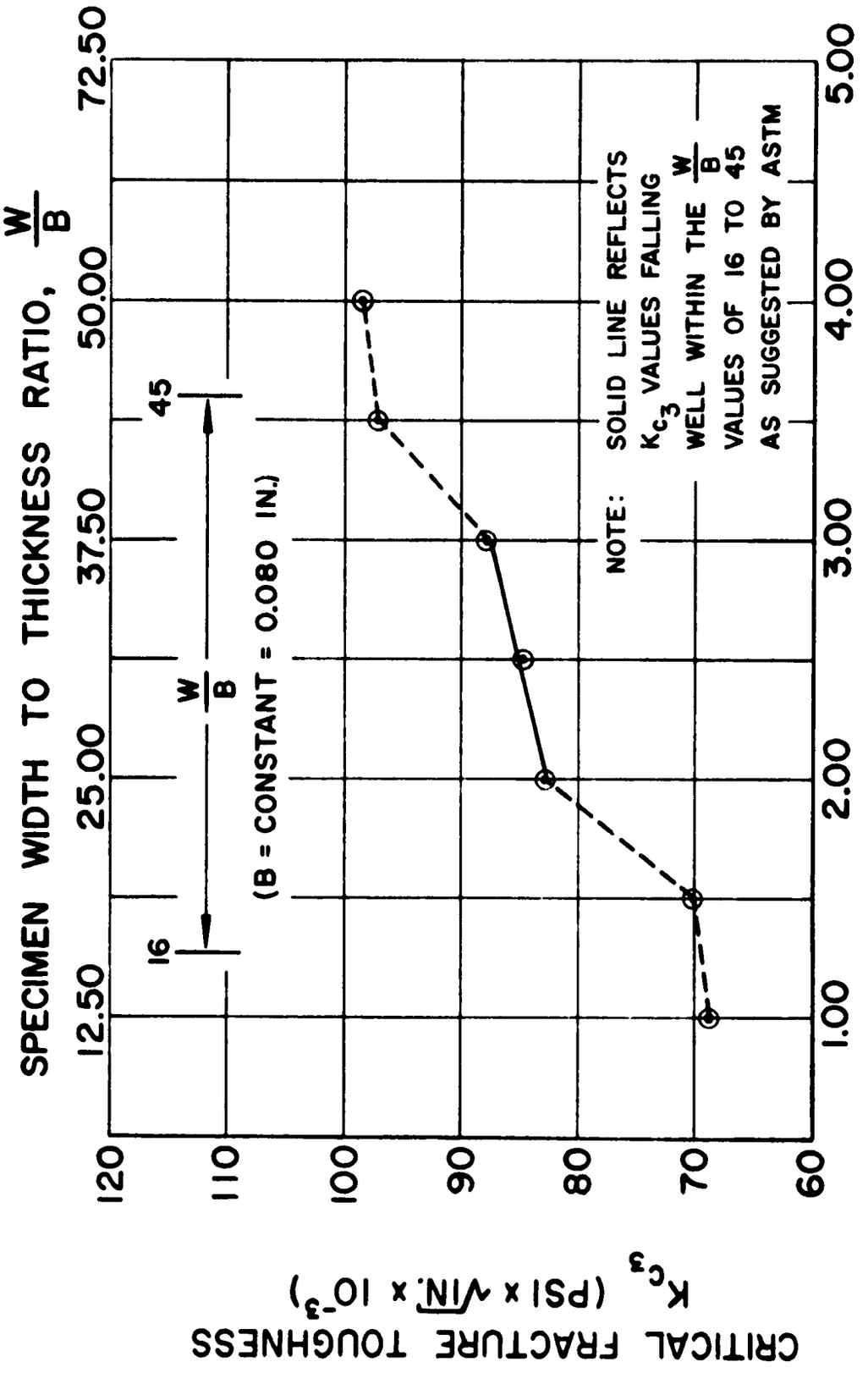

Figure 6b. Critical Fracture Toughness (K_{C3}) as a Function of Specimen Width (W)

is, on the basis of this work, speculative. However, the tenet that this would occur is supported by theoretical considerations if not by experimental evidence.[1]

Critical Fracture Toughness (K_{c3}) as a Function of the Initial Crack-Length-To-Specimen-Width Ratio

The observed relationship for K_{c3} and $\frac{2a_o}{W}$, shown in Figure 7b, suggests that the former is independent of the latter within the range $\frac{2a_o}{W} = 0.1 - 0.5$. Furthermore, there is no apparent reason to distinguish between the reliability of $\frac{2a_o}{W}$ values lying within the recommended range $\frac{2a_o}{W} = 0.3 - 0.4$ and those lying below this range. The same statement may be made with respect to $\frac{2a_o}{W}$ values lying above this range, with the exception of the single value of $\frac{2a_o}{W} = 0.6$. The magnitude of the corresponding K_{c3} coordinate, as this is reflected in its displacement relative to the other K_{c3} values, is attributed to the effect of the relatively severe restriction placed upon the zone available for plastic deformation by the existence of the high $\frac{2a_o}{W}$ ratio. The inability of such a restricted zone to permit an efficient redistribution of stresses and, hence, reduction of stress intensification via plastic strain is associated with a decrease in the values of σ_M and $(q_{c3})^{\frac{1}{2}}$ which, in turn, reflect a decrease in K_{c3}. The relationship between these quantities (shown earlier) is given by the general equation:

$$K_{c3} = \sigma_M (q_{c3} W)^{\frac{1}{2}}$$

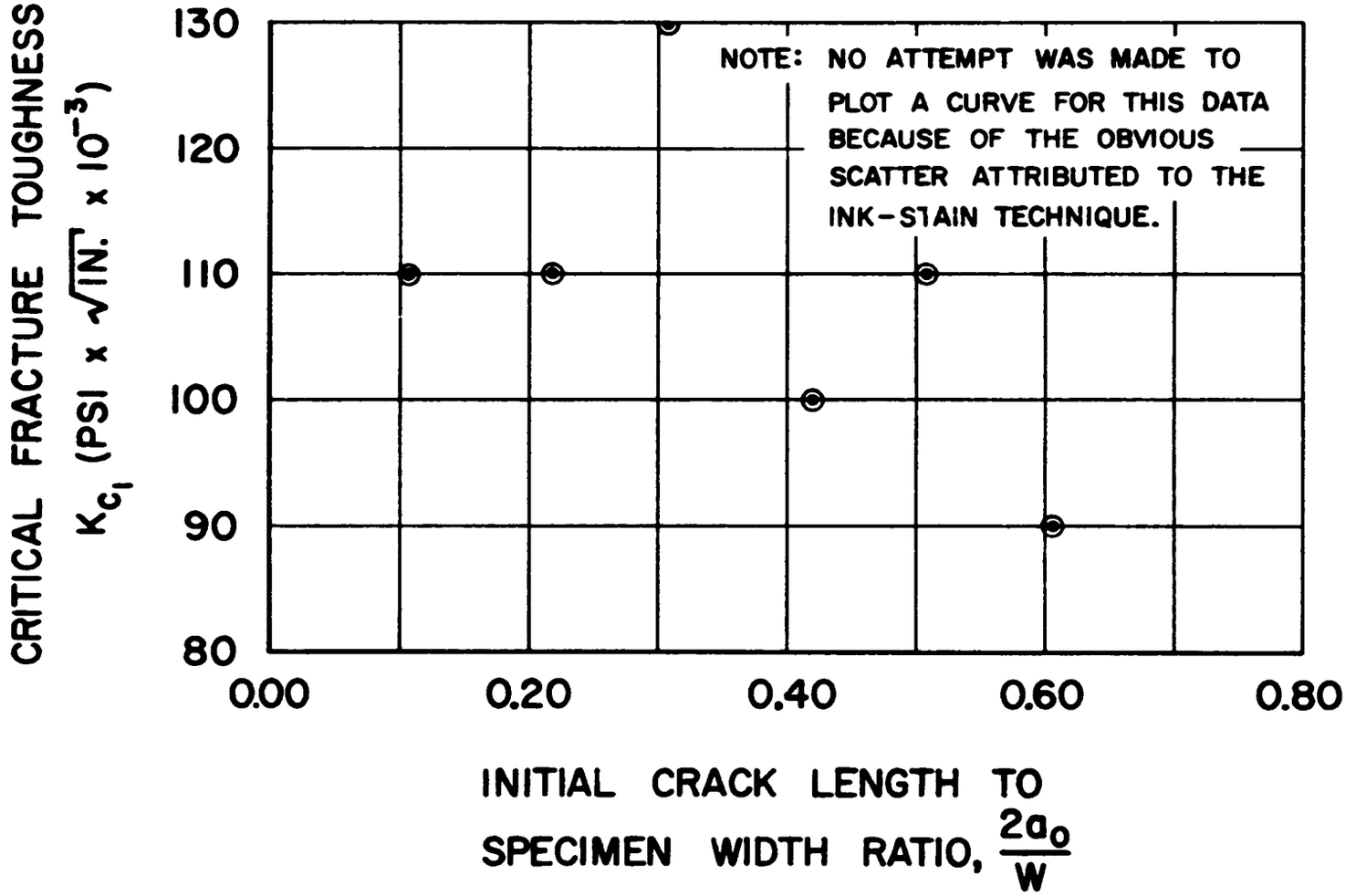

Figure 7a. Critical Fracture Toughness (K_{c1}) as a Function of Initial-Crack-Length-To-Specimen-Width Ratio ($2a_o/W$)

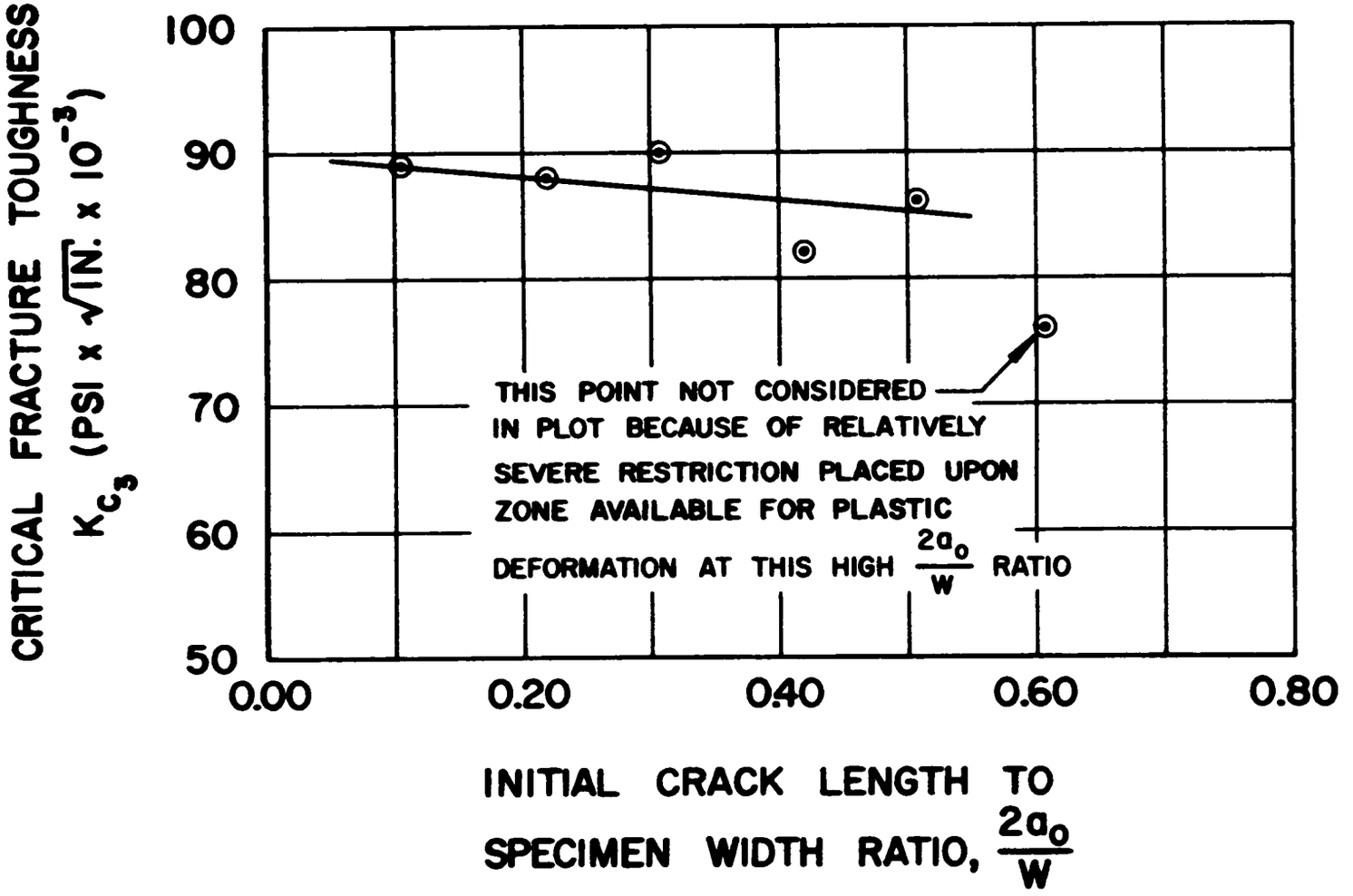

Figure 7b. Critical Fracture Toughness (K_{c3}) as a Function of Initial-Crack-Length-To-Specimen-Width-Ratio ($2a_o/W$)

Staining Method Compared to Fracture-Appearance Method for the Determination of Critical Fracture Toughness.

Values of K_{c1} were observed to be rather appreciably different from K_{c3} values as shown in Figures 6a, 6b, 7a, and 7b. The K_{c1} values consistently were of larger magnitude than the K_{c3} values and did not reflect an obvious independence of specimen geometry. This latter fact is attributed generally to the susceptibility of the staining method to human error in the processes of employing the technique, making the necessary measurements, and interpreting the results. Specifically, factors such as quantity of staining fluid introduced, its viscosity and ability to wet the particular surface, and, particularly, stain spatter may singly or collectively detract from the ability to determine representative results or to obtain suitable reproducibility. On the other hand, the determination of K_{c3} values is a relatively straight-forward process consisting mainly of simple, readily reproducible measurements.

With respect to the fact that the staining method was associated with K_c values of larger magnitude than were obtained by the fracture-appearance method, it appeared likely that this phenomenon resulted from the existence of apparent stained regions, which in reality, were actually of smaller dimensions than they appeared to be. It was reasoned that upon fracture of the specimen, the separated components, particularly the lower one, tended to rotate in a vertical

plane about their respective pin supports, thus causing excessive flow of stain in the direction opposite that of rotation. In order to minimize this effect, the practice of taping specimens to the grips was adopted.

The ratio of $\frac{2a}{2a_o}$ versus W values, shown in Figure 8, indicate the degree of scatter of slow-crack growth associated with the staining method. The average $\frac{2a}{2a_o}$ value (not shown) is 1.8 and, in fact, does not differ appreciable from the value of 1.6 reported by Kies, et al., to be commensurate with $P \geq 20$.[3] On the other hand, it is apparent that the $\frac{2a}{2a_o}$ values range from a high greater than 3 to a low less than 1.5. Furthermore, approximately 90 per cent of the $\frac{2a}{2a_o}$ ratios are distributed, collectively, so as to be above or below the value of 1.6. This degree of scatter further supports the belief that the fracture-appearance method may be relatively more reliable than the staining method.

The parameter K_{c1} was determined for a separate group of five specimens having the same geometry. The $\frac{2a}{2a_o}$ values ranged from 1.90 - 2.02 and reflected a maximum difference of 6.3 per cent. This difference generally was less than that observed for the bulk of K_{c1} values and was attributed to the use of constant specimen geometry. The reason the average value of $\frac{2a}{2a_o}$ was higher than that observed for the group of 84 specimens was not apparent.

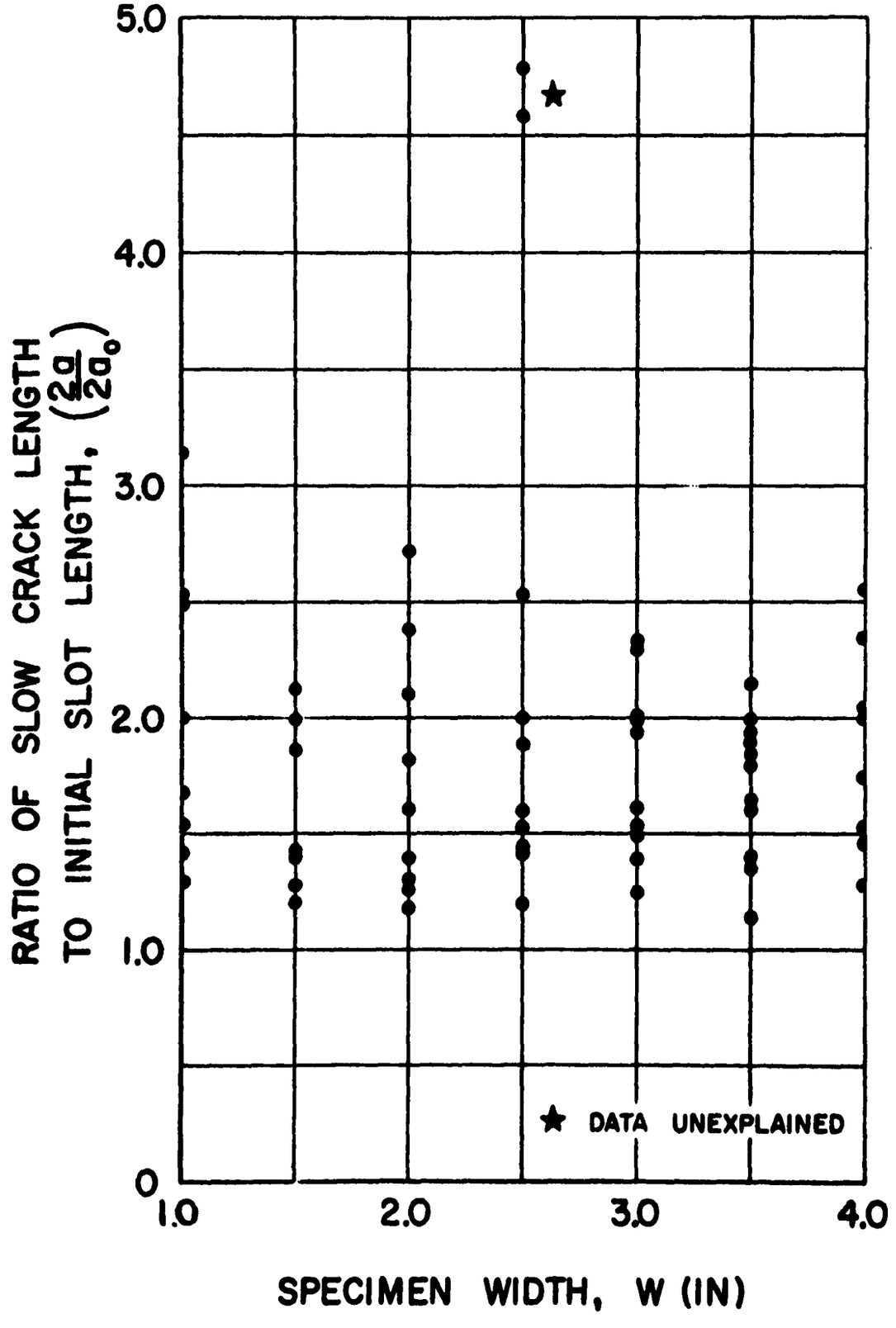

Figure 8. Ratio of Slow-Crack Length to Initial-Slot-Length ($2a/2a_o$) as a Function of Specimen Width (W)

Comparison of Fracture Toughness Data with Published Data

A comparison of fracture toughness data obtained in this instance with data obtained elsewhere involves what appear to be both similarities and dissimilarities. Warga has indicated for X-200 steel of thickness 0.080 in., yield strength 235,000 psi, and net section stress 69,000 to 94,000 psi, a corresponding range of G_c (staining method) values from 126 to 232.[4] Specimen type (center-notch; notch-to-width ratio 0.4) and dimensions (3 in. width, 12 in. length) were included in the range of specimens employed here. The present work includes data obtained for the same material of somewhat different yield strength (241,000 psi) and net section stress (134,000 psi), the average G_c value of which is 331. That such data do not lend themselves to direct comparison is indicated by considering that the $\sigma_{avg.N}/\sigma_{YS}$ reported by Warga is 0.35 as opposed to 0.55 (W = 3.0; average $2a_o$ = 0.4W) obtained here. On the other hand, the corresponding average G_c values are 179 as opposed to 331. Since an increase in the net section stress is associated with an increase in the fracture energy, G_c, the results would appear to be qualitatively in line, but resist direct comparison.

Warga has pointed out that a reasonable appraisal can be made of the limiting value of G_c (and K_c) and the corresponding strength level at which any particular high-strength steel would be suitable for use, provided certain assumptions are

made. He has shown, also, fracture toughness data expressed in terms of a common denominator, $\frac{\sigma_N}{\sigma_{YS}}$; this ratio constituting the basis of his contention.[4] Only by using this or a similar approach, then, is it possible to effect a satisfactory comparison of fracture toughness data.

Warga has indicated the limiting value for X-200 steel, at a yield strength of 195,000 psi, to be in excess of 1000.[4]

Orner and Hartbower have reported, for 0.080 in. X-200 steel, tempered at 700, 950 and 1050°F, G_c values of 176, 298 and 1195, respectively.[5]

Basis for Evaluating Fracture Toughness Data

Kies, et al., have suggested the use of minimum K_c and G_c values, with allowances for slow crack growth, based upon somewhat arbitrary assumptions. Thus, for σ_{YS} of 240,000 psi, $K_{c_{min}} = 764{,}000 \times (B)^{\frac{1}{2}}$.[4] On this basis, K_c values determined in the instance of the present work should approximate 214,000 psi. However, the largest single value of K_c actually observed was 169,200 psi. A similar consideration was made by Kies, et al., concerning $G_{c_{min}}$, that is, for σ_{YS} of 240,000 psi, $G_{c_{min}} = 19{,}300 \times B = 1545$.[3] The largest single value of G_c observed in the instance of the present work was 797.

The value of σ_N in the present work was, in every instance, of lesser magnitude than σ_{YS} of 241,000 psi; hence, the ratio of $\frac{\sigma_N}{\sigma_{YS}}$ was always less than unity. In view of these facts and

provided Warga's concept of unit ratio is, in reality, consistent with limiting conditions for satisfactory performance, the value of σ_{YS} for X-200 steel is 46,000 psi higher than should be employed in practice. The average G_c value (for crack-to-width ratios of 0.3 - 0.4) of 398, compared to reported values of $G_c = 1000$ at $\frac{\sigma_N}{\sigma_{YS}} = 1.0$.

With regard to what has been said above, attention should be directed to the fact that the principal objective of the present work was concerned with the effect of specimen geometry on critical fracture toughness. As such, the level of yield strength actually employed was incidental, so long as the strength-to-density ratio of the material employed was 700,000 psi/lb/in^3 minimum.

Despite the stated purpose of the present work, it is interesting to note that Manning has indicated H-11 and AISI 4340 may react differently when evaluated in terms of two different specimen geometries. This indicates that superior load carrying ability is not a unique characteristic of either, but reflects "subtle differences" in the behavior of steels subjected to equal stress concentration, that is, having identical specimen geometry.[6]

It would appear reasonable, in line with Manning's contention, that any attempt to assign an order of merit to high-strength steels should include a consideration of the effects of stress concentration.

Oil Versus Air Quenching of Test Specimens

Some consideration was given to whether oil or air quenching should be employed. Cursory tests, limited to hardness determinations on continuously cooled specimens and specimens cooled at discontinuous rates, failed to indicate any basis for favoring either oil or air as the quenching medium. In addition, the literature was not helpful in this regard. Oil quenching finally was chosen on the tenet that if a difference in response to hardening might exist, the use of oil would maximize the probability of developing a fully martensitic structure.

With respect to the above, it is possible that effects attendent upon either method of quenching might be reflected in associated fracture toughness parameters, with greater thermal stresses on the one hand and grain-boundary precipitation on the other. Larson has reported the existence of a grain-boundary film in air-quenched H-11 steel and no indication of this condition in the water-quenched structure. Because of this, a further study of the effects of the two quenchants on the fracture toughness of H-11 apparently is warrented.[7]

CONCLUSIONS

1. The range of $\frac{W}{B}$ values extending from 16 to 45 would appear to be somewhat broader than is consistent with the attainment of uniform values of K_{c3}. This possibility is supported by the observed 41 per cent difference in the extremes of the K_c values corresponding to the range recommended by the ASTM Committee.
2. The parameter K_{c3} appears to be independent of specimen geometry within a somewhat broader range of $\frac{2a_o}{W}$ values (0.1 - 0.5) than is recommended by the ASTM Committee.
3. The parameter K_{c1} was not obviously independent of speciment geometry. Whether the reason advanced to account for the generally observed relationship $K_{c1} > K_{c3}$ is valid, it is concluded on the basis of this work that K_{c3} values represent a more conservative evaluation of critical fracture toughness than do K_{c1} values. Furthermore, the parameter K_{c3} would appear to be quantitatively more reliable than the K_{c1} parameter. This is indicated because of the simplicity and accuracy involved in the determination of K_{c3}.

TERMINOLOGY

a : Slow crack length (in.)

a_o : Initial crack length from center line (in.)

a_s : Initial saw cut from center line (in.)

W : Specimen width (in.)

B : Specimen thickness (in.)

σ_{YS} : Yield strength (psi)

σ_N : Net fracture stress at onset of unstable crack propagation (psi)

σ_M : Maximum gross section stress at onset of unstable crack propagation (psi)

P_M : Maximum tensile load at onset of unstable crack propagation (lb)

P : Per cent shear

K_c : Critical fracture toughness parameter ($psi\sqrt{in.}$)

K_{c1} : Critical fracture toughness parameter associated with staining method ($psi\sqrt{in.}$)

K_{c3} : Critical fracture toughness parameter associated with the fracture-appearance method ($psi\sqrt{in.}$)

q_{c1} : Critical stress distribution factor associated with staining method

q_{c3} : Critical stress distribution factor associated with fracture-appearance method

G_c : Critical strain energy release rate $\frac{lb\text{-}in.}{in^2}$

T_r : Room temperature ^oF

E : Modulus of elasticity, psi

REFERENCES

1. "Fracture Testing of High-Strength Sheet Materials: A Report of a Special ASTM Committee," ASTM Bulletin, Number 243, January 1960.

2. Holms, A. G., "NRL-NASA-SRI Cooperative Study of High Strength Sheet Specimens Intended for Measuring Design Values of Fracture Toughness", Lewis Research Center, NASA. Paper presented at the Seventh Sagamore Ordnance Materials Research Conference, August 16-19, 1960.

3. J. A. Kies, H. Romine, H. L. Smith, H. Bernstein, "Minimum Toughness Requirements for High Strength Sheet Steel," Trans. of the American Society of Mechanical Engineers, Journal of Basic Engineering, March, 1961.

4. Joseph J. Warga, "Use of the Center Notch-Tensile Test to Evaluate Rocket-Chamber Materials", Welding Research, Vol. XXVI, Number 3, March, 1961.

5. George M. Orner and Carl E. Hartbower, "Notch Sensitivity in High-Strength Sheet Materials", Welding Research Supplement, April, 1960.

6. G. K. Manning, "How Should You Evaluate High-Strength Materials", Metal Progress, Vol. 80, No. 3, September, 1961.

7. J. E. Campbell, "Review of Recent Developments in the Evaluation of Special Metal Properties", DMIC Memorandum 94, Battelle Memorial Institute (OTS Publication 161244), March 28, 1961.

THE EFFECT OF TEMPERING TEMPERATURE, GRAIN SIZE, AND TEST TEMPERATURE ON FRACTURE TOUGHNESS OF HIGH-STRENGTH SHEET STEEL.

This investigation represents a continuation of a study pertaining to the effects of specimen geometry on fracture toughness characteristics of high-strength sheet steel.[1] Specifically, the objectives were to determine the effects of tempering temperature, grain size, and test temperature on the critical fracture toughness (K_c) of two high-strength sheet steels. The study proposed to:

(1) Determine the magnitude of K_c for specimens, having constant widths (W) and constant crack lengths ($2a_o$), tested at temperatures above and below room temperature.

(2) Determine the magnitude of K_c for specimens, having constant W and $2a_o$ values, tempered at different temperatures.

(3) Determine the magnitude of K_c for specimens, having constant W and $2a_o$ values and different ferrite grain sizes.

(4) Investigate the variation of K_c for specimens, having constant W and $2a_o$ values, tested at temperatures above and below room temperature.

(5) Investigate the variation of K_c for specimens, having constant W and $2a_o$ values, tempered at

different temperatures.

(6) Investigate the variation of K_c for specimens having constant W and $2a_o$ values and different ferrite grain sizes.

Each of the above six investigations was made for two types of high-strength sheet steel. Centrally-notched specimens were used for the investigations.

Apparatus and Procedure

All specimens used for this investigation were sheared from sheets of H-11 and X-200 steel. The average thickness of the sheets was 0.080 inch, and they were received in the sheroidized-annealed condition. The specimens used for these tests were referred to as Group 1, Group 2, and Group 3, respectively, for H-11 steel and Group 1, Group 2, and Group 3, respectively, for X-200 steel.

The longitudinal axis of each fracture toughness specimen corresponded to the rolling direction of the sheet. The dimensions of the specimen are shown in Figure 1. Holes for the pin-supported specimens were provided by drilling to 1/64 inch undersize and boring to the final dimension. The remaining machining operation consisted of drilling a 0.046 inch diameter hole located at the geometric center of the specimen.

A jeweler's saw, the blade of which was 0.005 inch thick, was used to cut a center slot ($2a_s$) in each specimen. Center slots subsequently were extended to predetermined lengths ($2a_o$) by means of fatigue stressing.

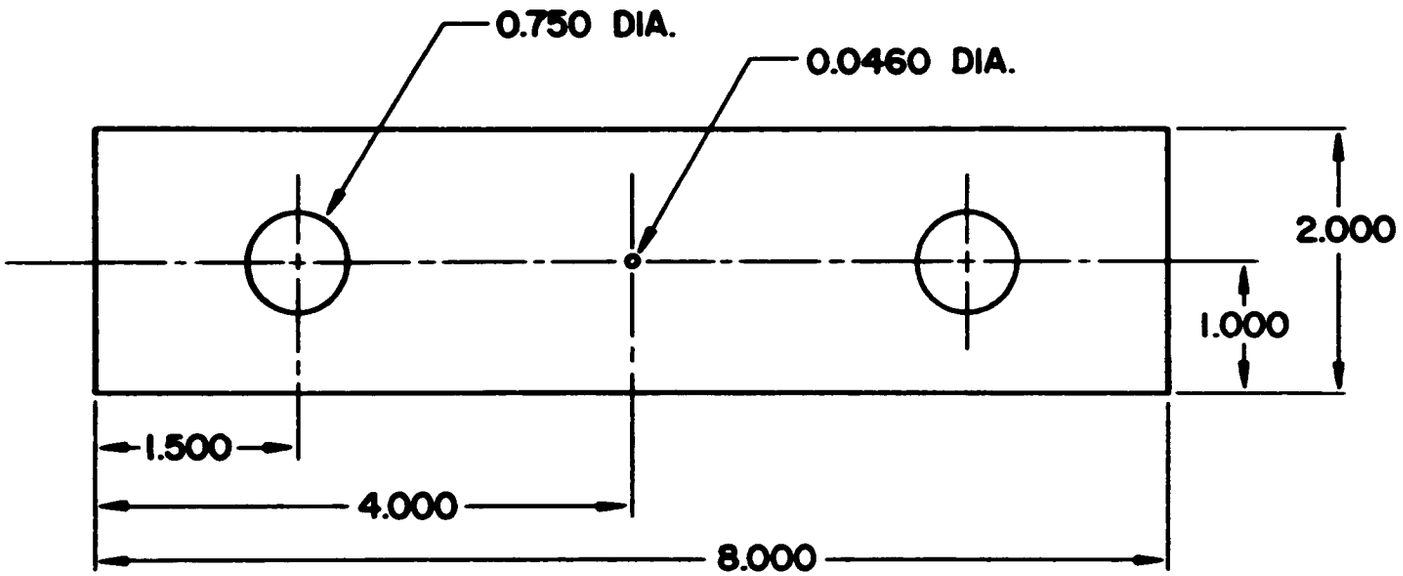

NOTE: 1. TOLERANCE ON ALL DIMENSIONS EXCEPT THAT OF PIN HOLES (SEE NOTE 2) ±0.001 IN.

2. PIN HOLE TOLERANCE $\frac{+0.0005}{-0.0000}$

Figure 1. Fracture Toughness Specimen

Each specimen, in turn, was mounted in a fatigue machine shown in Figure 2, which was regulated to produce a maximum tensile load and a minimum tensile load. Maximum and minimum loads were of such magnitudes that the corresponding net-section stresses in each specimen were 50% and 15%, respectively, of the yield strength (0.2% offset) of the material. A floodlight and a 3X magnifying glass were used to follow the crack growth to the length $2a_o$. In this manner, the fatigue loads and number of cycles required to produce the predetermined initial-crack length ($2a_o$) were determined for a limited number of specimens. These data permitted fatigue cracking of the remainder of the specimens simply by employing loads and numbers of cycles known to produce cracks of desired lengths. Fatigue data are shown in Table 1.

At the conclusion of the fatigue-cracking operation, Group 1 (H-11) specimens were heat treated to an ultimate tensile strength (room temperature) of approximately 230,000 psi. Eighteen specimens were used since there were nine test temperatures and duplicate specimens for each temperature. Heat treatment was conducted in an endothermic atmosphere having a dew-point temperature of 45°F. The specimens were austenitized at 1850°F for 30 minutes and then air cooled. Immediately afterward they were tempered for two hours at 975°F. After air cooling to room temperature, a second tempering treatment was conducted under the same conditions as the first.

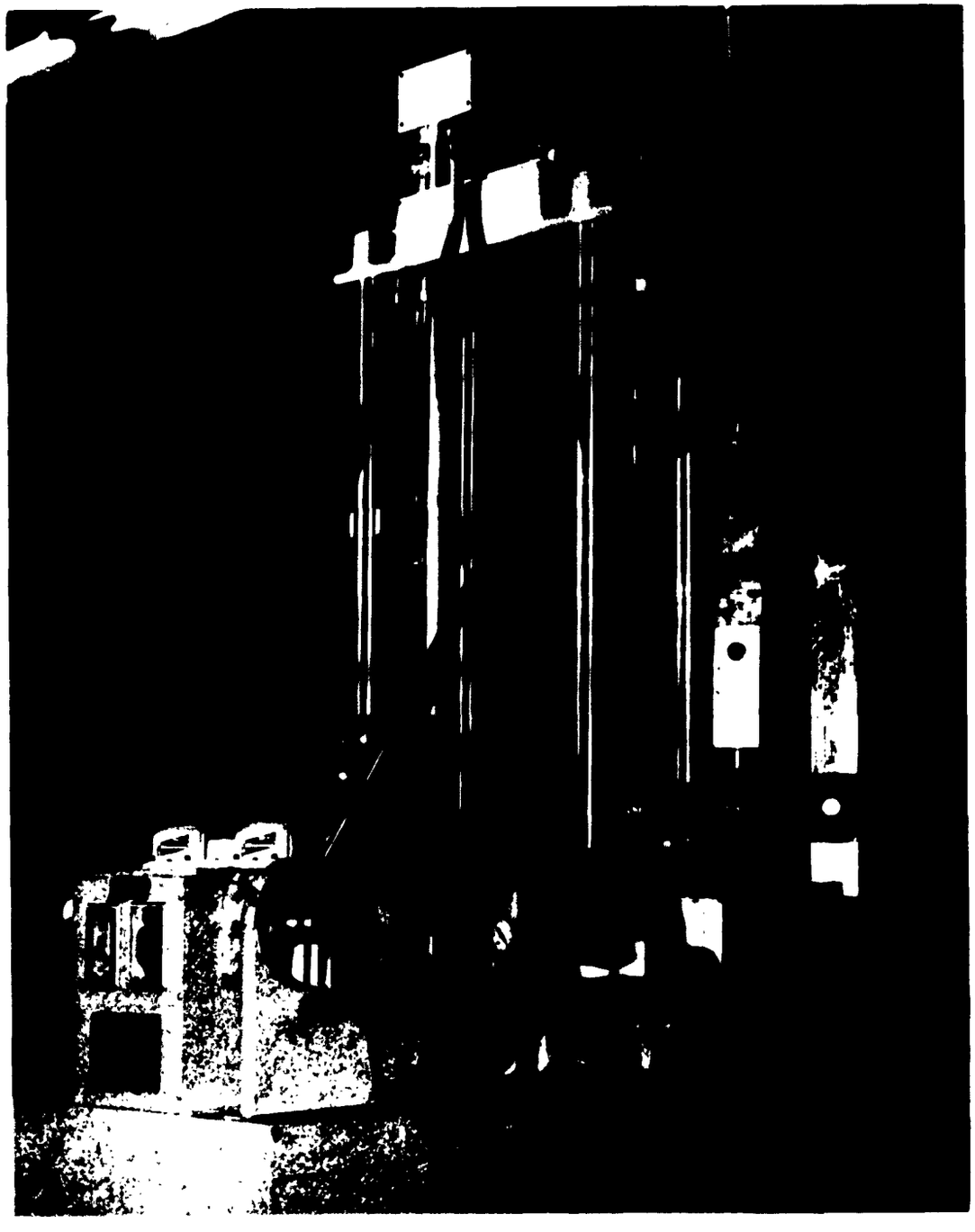

Figure 2. Fatigue Machine (Showing Positioning of Fracture Toughness Specimen)

No attempt was made to effect controlled decarburization of specimen surfaces. Rather, decarburization (as well as carburization) was avoided intentionally. Small quantities of H-11 steel were heat treated along with the test specimens in order to provide an indication of surface condition. Conclusions regarding surface condition were based on metallographic and hardness determinations. No evidence of decarburization was observed in any instance.

Eighteen standard tensile specimens were sheared from the same sheet of H-11 steel that was used for the corresponding fracture toughness test specimens. The longitudinal axis of each specimen was oriented in a direction parallel to the rolling direction of the sheet. The dimensions of the standard tensile-test specimen are indicated in Figure 3. These specimens were heat treated in the manner described for the fracture toughness specimens.

A universal testing machine, shown in Figure 4, was used to obtain the stress-strain data test for each of the standard tensile specimens. Type A-3, SR-4 strain gages were used to determine the strain values. In the first instance, one gage was mounted on each side of two of the standard tensile specimens. Two gages per specimen were used in order that one set of gage readings could be used to serve as a check on the other, However, it was found that the strain values for the gage one side of the specimen corresponded so closely with those for the gage on the opposite side of the specimen that only one gage was used for each of the remaining specimens.

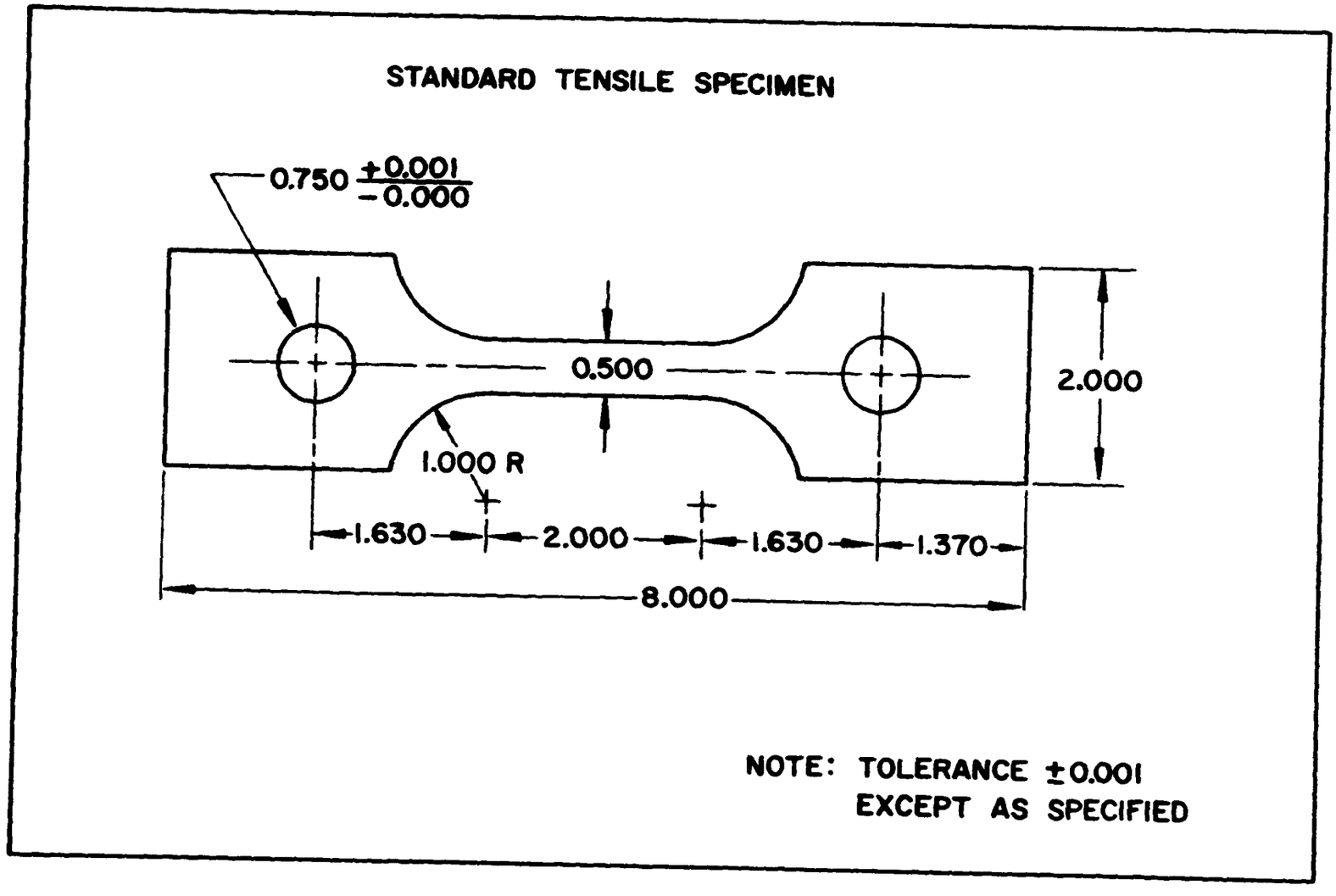

Figure 3. Standard Tensile Specimen

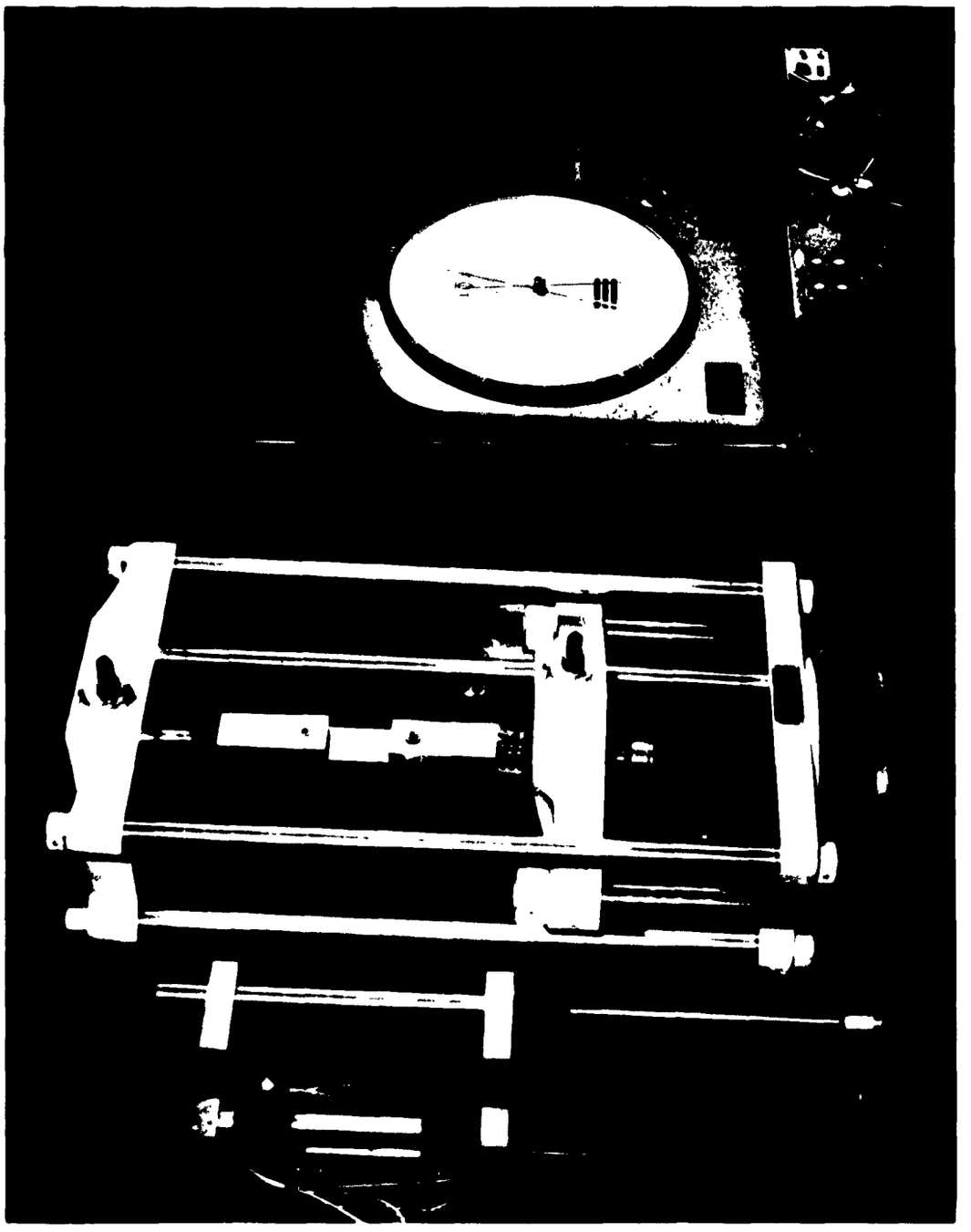

Figure 4. Universal Testing Machine (Showing Positioning of Fracture Toughness Specimen)

One standard tensile specimen was provided for each fracture toughness specimen. As was the case for the fracture toughness specimens, there were duplicate standard tensile specimens for each of the nine test temperatures. These temperatures were 300, 150, 100, 50, 0, -50, -100, -150, and -200°F. The furnace used to maintain the above-room test temperatures is shown in Figure 5. A specially constructed cryostatic shown in Figure 6, was used in maintaining the below-room test temperatures.

A stress-strain curve was plotted for each standard tensile specimen in order to determine the yield strength (0.2% offset).

The universal testing machine also was used to determine the maximum tensile load for each fracture toughness specimen. However, since fracture toughness has been observed to be sensitive to loading rates, a variable load pacer was used to maintain a constant loading rate of 3500 lb/min for each specimen.[3]

After testing the fracture toughness specimens, the fracture-appearance or per cent shear method was used to determine K_{c3} values (Table 2). The fracture appearance method consists of measuring the shear lip, as shown in Figure 7, and expressing the shear-lip distance as a percentage of the total specimen width. The shear-lip measure- was made at a distance of twice the specimen width (2B) from the extreme specimen edge. The measurement was made by using

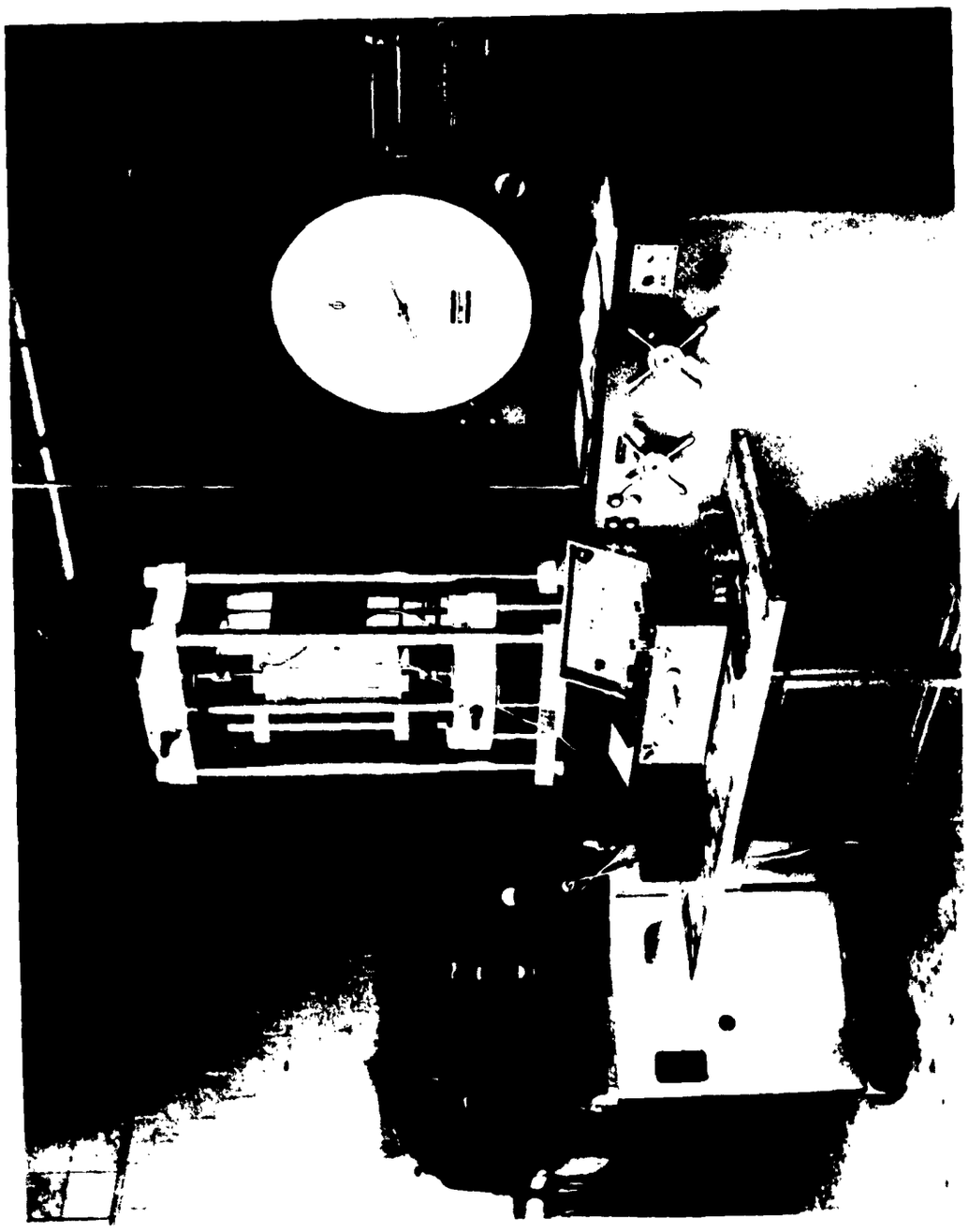

Figure 5. Furnace, In Position on Universal Testing Machine

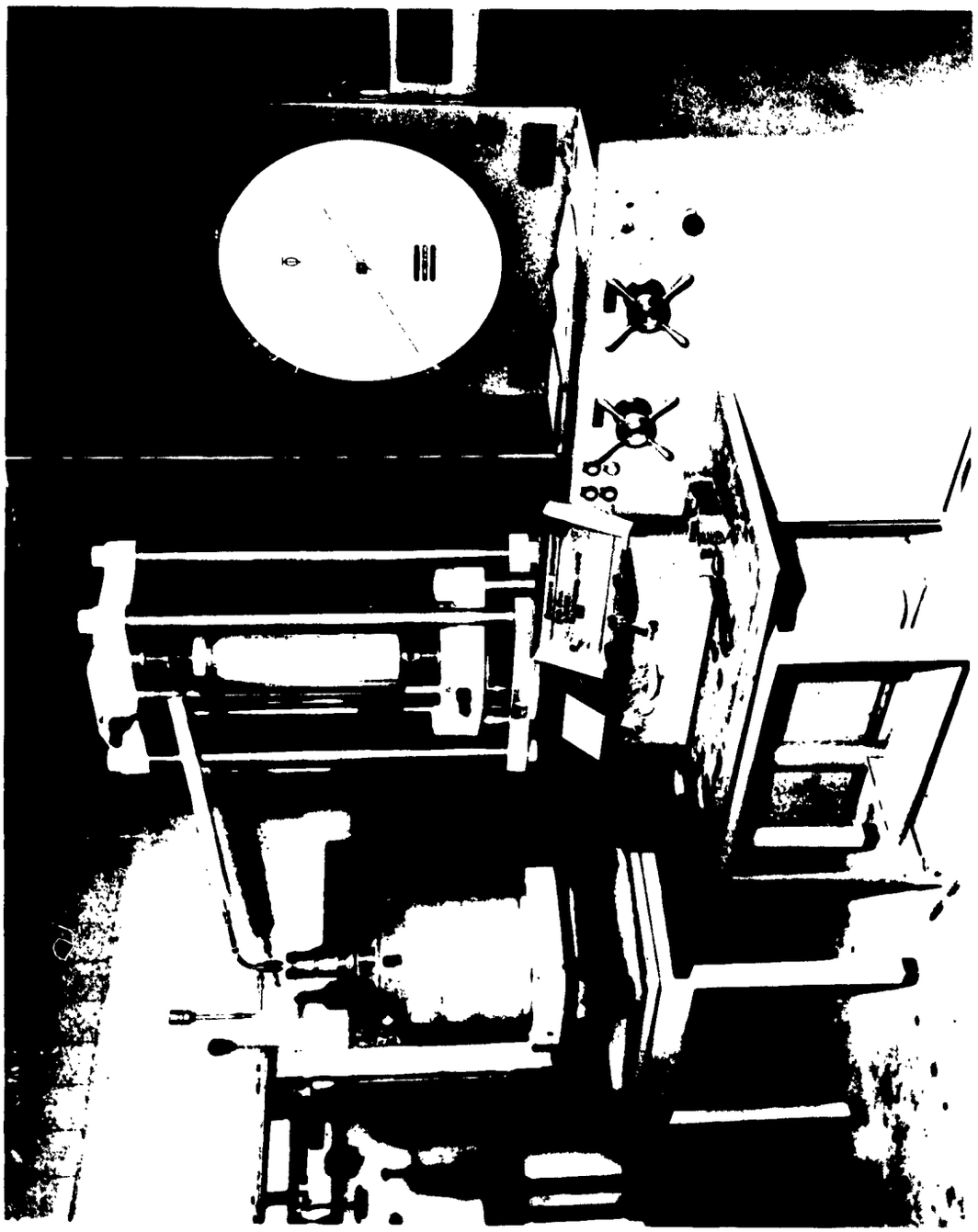

Figure 6. Cryostat, In Position on Universal Testing Machine

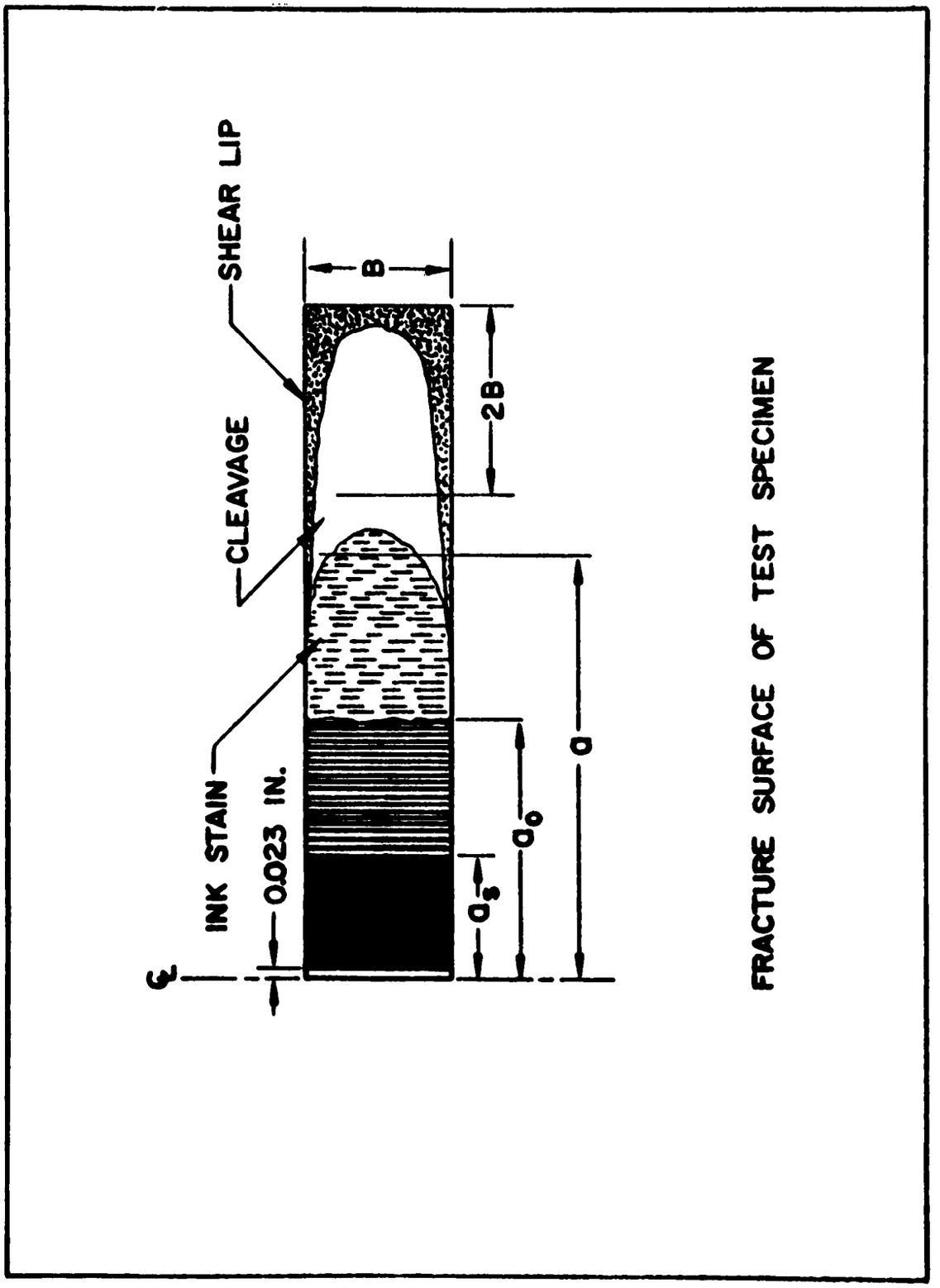

Figure 7. Fracture Surface of Test Specimen

a 60X stereoscopic microscope equipped with a calibrated reticle which could be read to 0.001 inch. Each fracture surface of the fracture toughness specimens consisted of a generally flat cleavage surface bordered by a shear lip.

The shear values then were used in the determination of q_{c3} values in order to arrive at K_{c3} from the following equation:

$$(1)\quad K_{c3} = \sigma_M (q_{c3} W)^{\frac{1}{2}}$$

in which $\sigma_M = \frac{P_M}{WB}$

and q_{c3} = stress distribution factor.

The value of q_{c3} was determined by using the following equations:

$$(2)\quad 2\tan^{-1} q_{c3} - \frac{q_{c3}}{1+q_{c3}^2} = \frac{2\pi a_o}{W} + 2C + \tfrac{1}{2}\left[\frac{\sigma_M}{\sigma_{YS}}\right]^2 q_{c3}$$

which can be expressed in the following form:

$$\frac{\pi a_o}{W} + C = \tan^{-1} q_{c3} - \frac{0.5 q_{c3}}{1+q_{c3}^2} - \tfrac{1}{4} q_{c3}\left[\frac{\sigma_M}{\sigma_{YS}}\right]^2$$

It is apparent that this latter form of equation (2) is the equation of a straight line having a negative slope of $\frac{1}{4}q_{c3}$ and an ordinate intercept of $(\tan^{-1} q_{c3} - \frac{0.5q_{c3}}{1+q_{c3}^2})$

The term "C" in equation (2) is an empirical correction term based on the running crack shear-lip fraction "P" and is determined from the following equation:

(3) $C = 4.7\ (P - 0.43)\ B/W$

Each "P" (per cent shear) value was substituted into equation (3) in order to determine, ultimately, the value of the ordinate "y". The equation for "y" is shown as follows:

$$y = \frac{\pi a_o}{W} + C.$$

A number of straight lines were plotted using equation (2) which included the range of $\left[\frac{\pi a_o}{W} + C\right]$ and $\left[\frac{\sigma_M}{\sigma_{YS}}\right]^2$ values determined during the investigation. The values of q_{c3} were determined by entering the $\left[\frac{\pi a_o}{W} + C\right]$ value and corresponding $\left[\frac{\sigma_M}{\sigma_{YS}}\right]^2$ value into the q_{c3} plot[1] (not shown) and reading the corresponding q_{c3} value.

The q_{c3} values then were indirectly used in the determination of slow-growth (2a) values. Due to the fact that the fracture toughness value for a given material is independent of the method of determination, $q_{c1} = q_{c3}$. Therefore, substituting the value of q_{c1} for q_{c3} and using the corresponding $\left[\frac{\sigma_M}{\sigma_{YS}}\right]^2$ value, a $\frac{\pi a}{W}$ value was determined from the q_{c1} plot[1]

(not shown). Using the $\frac{\pi a}{W}$ value, a corresponding 2a value was achieved without the actual application of a stain. The 2a value was used in the determination of the net-fracture stress (σ_N).

The next group of H-11 fracture toughness specimens was tested at essentially-constant room temperature. The eighteen specimens comprising this group (Group 2) consisted of nine pairs of duplicate specimens. These specimens, which had been previously fatigue-cracked, were austenitized at 1850°F for 30 minutes and then air cooled. Heat treatment was conducted in an endothermic atmosphere having a dew point temperature of 45°F. Immediately after cooling from the austenitizing temperature, one pair of the specimens was tempered for two hours at 400°F. After air cooling to room temperature, this pair of specimens was given a second tempering treatment under the same conditions as the first.

Duplicate standard tensile-test specimens were heat treated in the manner described for the fracture-toughness specimens.

A second pair of Group 2 (H-11) fracture toughness specimens and standard tensile-test specimens were heat treated as before except that the tempering temperature was increased to 500°F.

The remaining Group 2 (H-11) fracture toughness specimens and standard tensile-test specimens were heat treated in the manner outlined above except that the tempering temperature was increased in 100°F increments for each successive pair. This procedure was continued until the last specimens had been tempered at 1200°F.

The tensile-testing procedure used for Group 1 (H-11) fracture toughness specimens was employed for Group 2 (H-11) fracture toughness specimens. The K_{c3} values also were calculated in the same manner.

The yield strength values of the standard tensile-test specimens were determined as before.

Group 3 (H-11) consisted of nineteen fracture toughness specimens. These specimens were austenitized at 2050°F instead of 1850°F as was employed for Groups 1 and 2 (H-11) specimens. The austenitizing temperature was increased for Group 3 (H-11) specimens in order to coarsen the grain size. The grain size of Group 1 (H-11) specimens was ASTM No. 8 The grain size of Group 3 (H-11) specimens was ASTM No. 6-7

Two Group 3 (H-11) fracture toughness specimens were tested at each of the following temperatures: 200, 150, 100, 50, 0, -50, -100, -150, and -200°F. A single fracture toughness specimen was tested at -300°F since some difficulty was encountered in maintaining this temperature.

The procedure employed previously was used for the determination of K_{c3} values.

A standard tensile-test specimen was provided for, and heat treated with, 19 Group 3 (H-11) fracture toughness specimens. The test temperatures used for the standard tensile-test specimens were the same as those used for the corresponding fracture toughness specimens. The yield strengths of the standard tensile-test specimens were determined as before.

The tensile-testing procedure used for Group 1 (H-11) fracture toughness specimens was employed for Group 2 (H-11) fracture toughness specimens. The K_{c3} values also were calculated in the same manner.

The yield strength values of the standard tensile-test specimens were determined as before.

Group 3 (H-11) consisted of nineteen fracture toughness specimens. These specimens were austenitized at 2050°F instead of 1850°F as was employed for Groups 1 and 2 (H-11) specimens. The austenitizing temperature was increased for Group 3 (H-11) specimens in order to coarsen the grain size. The grain size of Group 1 (H-11) specimens was ASTM No. 8 The grain size of Group 3 (H-11) specimens was ASTM No. 6-7

Two Group 3 (H-11) fracture toughness specimens were tested at each of the following temperatures: 200, 150, 100, 50, 0, -50, -100, -150, and -200°F. A single fracture toughness specimen was tested at -300°F since some difficulty was encountered in maintaining this temperature.

The procedure employed previously was used for the determination of K_{c3} values.

A standard tensile-test specimen was provided for, and heat treated with, 19 Group 3 (H-11) fracture toughness specimens. The test temperatures used for the standard tensile-test specimens were the same as those used for the corresponding fracture toughness specimens. The yield strengths of the standard tensile-test specimens were determined as before.

At the conclusion of testing of the H-11 fracture toughness and standard tensile-test specimens, a similar testing program was followed for X-200 fracture toughness specimens and standard tensile-test specimens. The heat treating procedures for Groups 1, 2, and 3 of X-200 steel corresponded to the procedures used for Groups 1, 2, and 3, respectively, of the H-11 steel.

Heat-treating and test temperatures for specimens of X-200 steel were as follows:

Group 1: Austenitizing temperature: 1750°F
Tempering temperature: 800°F
Test temperatures: 150, 100, 75, 25, 0, -25, -50, -75, -100, and -150°F

Group 2: Austenitizing temperature: 1750°F
Tempering temperatures: 400, 500, 600, 700, 800, 900, 1000, 1100, 1200, and 1300°F
Test temperature: Approximately 82°F

Group 3: Austenitizing temperature: 1950°F
Tempering temperature: 800°F
Test Temperatures: 150, 100, 50, 25, 0, -25, -20, -75, -100, and -150°F

The grain size of Group 1 (X-200) specimens was ASTM No. 7-8
The grain size of Group 3 (X-200) specimens was ASTM No. 6-7

DISCUSSION OF RESULTS

Reduction of Data

The scales employed in the graphical representation of K_{c3} values are consistent with the estimated accuracy involved in the accumulation of corresponding data. Each point plotted, on any particular graph, represents a single determination.

The fracture-appearance method of evaluating K_{c3} was employed because:

1. Previous experience has indicated the fracture-appearance method to be relatively more reliable than the staining method.[1]
2. The staining method does not lend itself to the determination of fracture-appearance transistion temperature (FATT).[2]

Heat Treatment

Specimens of X-200 and H-11 steels were air cooled rather than oil quenched from their respective austenitizing temperatures in order to minimize any tendency toward distortion and to simplify the hardening procedure. Specimens were held in a fixture (Figure 8) during austenitizing and clamped during tempering. These procedures were effective in minimizing distortion.

Ductile-Brittle Criterion

The net-fracture stress curve (Figure 25) for H-11 intersects the yield-strength curve at $\sigma_N / \sigma_{YS} = 1.0$. The point of intersection corresponds to a tempering temperature of 975°F,

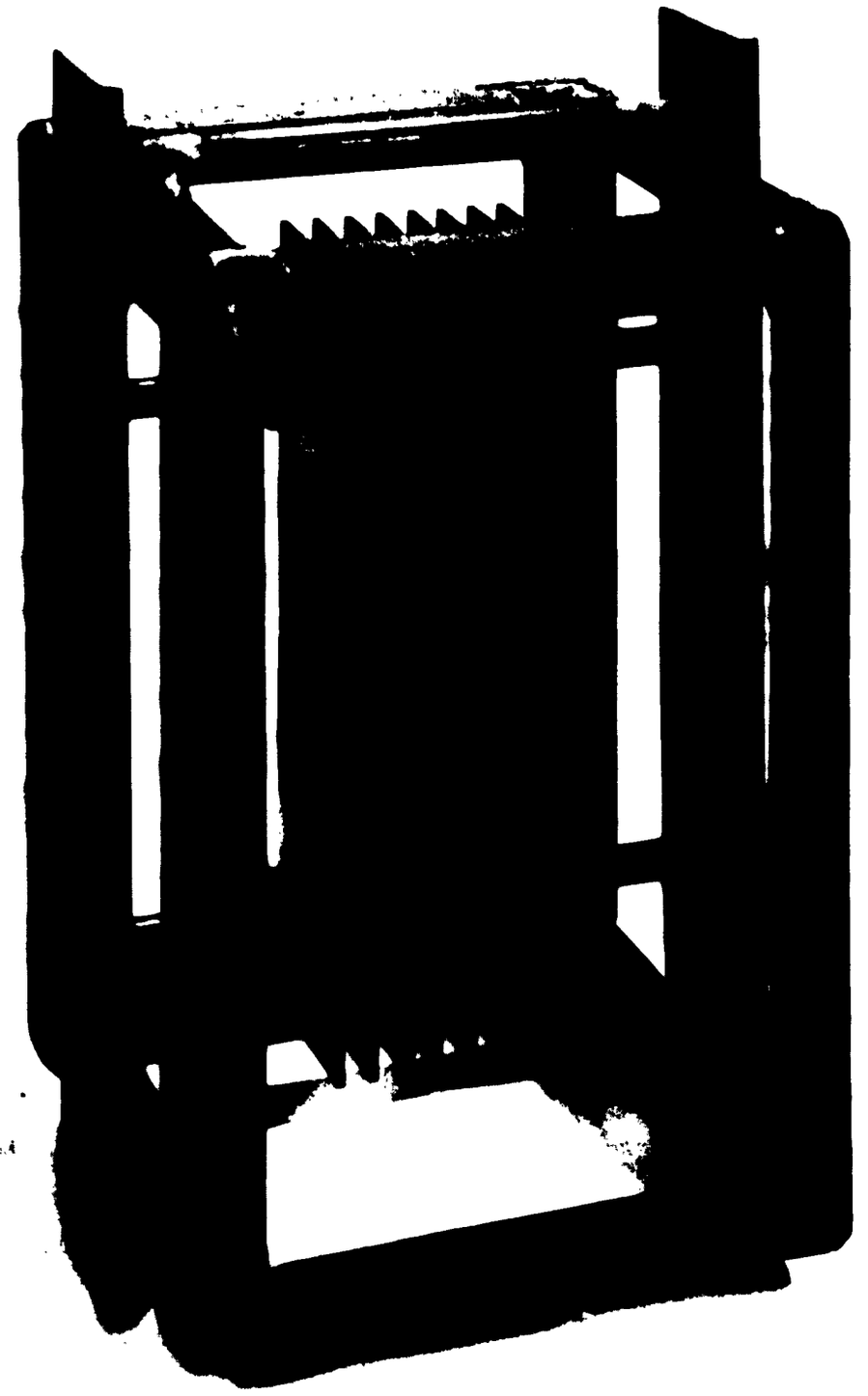

Figure 8. Specimen Heat-Treating Fixture

this temperature being the actual temperature employed. Similarly, with respect to X-200 (Figure 14) the ratio $\sigma_N / \sigma_{YS} = 1.0$ occurs at a tempering temperature of 900°F which is 100°F above the tempering temperature employed. On this basis H-11, in the condition employed, was notch ductile; whereas, X-200, in the condition employed, was something less than notch ductile.

Critical Fracture Toughness as a Function of Ferrite Grain Size

A well defined fracture-appearance transition temperature (FATT) generally was not observed for either H-11 or X-200 specimens. This fact is attributed to: (a) the high yield-strength level (190,000 psi and 205,000 psi, respectively, at room temperature) in which condition each steel was evaluated, and (b) the use of test temperatures which generally were below the limit required for transition from P<100 per cent to P = 100 per cent. Similar behavior has been reported elsewhere.[3]

The FATT for Group 1 (H-11) specimens, austenitized and tempered at recommended[4] temperatures of 1850 and 975°F, respectively, was observed to be 150°F (Figure 20). However, the use of Group 3 (H-11) specimens austenitized at a temperature (2050°F) 200°F higher than recommended, and tempered at the same tempering temperature, resulted in a maximum P = 55 per cent at a test temperature of 200°F; hence, no FATT was observed. The difference in behavior is attributed to the coarser grain size and the resulting decrease in toughness.

With respect to X-200 specimens, no FATT was observed (Figures 9-12 and 15-18). The combination of recommended[4] austenitizing temperature (1750°F) and relatively low tempering temperatures (800°F) was consistent with a maximum value of P = 36 per cent. The combination of higher than recommended austenitizing temperature and relatively low tempering temperature for Group 3 specimens was consistent with a maximum value of P = 28 per cent.

The effect of the relatively low tempering temperature alone was to raise FATT, for which P = 100 per cent, above that of the highest test temperature. The FATT apparently was further raised by incorporating the factor of coarse grain size with that of relatively low tempering temperature since, by so doing, the value of P was reduced from 36 to 28 per cent. The increase in transition temperature accompanying increase in grain size has been reported elsewhere.[5]

Critical Fracture Toughness, Fracture Appearance, Net-Fracture Stress, and Ratio of Net-Fracture Stress - To - Yield Strength as a Function of Test Temperature

The geometries of curves showing K_{c3}, P, σ_N, and σ_N / σ_{YS} as a function of test temperature (Figures 9-12, 15-18, 19-22, and 25-28) were quite similar. Curves generally displayed an unexplained hump to the vicinity of the low-temperature end of the temperature range. Although the equations for the curves were not determined, the relationship between the above-mentioned quantities and test temperature appears to be of the exponential type.

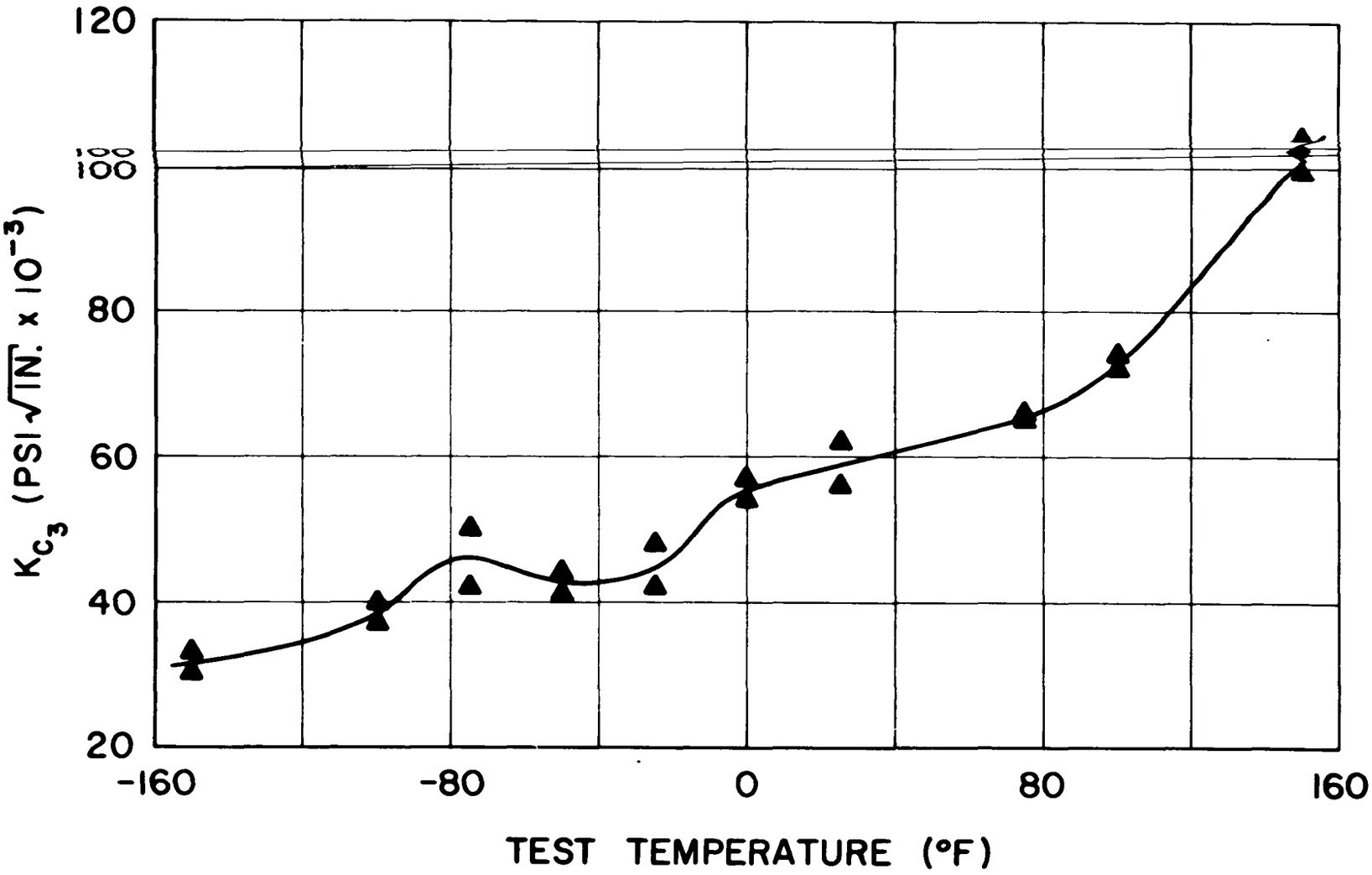

Figure 9. Critical Fracture Toughness (K_{C3}) as a Function of Test Temperature for Group 1 (X-200)

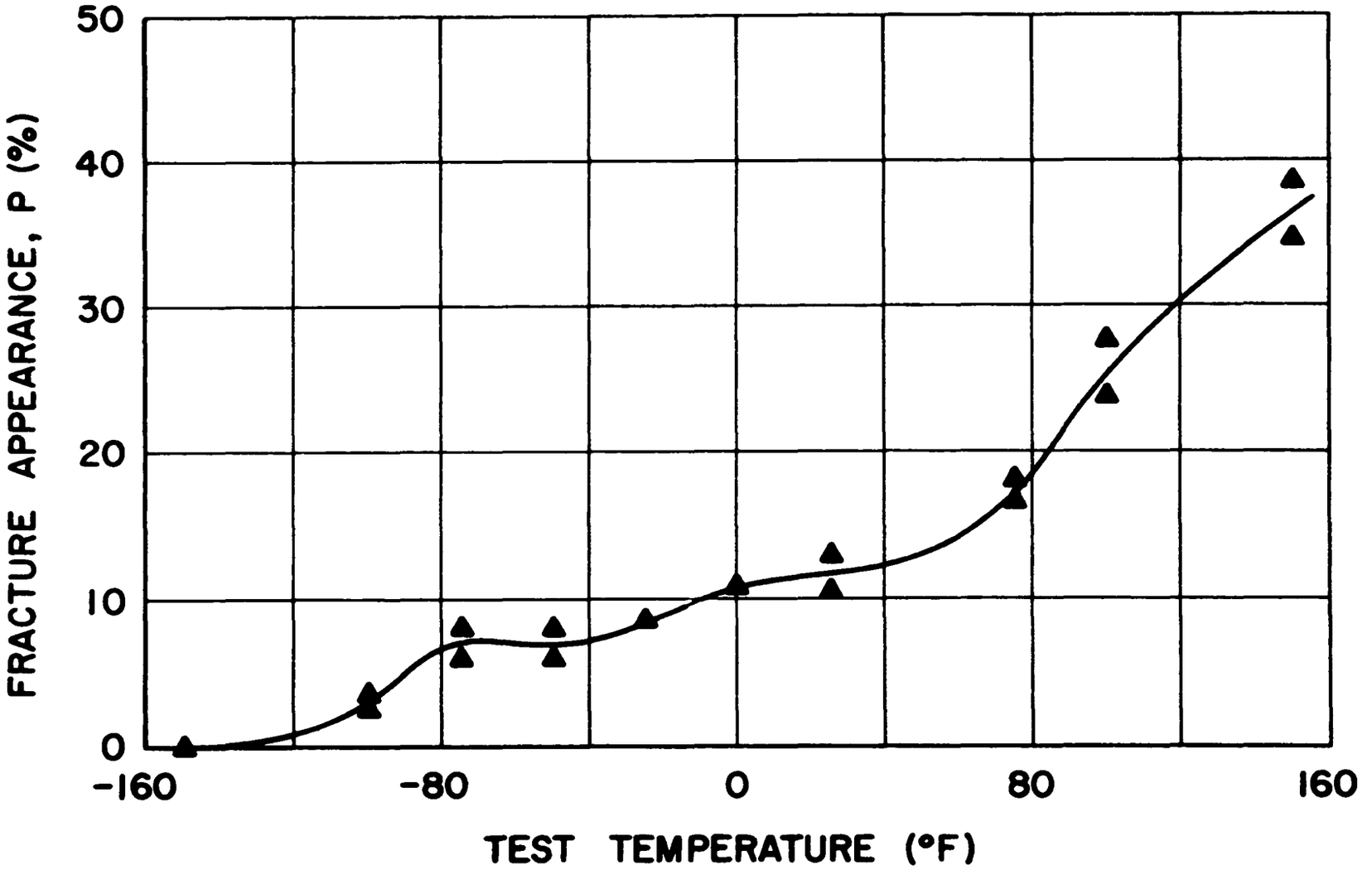

Figure 10. Fracture Appearance (P) as a Function of Test Temperature For Group 1 (X-200)

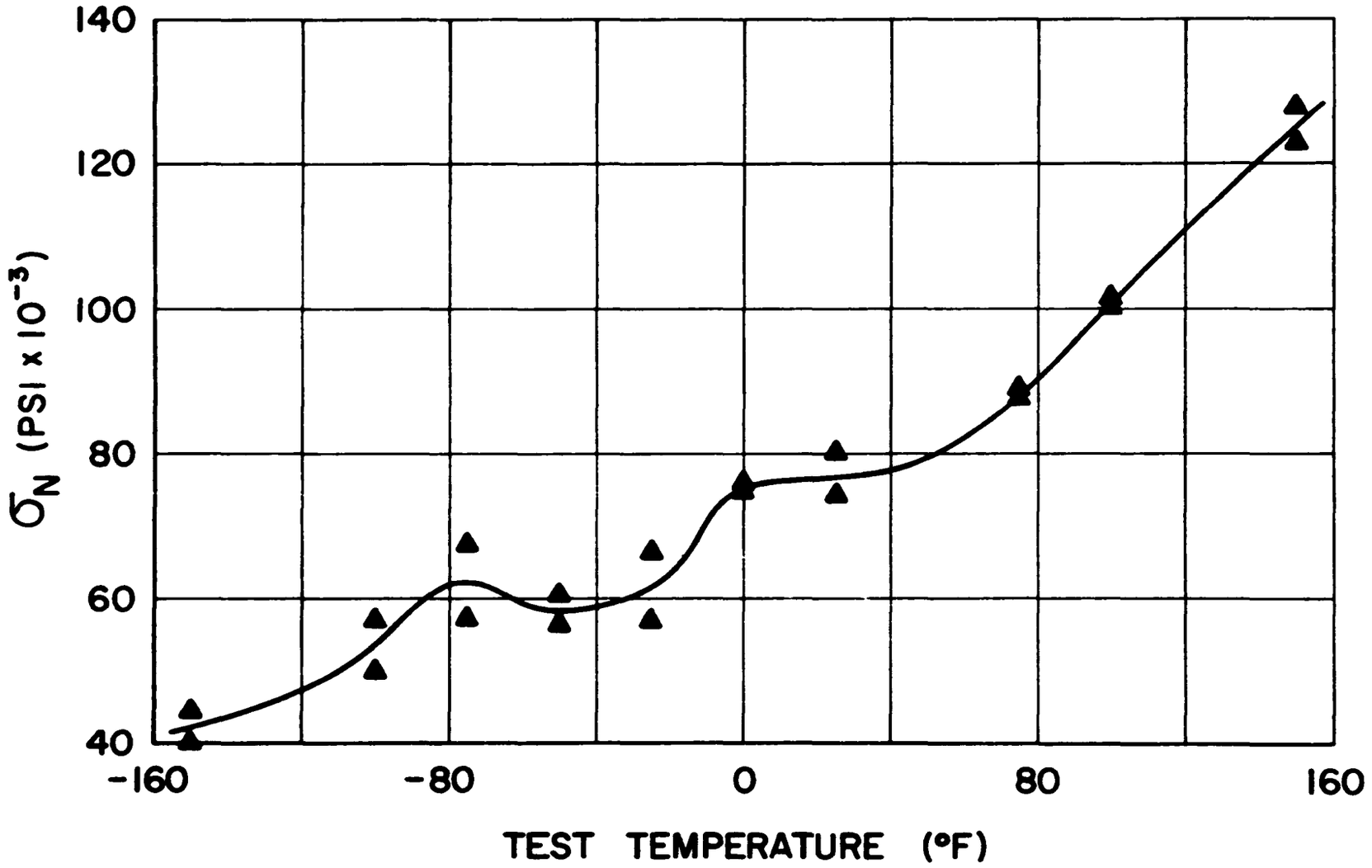

Figure 11. Net-Fracture Stress (σ_N) as a Function of Test Temperature For Group 1 (X-200)

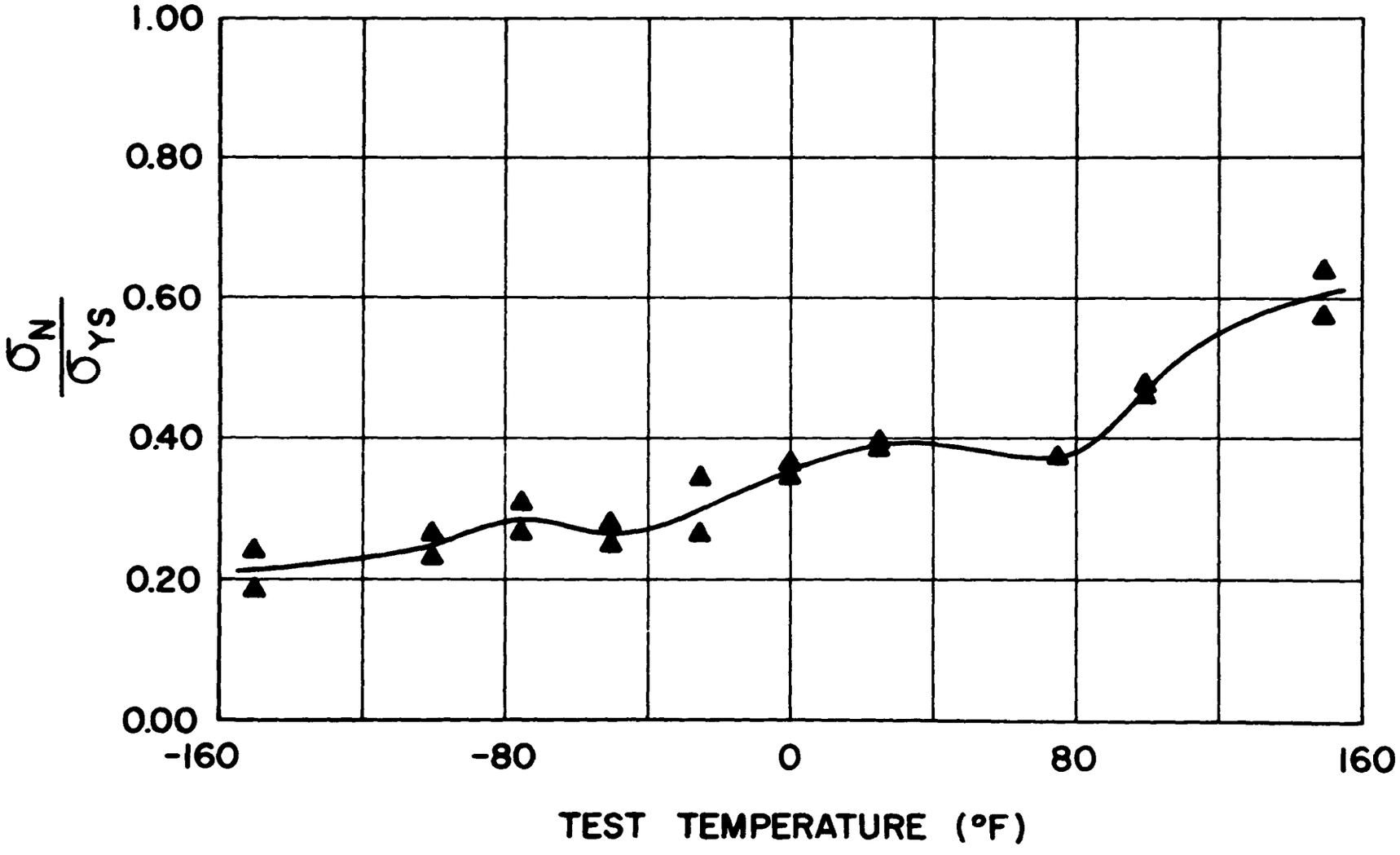

Figure 12. Ratio of Net-Fracture Stress-To-Yield-Strength (σ_N / σ_{YS}) as A Function of Test Temperature for Group 1 (X-200)

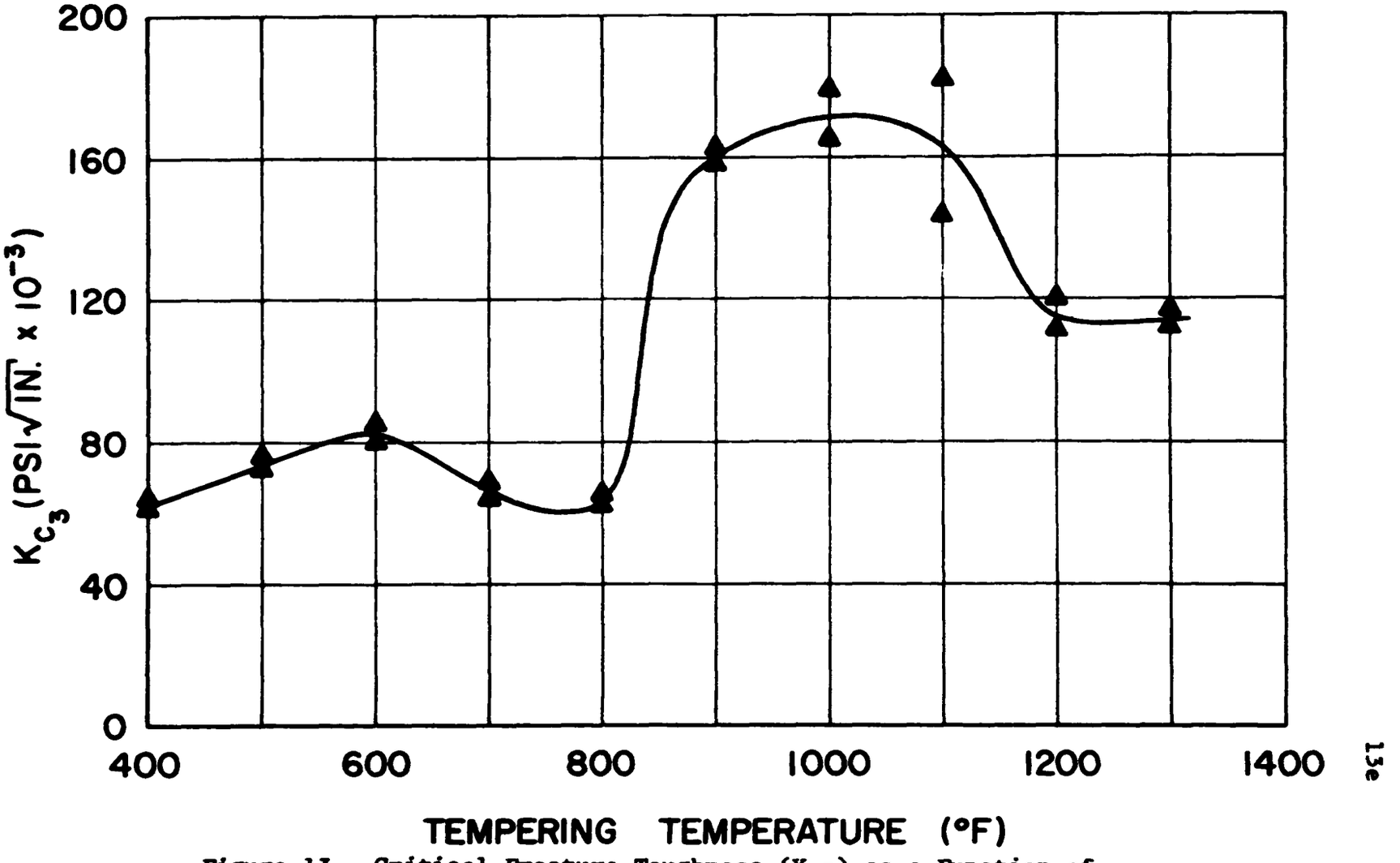

Figure 13. Critical Fracture Toughness (K_{C3}) as a Function of Tempering Temperature for Group 2 (X-200)

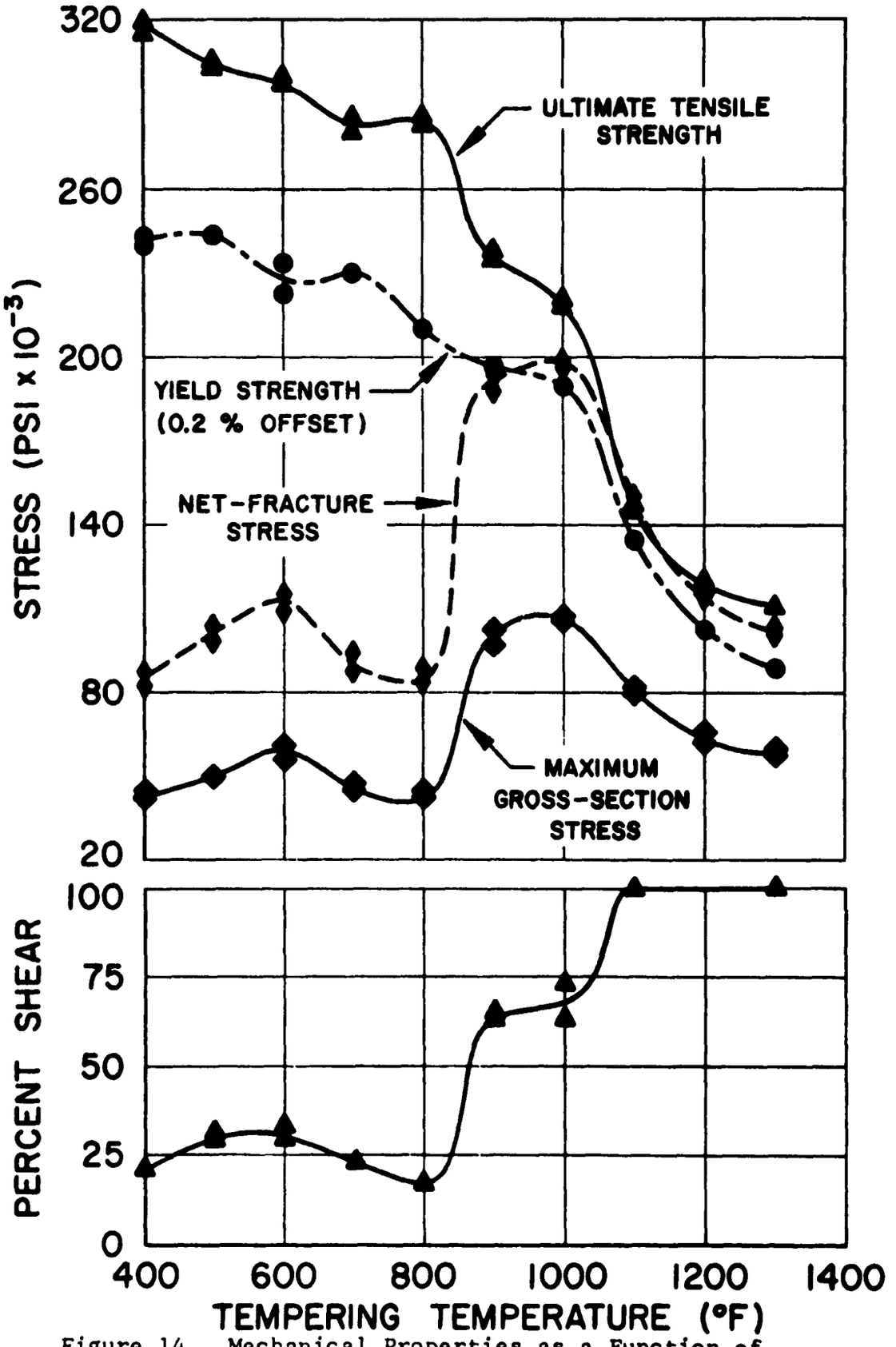

Figure 14. Mechanical Properties as a Function of Tempering Temperature for Group 2 (X-200)

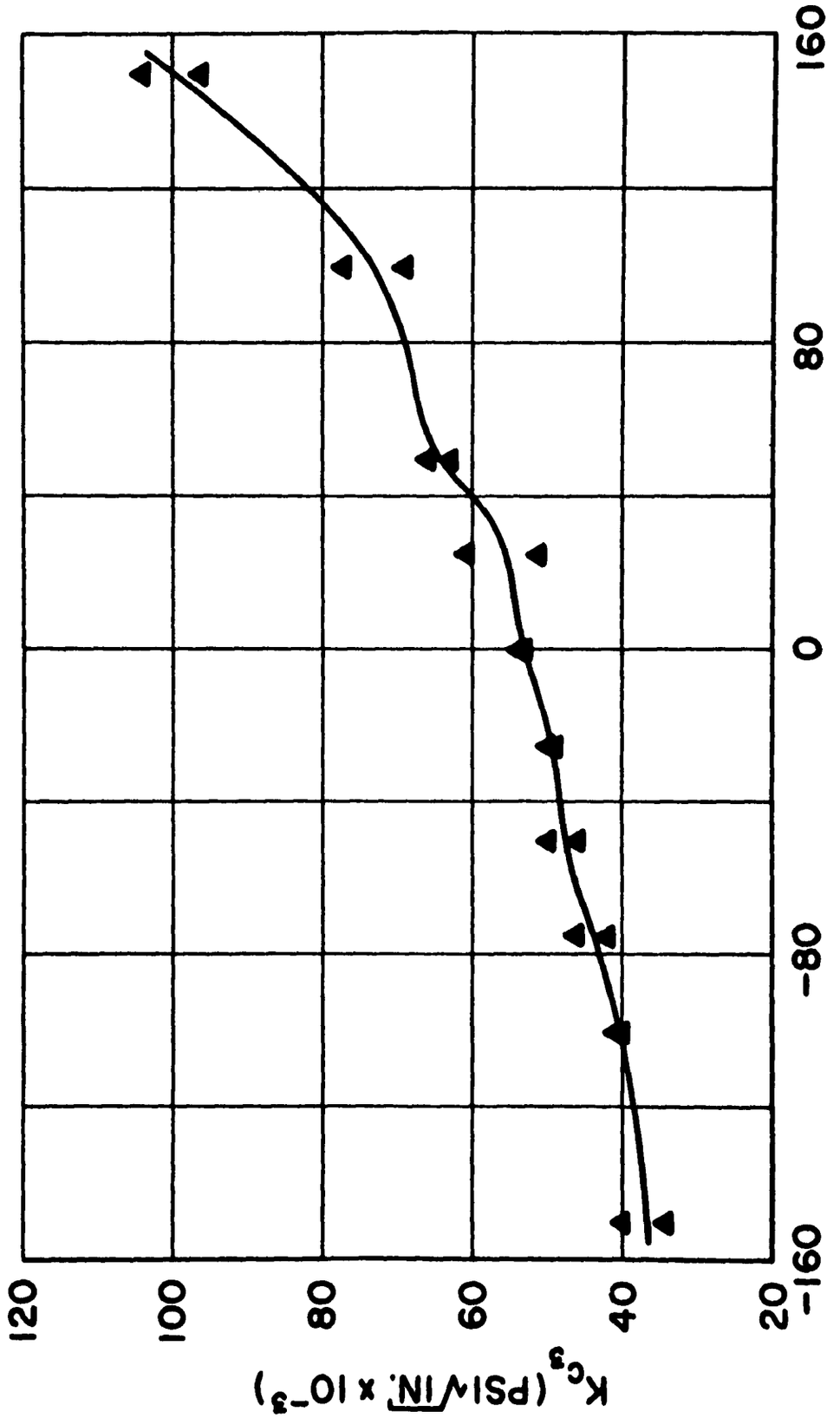

Figure 15. Critical Fracture Toughness (K_{c3}) as a Function of Test Temperature for Group 3 (X-200)

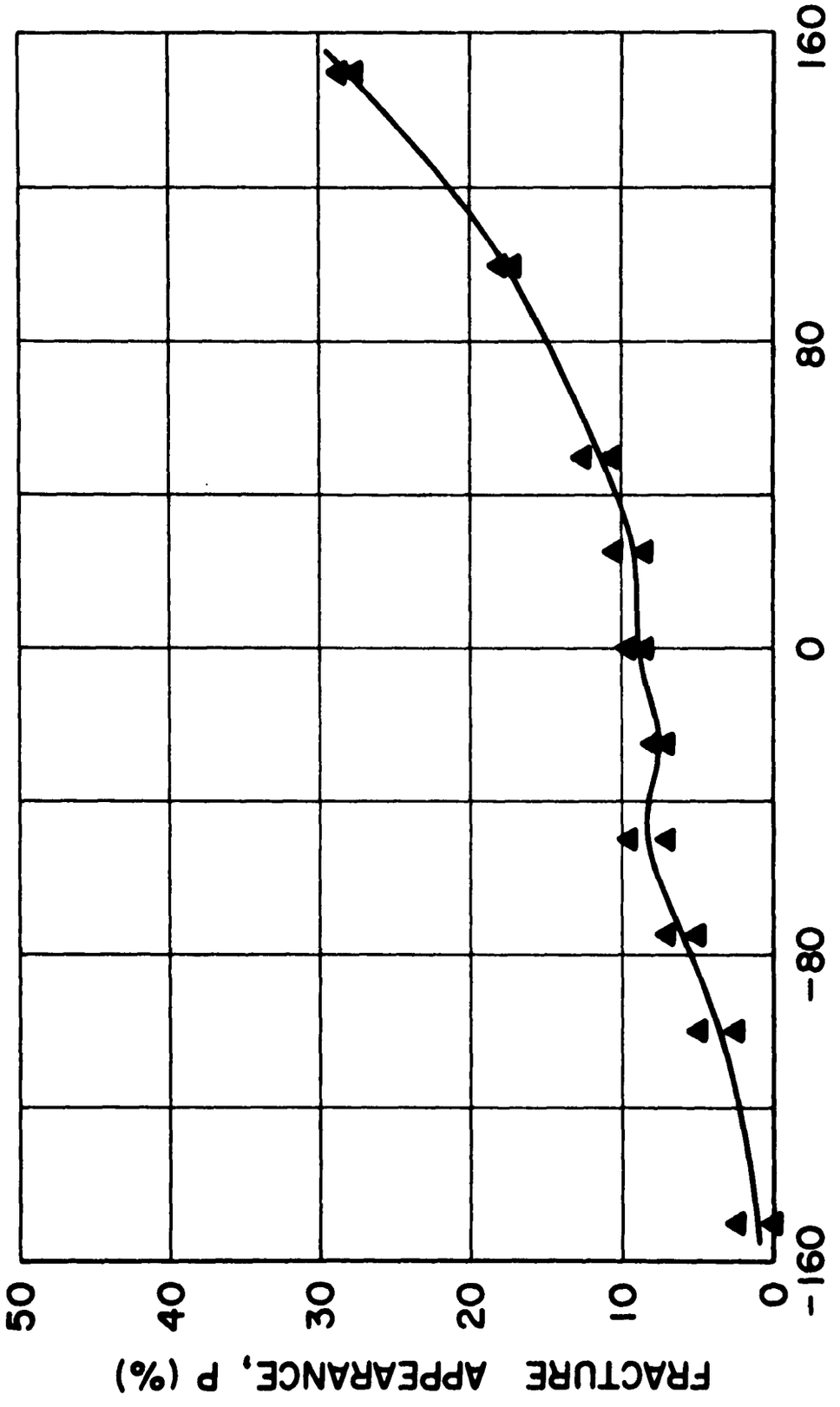

Figure 16. Fracture Appearance (P) as a Function of Test Temperature for Group 3 (X-200)

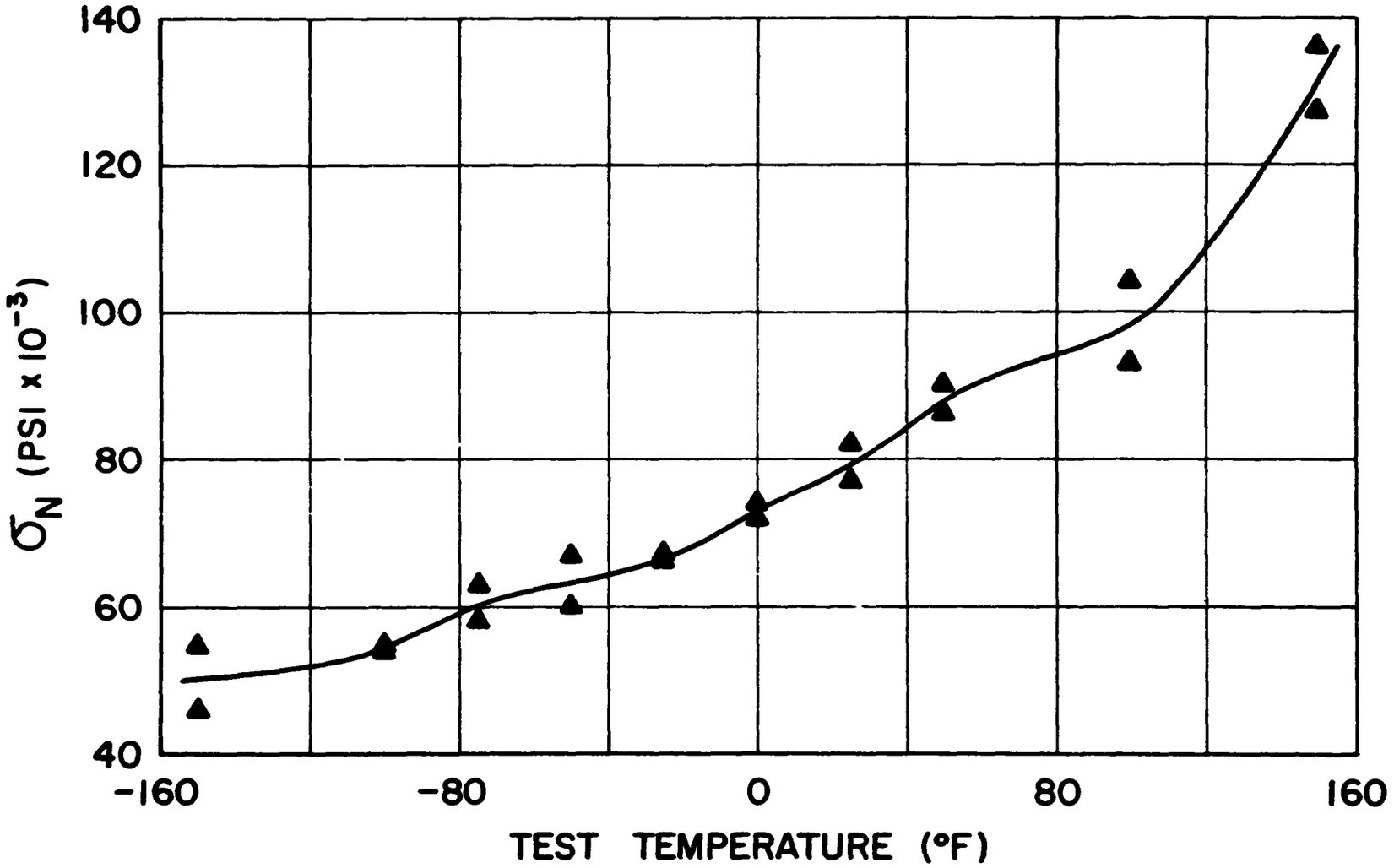

Figure 17. Net-Fracture Stress (σ_N) as a Function of Test Temperature for Group 3 (X-200)

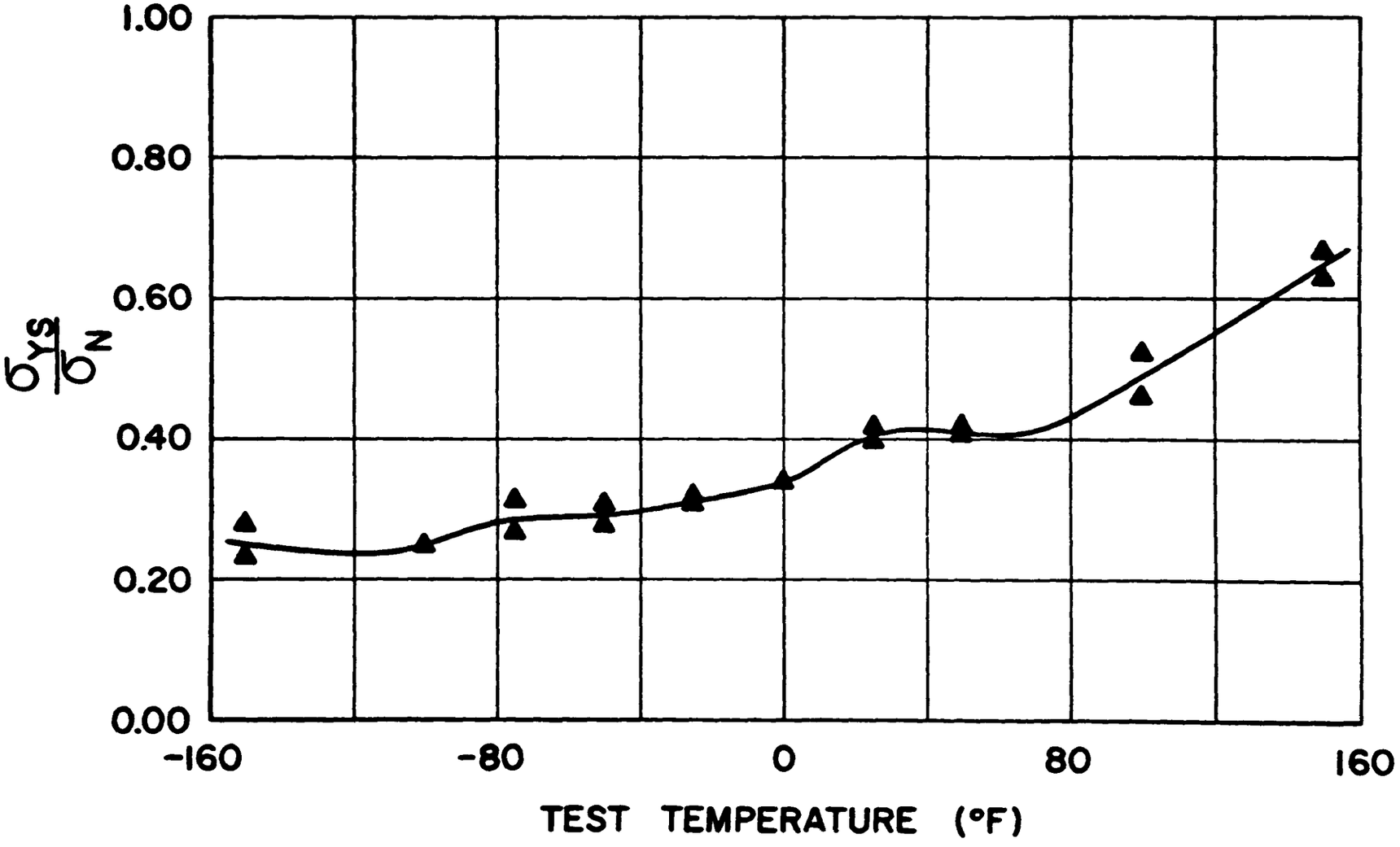

Figure 18. Ratio of Net-Fracture Stress-To-Yield Strength (σ_N/σ_{YS}) as a Function of Test Temperature For Group 3 (X-200)

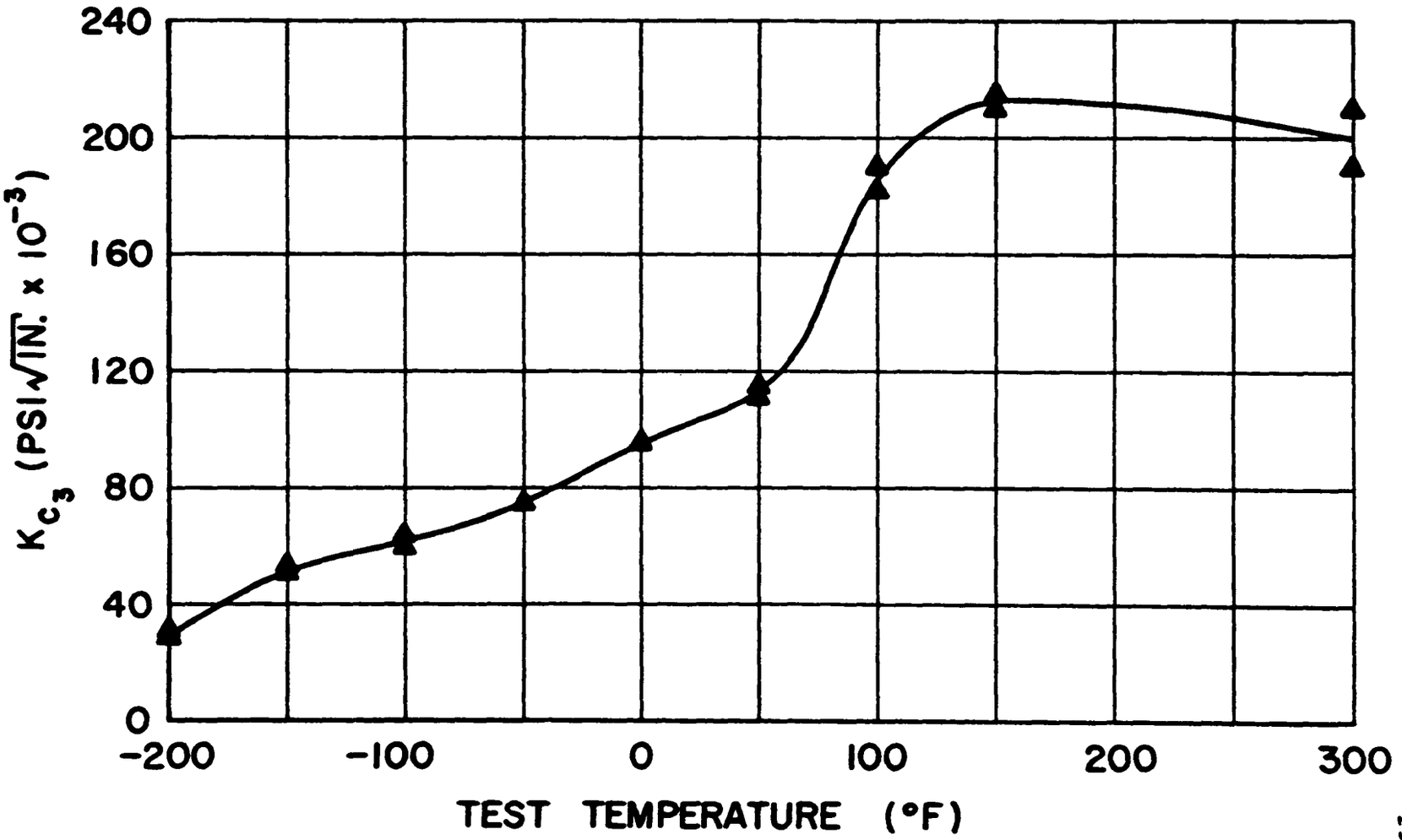

Figure 19. Critical Fracture Toughness (K_{c3}) as a Function of Test Temperature For Group 1 (H-11)

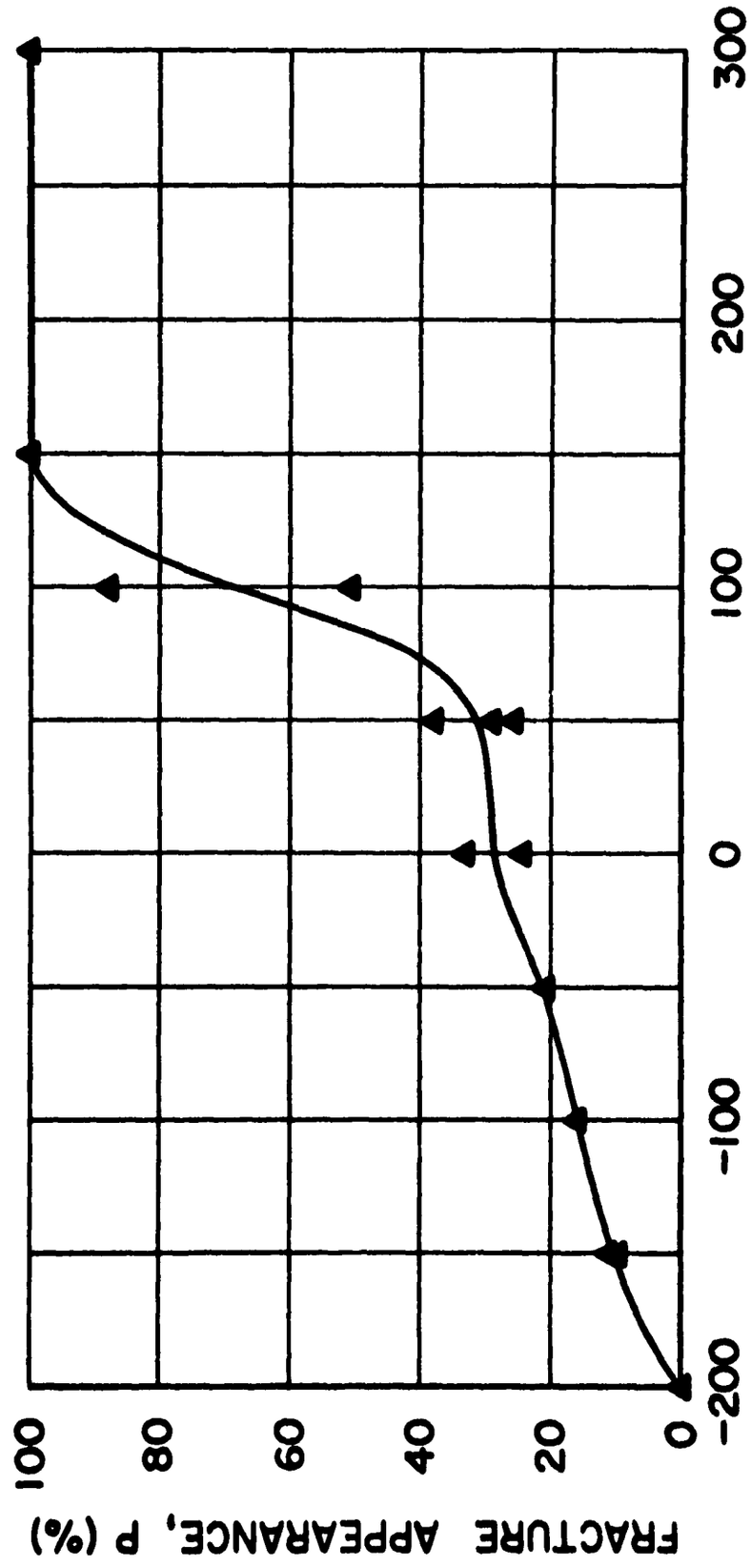

Figure 20. Fracture Appearance (P) as a Function of Test Temperature For Group 1 (H-11)

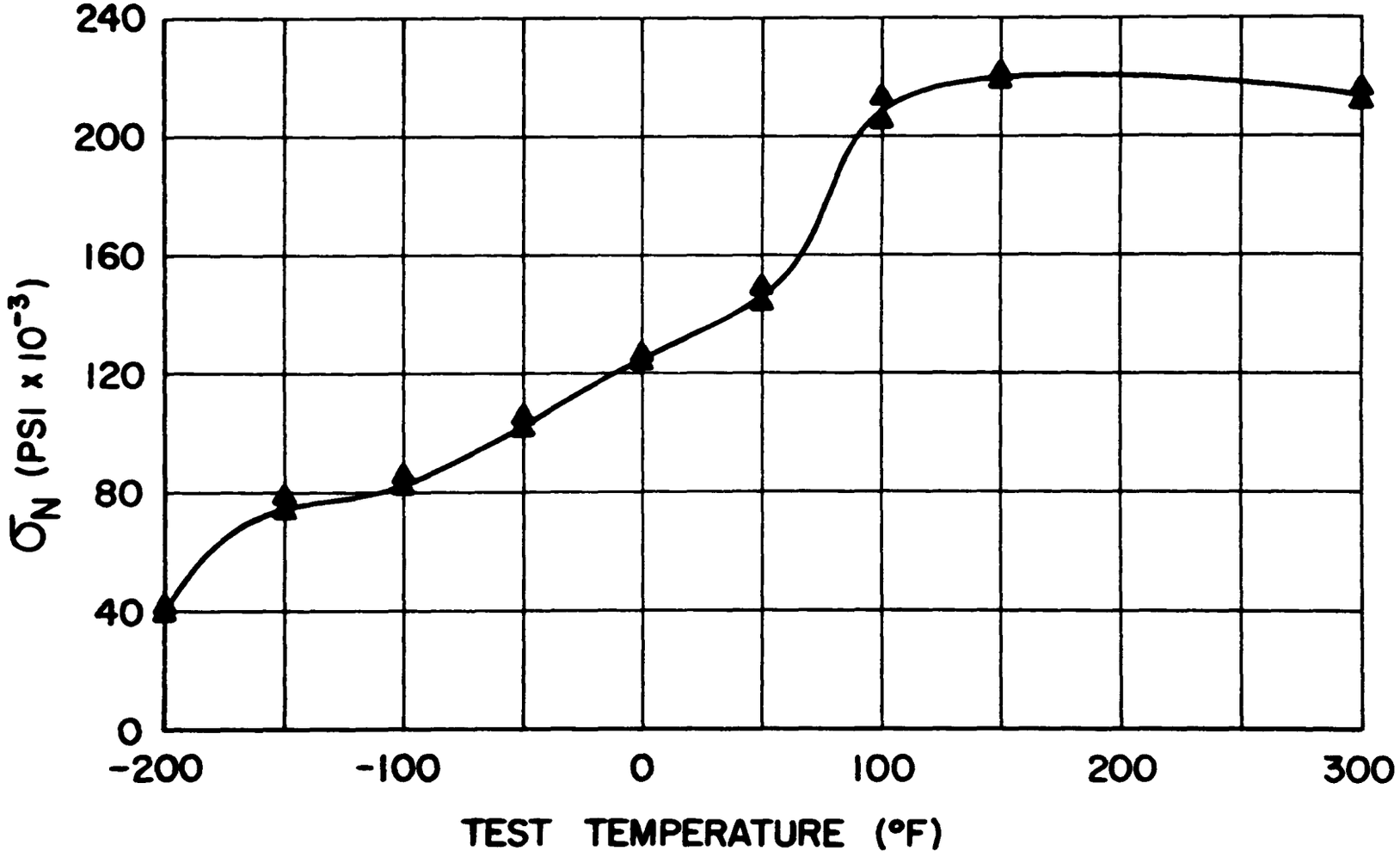

Figure 21. Net-Fracture Stress (σ_N) as a Function of Test Temperature For Group 1 (H-11)

13m

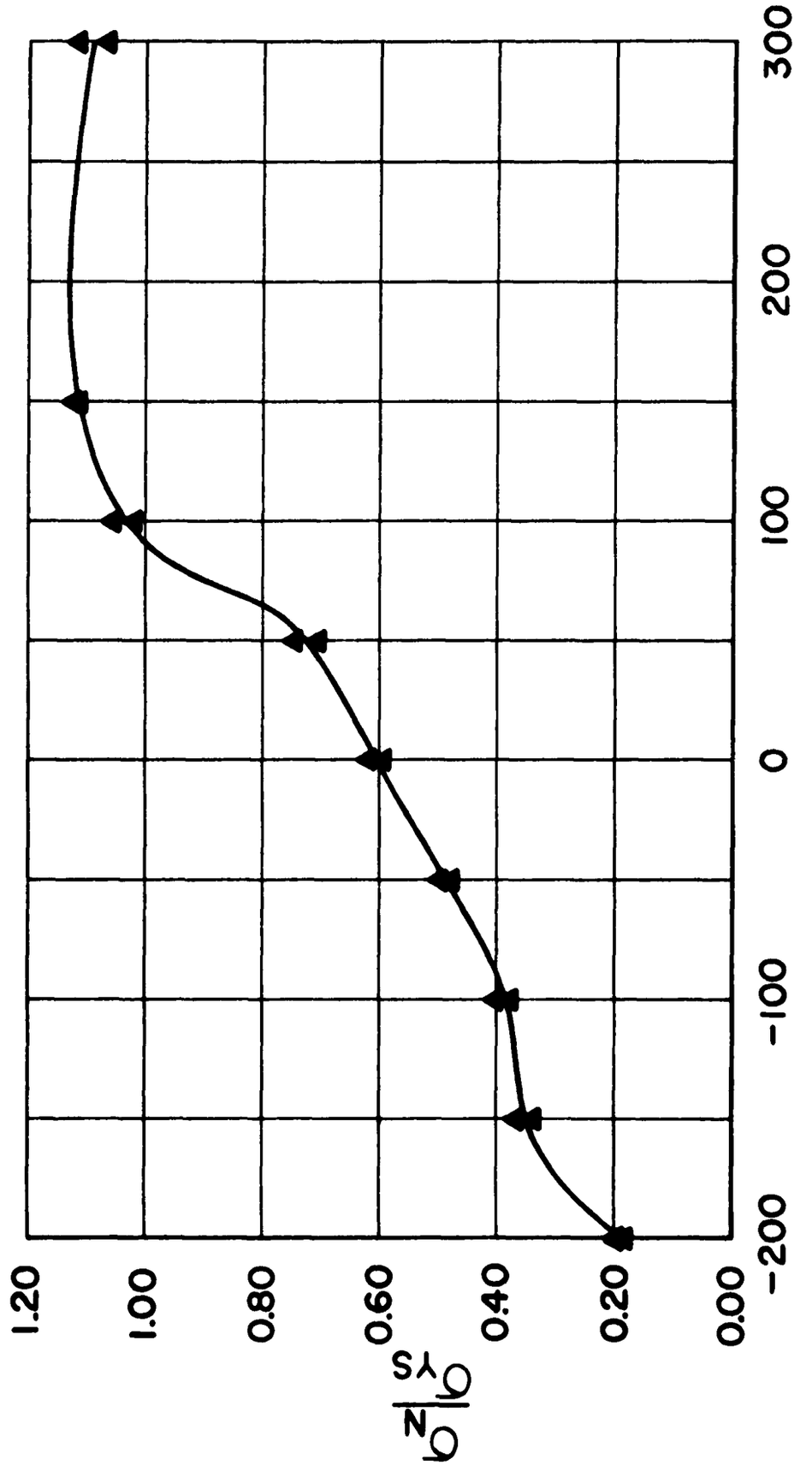

Figure 22. Ratio of Net-Fracture Stress-To-Yield Strength (σ_N / σ_{YS}) as a Function of Test Temperature For Group 1 (H-11)

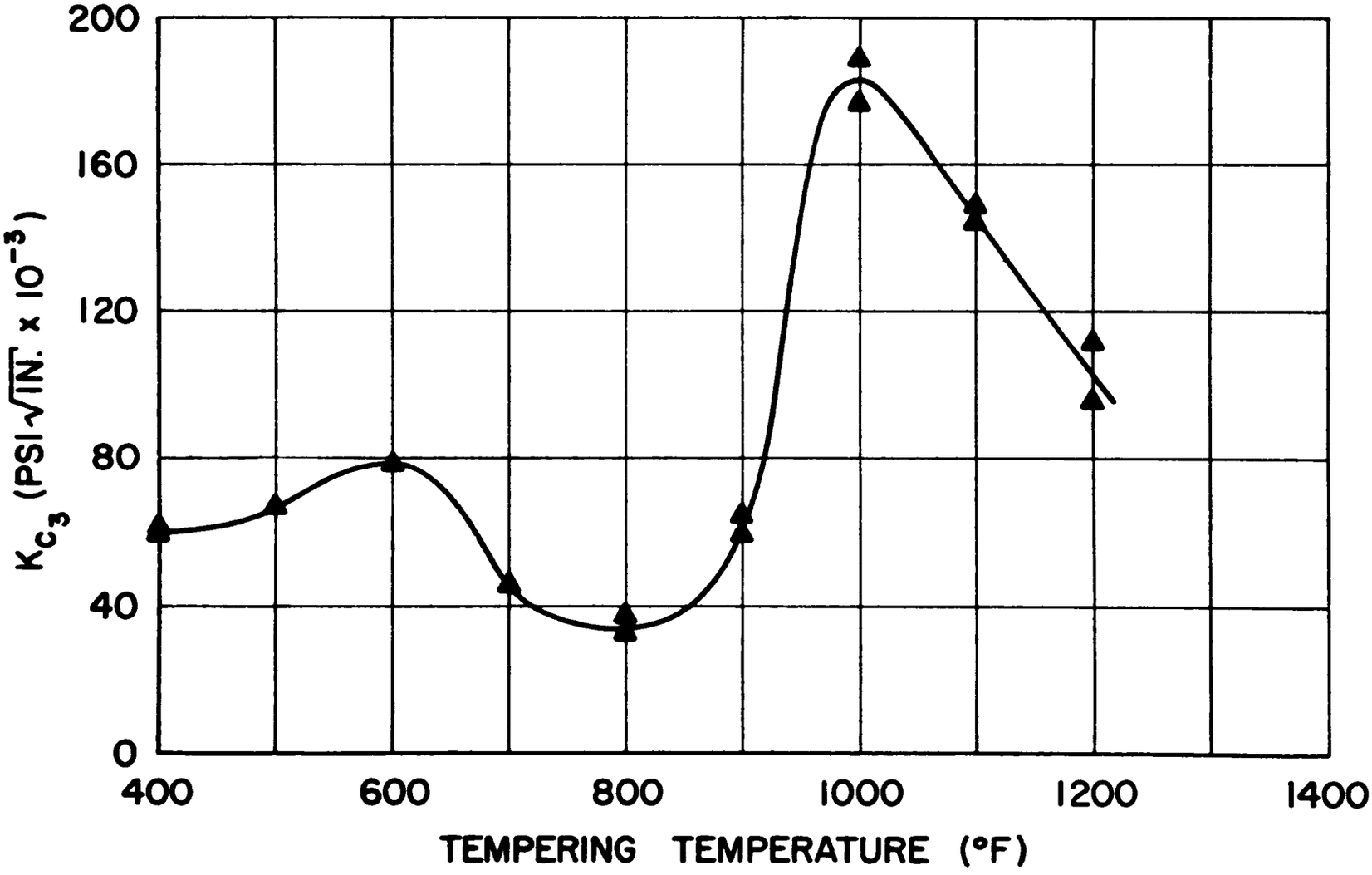

Figure 23. Critical Fracture Toughness (K_{c3}) as a Function of Tempering Temperature for Group 2 (H-11)

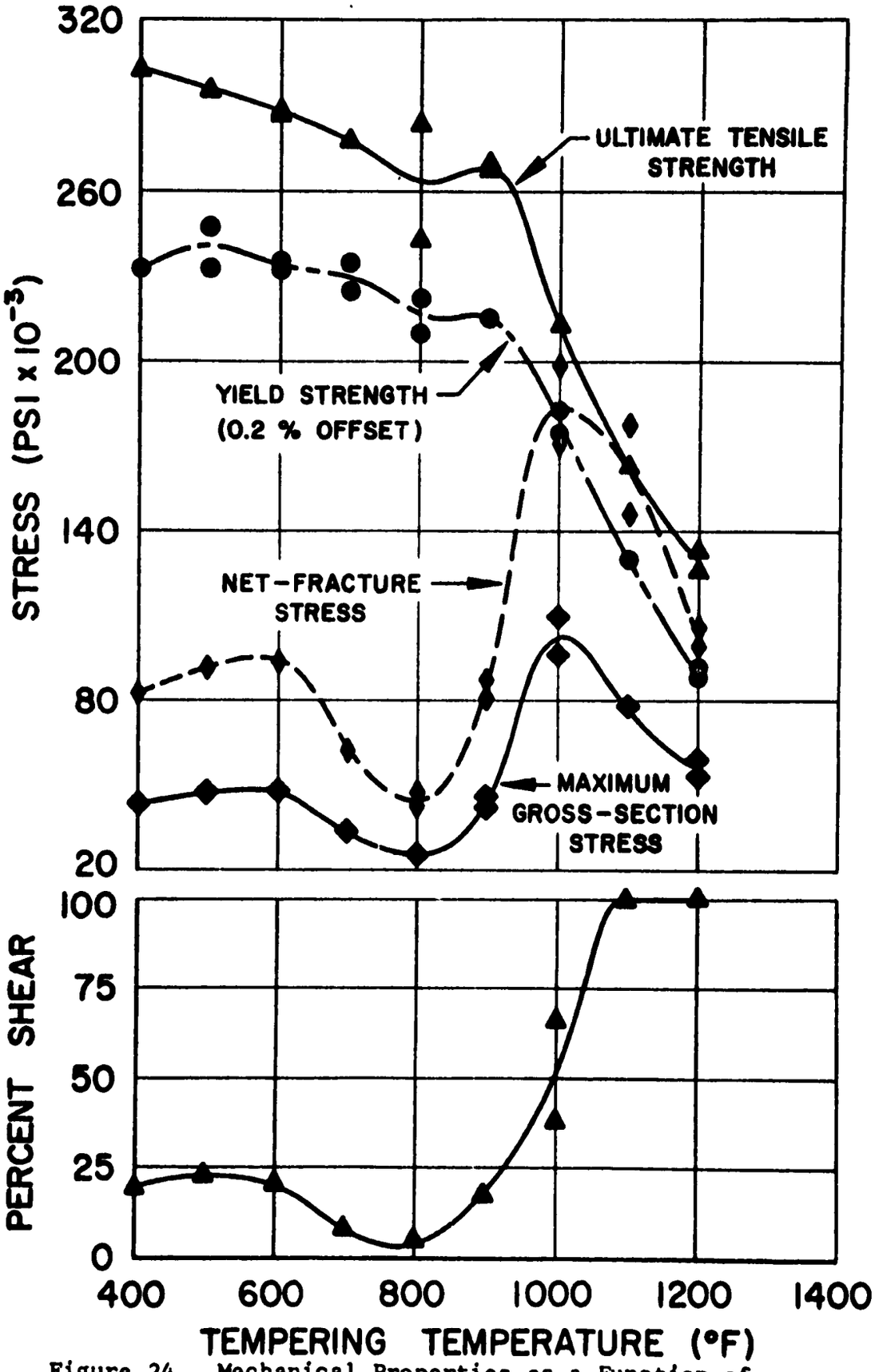

Figure 24. Mechanical Properties as a Function of Tempering Temperature for Group 2 (H-11)

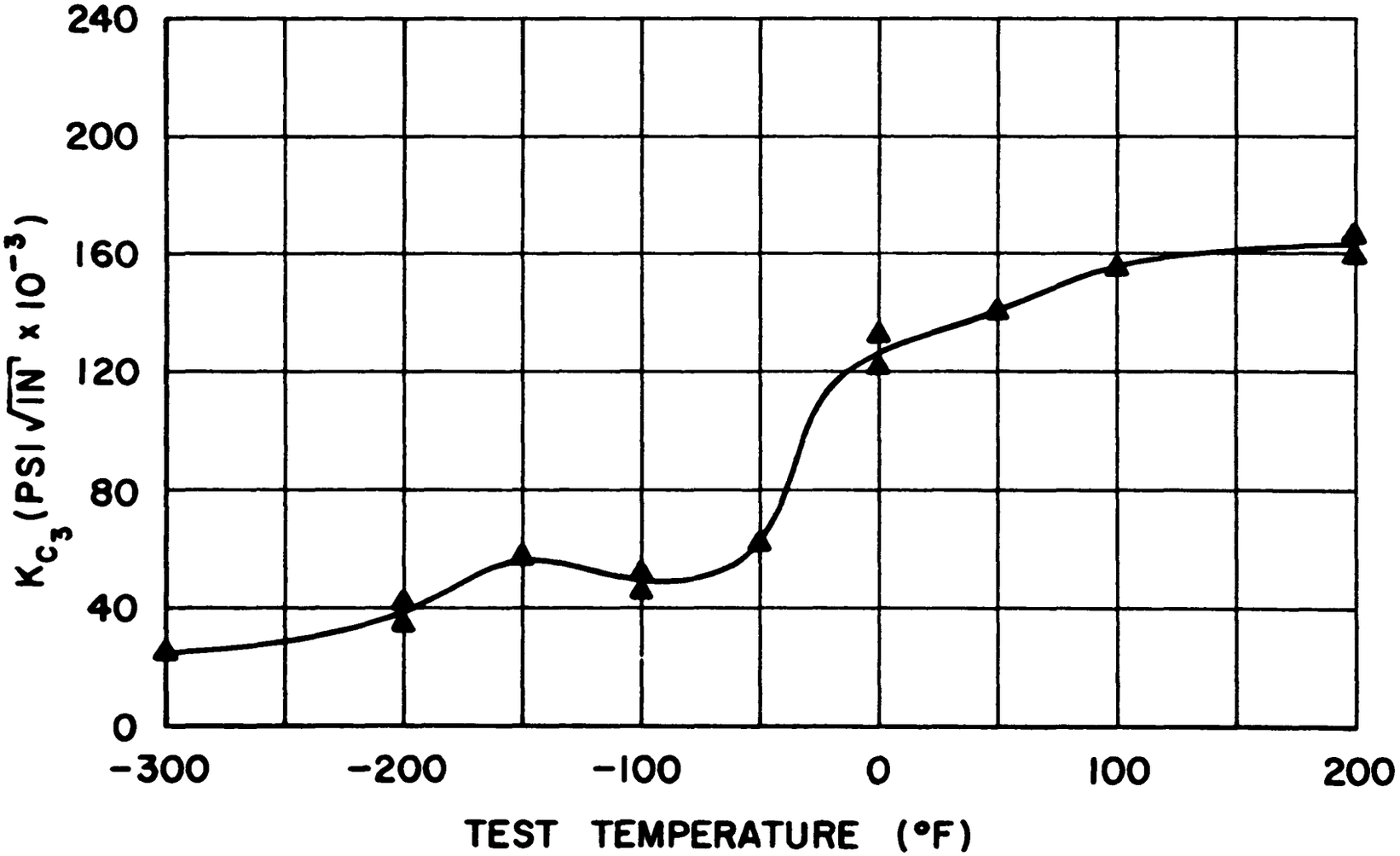

Figure 25. Critical Fracture Toughness (K_{c3}) as a Function of Test Temperature for Group 3 (H-11)

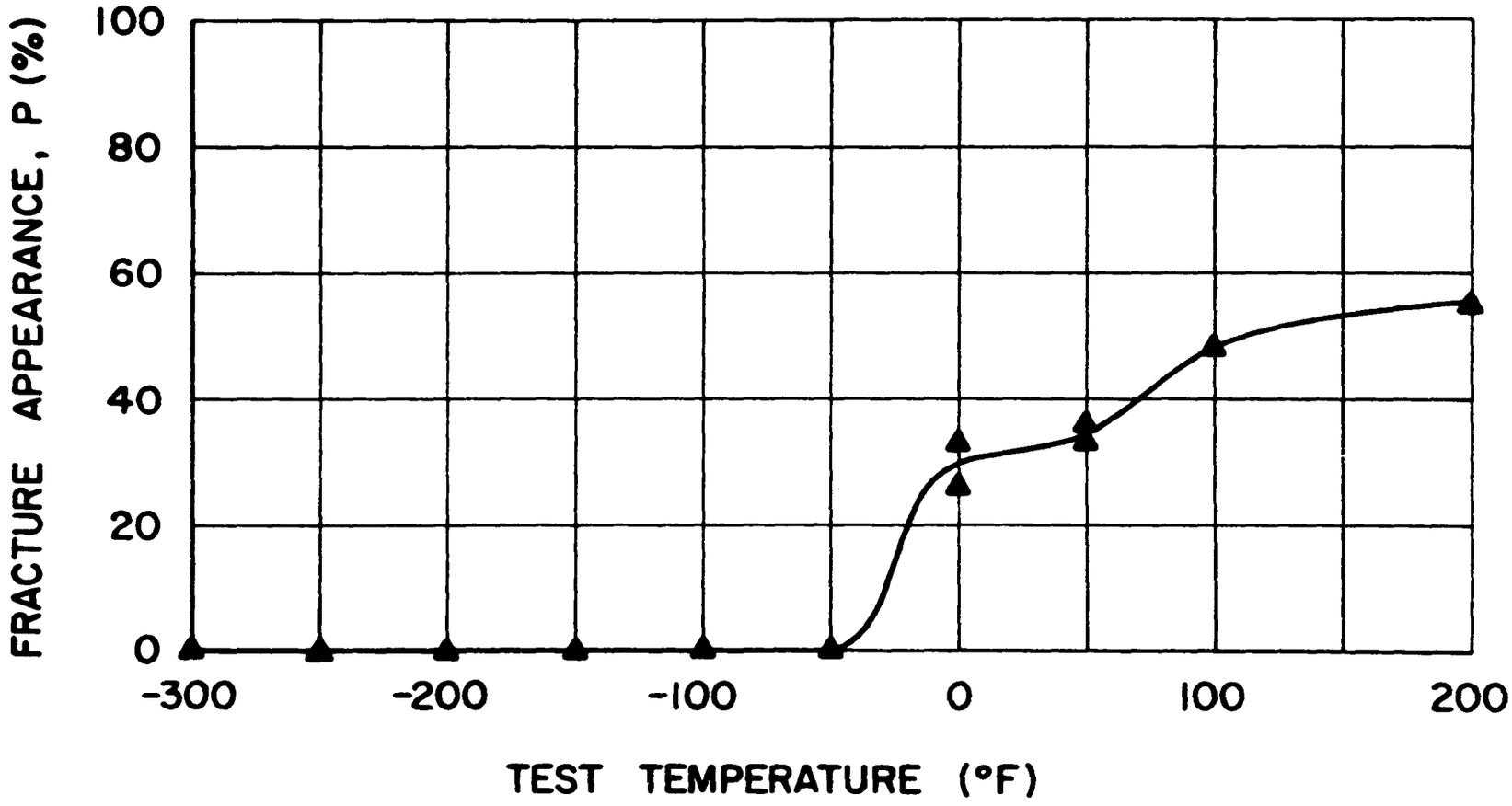

Figure 26. Fracture Appearance (P) as a Function of Test Temperature for Group (H-11)

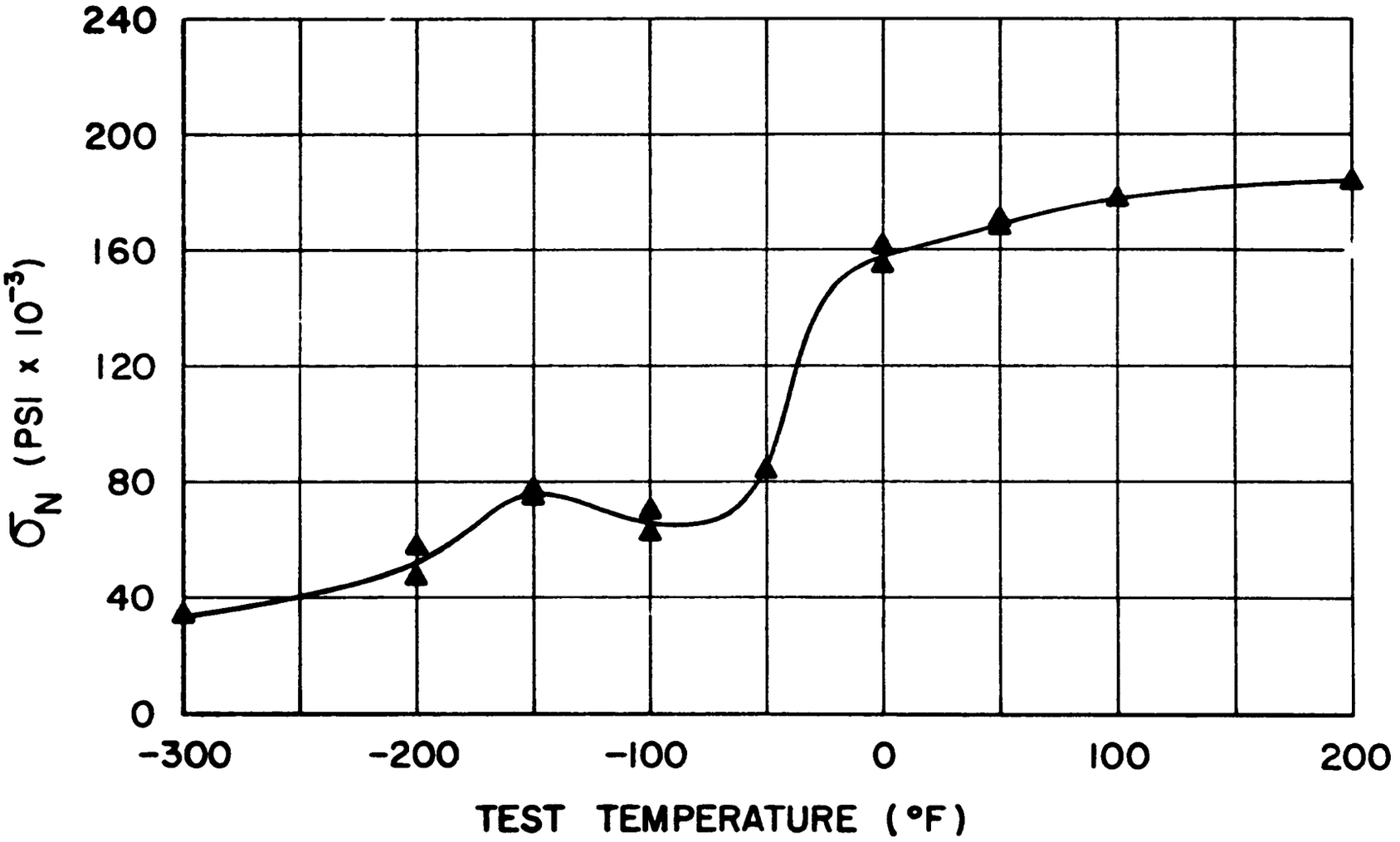

Figure 27. Net-Fracture Stress (σ_N) as a Function of Test Temperature For Group 3 (H-11)

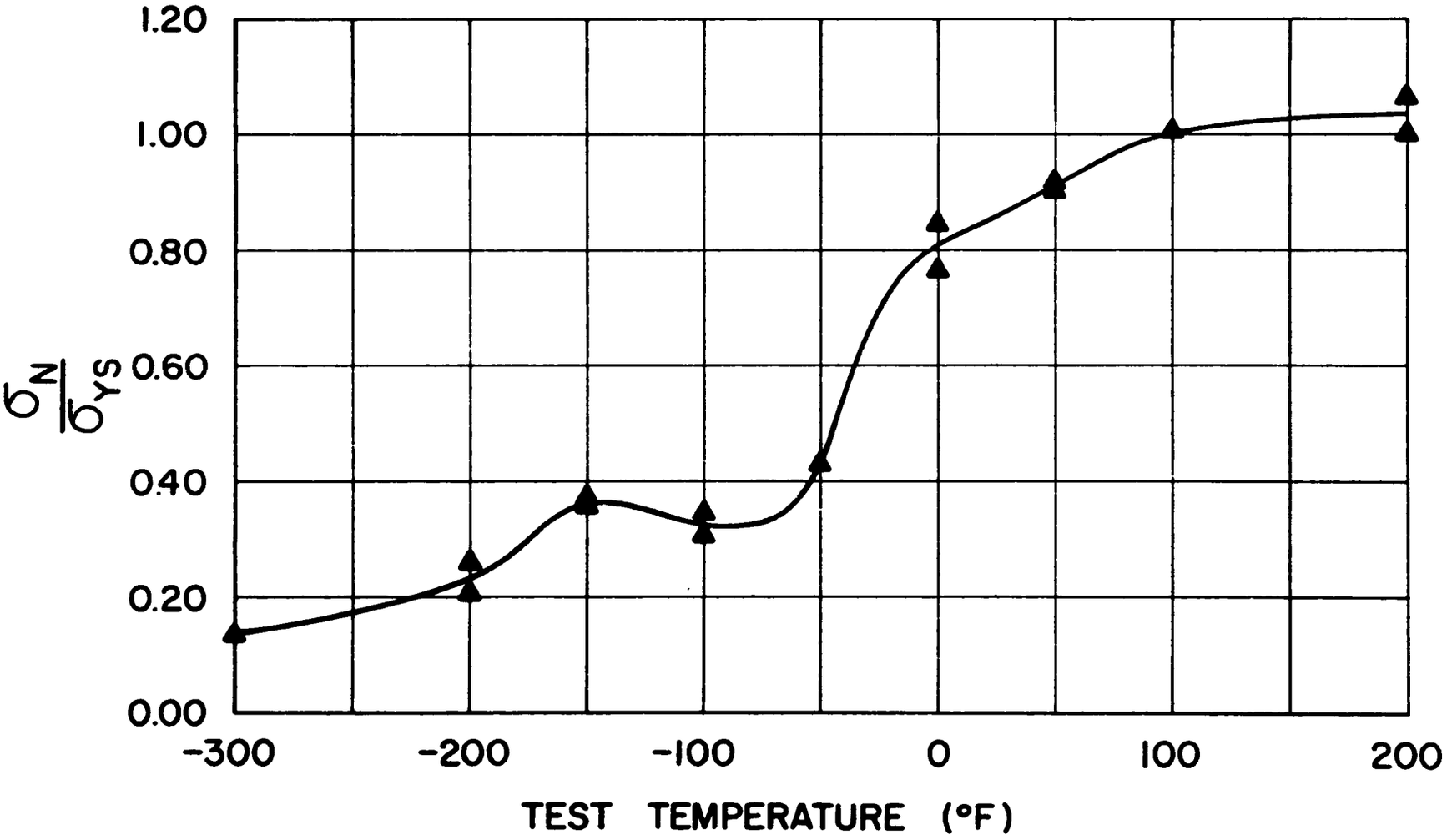

Figure 28. Ratio of Net-Fracture Stress-To-Yield Strength (σ_N / σ_{YS}) as a Function of Test Temperature for Group 3 (H-11)

A. Critical Fracture Toughness as a Function of Test Temperature.

The rather negligible difference in K_{c3} values associated with Group 1 and Group 3 specimens of X-200 (Figures 9-12 and 15-18) is believed to reflect the superimposed effects of: (a) a relatively low tempering temperature for both groups, and (b) a higher than recommended austenitizing temperature for Group 3.

If the tempering temperature had been the recommended $1000^{o}F$[4], instead of $800^{o}F$, the effect of grain coarsening probably would have been more apparent.

Group 1 (H-11) specimens, reflected a minimum K_{c3} value of 30,000 psi $\sqrt{in.}$ at $-200^{o}F$ (Figures 19-22). As the test temperature was increased, the values of K_{c3} increased exponentially to a maximum of approximately 220,000 psi $\sqrt{in.}$ Group 3, which reflects a coarser grain size than that of Group 1, has approximately the same minimum K_{c3} value; whereas, the maximum K_{c3} value for Group 3 was 164,000 psi $\sqrt{in.}$. This decrease of approximately 25% in the maximum value of K_{c3} is attributed entirely to the coarsened grain size (Figures 25-28).

B. Fracture Appearance as a Function of Test Temperature

The rather negligible difference in P values associated with Group 1 and Group 3 specimens of X-200 (Figures 9-12 and 15-18) can be explained on the basis of the two reasons, pertaining to the same steel, advanced in "A" to account for the effect of test temperature on K_{c3}.

The effect of test temperature on P, in the instance of Group 1 (H-11) specimens (Figure 20), reflected, as mentioned earlier, an FATT of 150°F. As the temperature decreased, P appeared to decrease exponentially to a minimum value of zero at -200°F.

The coarsened grain size of Group 3 (H-11) specimens was responsible for a shift in the FATT such that it exceeded the test temperature, (Figure 26). Accompanying the shift in FATT was a shift in the value P = zero to a test temperature of -50°F.

C. Net Section Stress as a Function of Test Temperature

The rather negligible difference in σ_N values associated with Group 1 and Group 3 specimens of X-200 (Figures 9-12 and 15-18) can be explained on the basis of the two reasons, pertaining to the same steel, advanced in "A".

The distinction between σ_N values associated with Group 1 and Group 3 specimens of H-11 (Figures 19-22 and 25-28) exists because of the two reasons, pertaining to the same steel, advanced in "A".

D. The Ratio of σ_N / σ_{YS} values associated with Groups 1 and 3 (X-200) specimens is, on the same basis as that employed earlier, accounted for by considering the combined effects of tempering and austenitizing temperatures (Figures 12 and 18). The somewhat more pronounced difference in σ_N / σ_{YS} values associated with Group 1 and Group 3 (H-11) specimens is attributed solely

to the deleterious effect of grain size on fracture toughness. In support of this statement, it is apparent from Figures 22 and 28, and 13 and 19 that the magnitude of σ_N / σ_{YS} for H-11 specimens is appreciably larger than σ_N / σ_{YS} for X-200 specimens over the entire range of test temperatures common to both. At the test temperature of 150°F the value of this ratio is 1.04-1.12 for H-11 specimens, but only 0.60-0.65 for X-200 specimens.

Critical Fracture Toughness as a Function of Tempering Temperature

The relationship between K_{c3} and tempering temperature for Group 2 (X-200 and H-11) specimens is shown in Figures 13 and 23. The curves are quite similar and exhibit the following features: (a) relief of residual stresses, accompanied by an increase in K_{c3}, from 400 - 600°F, (b) possibly, precipitation of carbides coherently aligned with the martensitic matrix, or transformation of a residual quantity of retained austenite, accompanied by, in either event, a decrease in the value of K_{c3}. In the instance of X-200 specimens, K_{c3} decreased to the initial minimum value observed for the 400°F tempering temperature while K_{c3} for H-11 specimens decreased to a value almost one-half that observed for the same tempering temperature. These changes occurred over the range 600 - 800°F. (c) The increase in extent of carbide precipitation and ferrite formation may account for the marked increase in the values of

K_c from 800 - 1000°F. (d) Agglomeration of carbides and increase in mean-free ferrite path probably accounts for the precipitous decrease in K_{c3} from 1000 - 1200°F.

CONCLUSIONS

1. The effect of tempering temperature on K_{c3} was, in the instance of X-200 steel, essentially constant from 400 to 800°F, inclusive. However, from 900 to 1300°F, inclusive, the average K_{c3} value was observed to increase by more than a factor of two. The value of P=100 per cent (FATT = T_r) corresponded to a strength level commensurate with 1100°F tempering temperature. The effect of tempering temperature on K_{c3} was, in the instance of H-11 steel essentially constant from 400 to 900°F, inclusive. However, from 1000 to 1200°F, inclusive, the average K_{c3} value was observed to increase by more than a factor of two. Anomolously, the value of P = 100 per cent also corresponded to a strength level commensurate with a 1100°F tempering temperature. The increase in K_{c3} values for both X-200 and H-11 steels, is attributed to the increase in σ_N / σ_{YS} from $\sigma_N / \sigma_{YS} < 1.0$ to $\sigma_N / \sigma_{YS} \geq 1.0$.
2. On the basis of strength level, commensurate with the tempering temperatures employed, H-11 steel was notch ductile; whereas, X-200 steel was somewhat less than notch ductile.
3. Increasing ferrite grain size was shown to have an adverse effect on the parameter K_{c3} and quantities such as P, σ_N, and σ_N / σ_{YS}. As ferrite grain size increases, FATT is displaced in the direction of higher temperatures.

TERMINOLOGY

a : Slow crack length (in.)

a_o : Initial crack length from center line (in.)

a_s : Initial saw cut from center line (in.)

W : Specimen width (in.)

B : Specimen thickness (in.)

σ_{YS} : Yield strength (psi)

σ_N : Net fracture stress at onset of unstable crack propagation (psi)

σ_M : Maximum gross section stress at onset of unstable crack propagation (psi)

P_M : Maximum tensile load at onset of unstable crack propagation (lb)

P : Per cent shear

K_c : Critical fracture toughness parameter (psi in.)

K_{c3} : Critical fracture toughness parameter associated with the fracture-appearance method (psi in.)

q_{c3} : Critical stress distribution factor associated with fracture-appearance method (dimensionless)

T_r : Room temperature (^oF)

FATT : Fracture appearance transition temperature, that is, the lowest temperature at which the mode of fracture is 100 per cent shear (^oF)

REFERENCES

1. H. W. Maynor, R. E. Mueller, and E. O. Jones, Jr., "The Effect of Specimen Geometry on Critical Fracture Toughness of High-Strength Sheet Steels", submitted to ASTM,

2. "Fracture Testing of High-Strength Sheet Materials: A Report of a Special ASTM Committee, ASTM Bulletin, Number 244, February, 1960.

3. G. K. Manning, "How Should You Evaluate High-Strength Materials?", Metal Progress, Vol. 80, No. 3, September 1961.

4. R. J. Fiorentino, D. B. Roach, and A. M. Hall, "Heat Treatment of High-Strength Steels for Air Frame Applications", DMIC Report 119, p. 41, November 27, 1959.

5. J. H. Gross and R. D. Stout, "The Effect of Microstructure on Notch Toughness - Part III", Welding Research, Vol. XXI, No. 2, February, 1956.

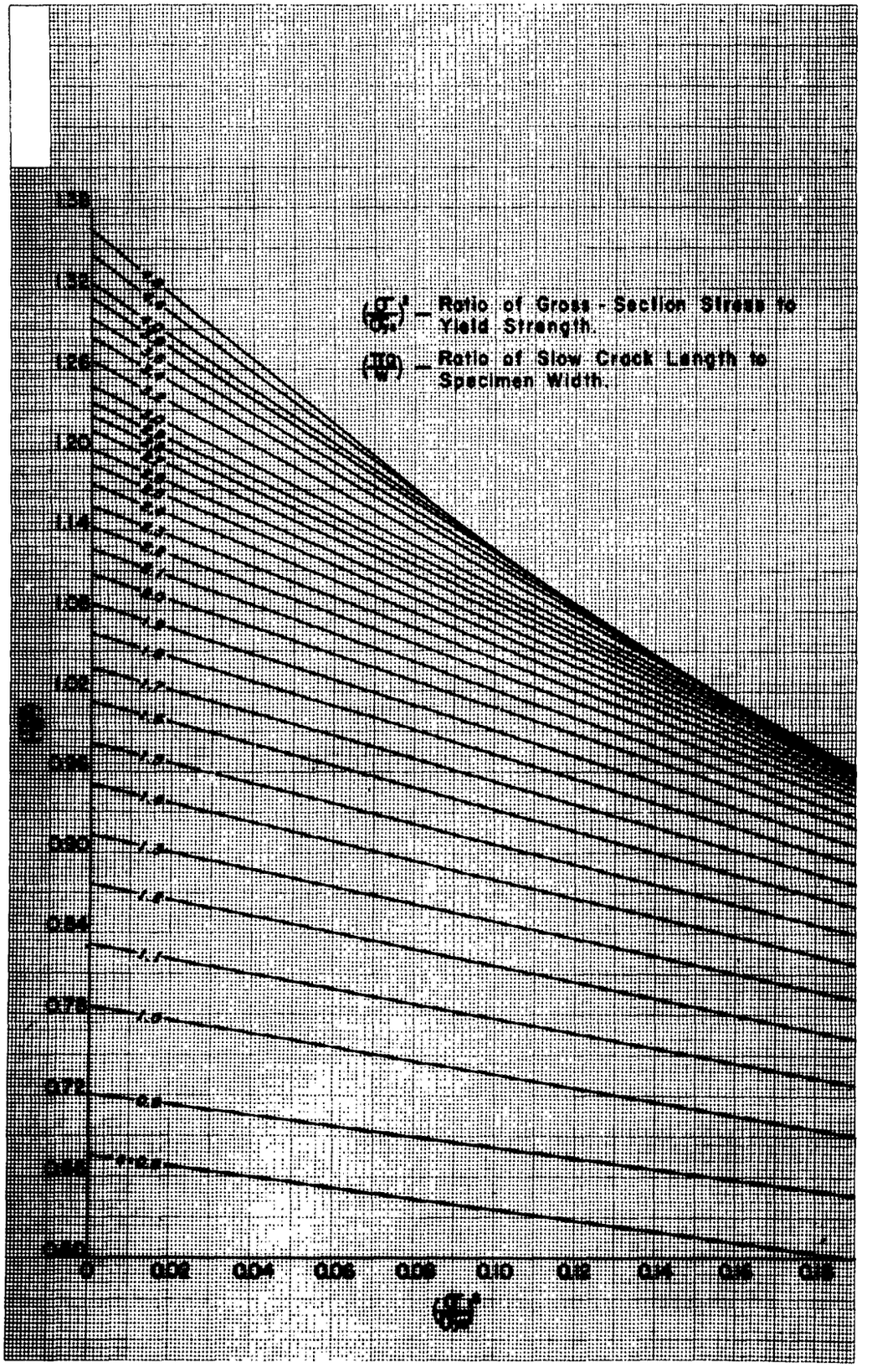

Critical Stress Distribution Factor Curve (q_{c1}

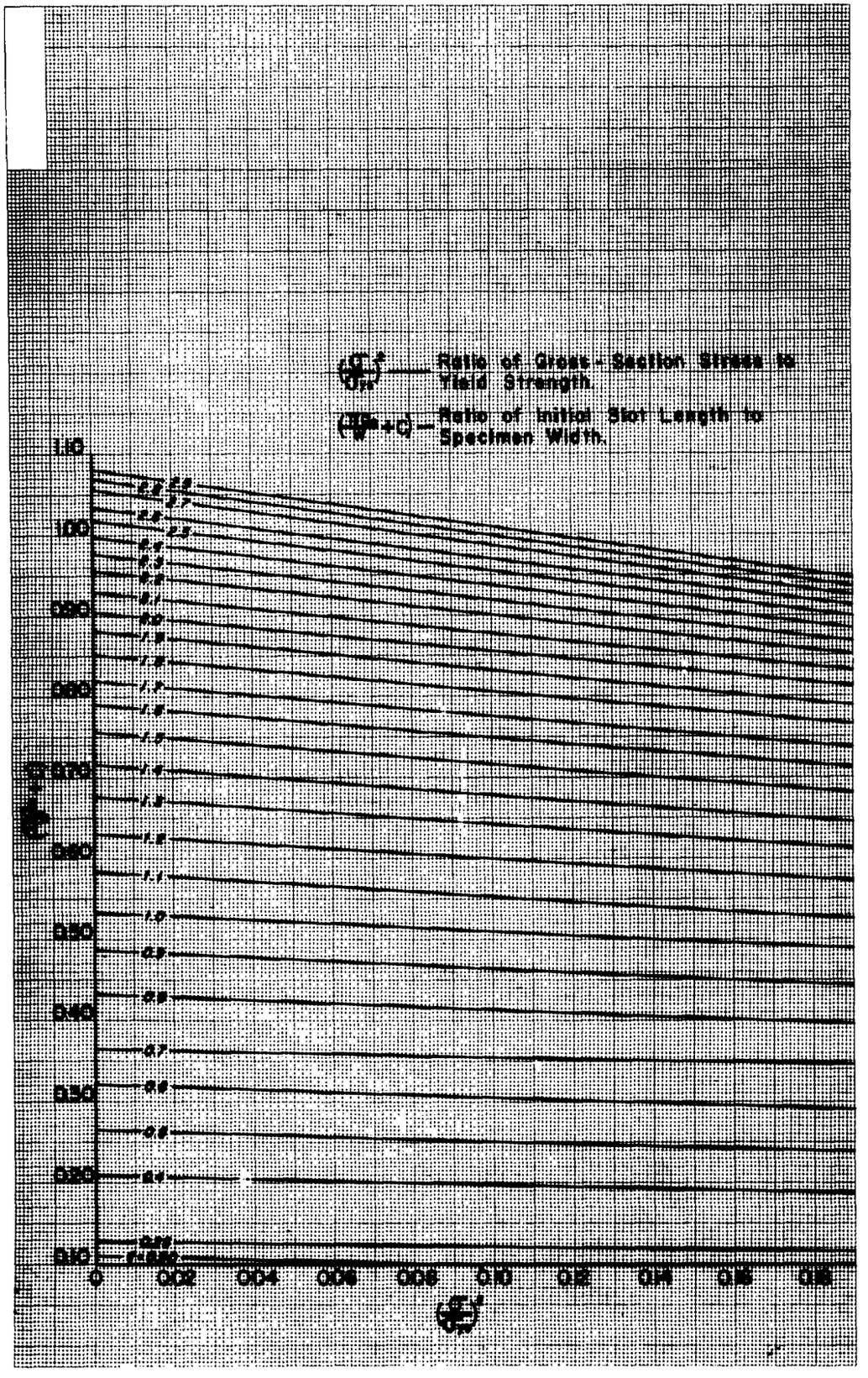

Critical Stress Distribution Factor Curve (q_{c3})

TABLE 1
FATIGUE CRACKING DATA

Specimen Width (in.)	Crack-to-width ratio	Specimen Number *	$2a_s$ (in.)	Fatigue Loads Max. Load (lb)	Min. Load (lb)	Cycles	$2a_o$ (in.)
** 1.00	0.1W	81	0.095	2900	900	51,800	- -
1.00	0.2W	80	0.170	2500	800	48,100	0.175
1.00	0.2W	82	0.177	2500	800	58,500	0.208
1.00	0.3W	71	0.219	2300	700	92,500	0.290
1.00	0.3W	72	0.216	2300	700	85,800	0.330
1.00	0.4W	73	0.204	2300	700	104,100	0.445
1.00	0.4W	76	0.279	2200	800	110,600	0.450
1.00	0.5W	77	0.267	2300	800	107,300	0.575
1.00	0.5W	78	0.270	2300	800	88,500	0.505
**1.50	0.1W	60	0.129	4400	1400	30,000	- -
1.50	0.2W	61	0.276	3900	1200	33,000	0.374
1.50	0.2W	62	0.297	3900	1200	17,600	0.328
1.50	0.3W	63	0.346	3700	1200	38,300	0.481
1.50	0.3W	64	0.346	3700	1200	38,100	0.471
1.50	0.4W	65	0.350	3700	1200	58,500	0.694
1.50	0.4W	66	0.345	3700	1200	58,500	0.641
**1.50	0.5W	67	0.430	3300	1100	57,800	- -
**1.50	0.5W	68	0.453	3300	1100	73,200	- -
1.50	0.6W	69	0.448	3300	1100	68,600	0.980
1.50	0.6W	70	0.440	3300	1100	67,000	0.925

* Thickness for all specimens was 0.085 inches.
** Specimens failed through pin holes.

FATIGUE CRACKING DATA (cont.)

Specimen Width (in.)	Crack-to-width ratio	Specimen number*	$2a_s$ (in.)	Fatigue Loads Max. Load	Min. Load	Cycles	$2a_o$ (in.)
**2.00	0.1W	50	0.204	6000	1800	33,400	- -
2.00	0.1W	55	0.198	6000	1800	30,300	0.229
2.00	0.2W	56	0.384	5000	1600	65,600	0.550
2.00	0.2W	57	0.390	5000	1600	40,700	0.565
2.00	0.3W	46	0.412	4000	1300	126,800	0.629
2.00	0.3W	47	0.422	4000	1300	87,100	0.644
2.00	0.4W	48	0.404	4000	1300	138,100	0.826
2.00	0.4W	51	0.415	4000	1300	137,800	0.823
2.00	0.5W	49	0.420	4000	1300	168,400	1.032
2.00	0.5W	52	0.423	4000	1300	127,100	1.060
2.00	0.6W	53	0.420	4000	1300	144,200	1.219
2.00	0.6W	54	0.426	4000	1300	139,000	1.216
2.50	0.1W	34	0.242	7400	2200	40,000	0.245
2.50	0.1W	35	0.221	7400	2200	35,800	0.225
2.50	0.2W	36	0.493	6600	2000	18,400	0.540
2.50	0.2W	37	0.478	6600	2000	20,000	0.555
2.50	0.3W	40	0.649	6200	1900	42,000	0.955
2.50	0.3W	41	0.645	6200	1900	31,400	0.845
2.50	0.4W	39	0.646	6200	1900	48,400	1.020
2.50	0.4W	45	0.988	4900	1500	25,500	1.115
2.50	0.5W	38	0.622	6200	1900	67,400	1.265
2.50	0.5W	42	0.631	6200	1900	77,200	1.250
2.50	0.6W	43	0.640	6200	1900	74,000	1.450
2.50	0.6W	44	1.006	4900	1500	74,300	1.600

* Thickness for all specimens was 0.085 inches.
** Specimens failed through pin holes.

FATIGUE CRACKING DATA (cont.)

Specimen Width (in.)	Crack-to-width ratio	Specimen Number*	$2a_s$ (in.)	Fatigue Load Max. Load (lb)	Fatigue Load Min. Load (lb)	Cycles	$2a_o$ (in.)
**3.00	0.1W	24	0.273	9200	2750	38,000	- -
3.00	0.1W	25	0.273	9200	2750	30,000	0.314
3.00	0.2W	26	0.594	8100	2400	16,800	0.783
3.00	0.2W	27	0.543	8100	2400	33,000	0.703
3.00	0.3W	28	0.738	7400	2200	28,000	0.945
3.00	0.3W	29	0.726	7400	2200	32,600	0.935
3.00	0.4W	30	0.729	7400	2200	56,200	1.220
3.00	0.4W	31	0.744	7400	2200	50,400	1.225
3.00	0.5W	22	0.759	7400	2200	66,700	1.490
3.00	0.5W	23	1.170	6000	1700	34,800	1.515
3.00	0.6W	33	0.759	7400	2200	84,400	1.801
3.00	0.6W	32	1.200	6000	1700	45,200	1.812
3.50	0.1W	12	0.348	10,300	3100	15,000	0.425
3.50	0.1W	13	0.339	10,300	3100	20,000	0.384
3.50	0.2W	14	0.681	9300	2800	14,900	0.829
3.50	0.2W	15	0.693	9300	2800	10,000	0.760
3.50	0.3W	16	0.810	8900	2600	13,200	0.967
3.50	0.3W	17	0.846	8900	2600	11,500	0.945
3.50	0.4W	18	0.813	8900	2600	40,200	1.451
3.50	0.4W	19	0.813	8900	2600	37,100	1.425
3.50	0.5W	20	0.804	8900	2600	49,300	1.775
3.50	0.5W	21	0.837	8900	2600	45,100	1.764
3.50	0.6W	11	0.837	8900	1900	23,100	2.071
3.50	0.6W	58	1.620	6300	1900	22,800	2.090

* Thickness for all specimens was 0.085 inches.
** Specimens failed through pin holes.

FATIGUE CRACKING DATA (cont.)

Specimen Width (in.)	Crack-to-width ratio	Specimen Number*	$2a_s$ (in.)	Fatigue Loads Max. Load (lb)	Min. Load (lb)	Cycles	2ao (in.)
4.00	0.2W	3	0.780	10,000	3200	8000	0.850
4.00	0.2W	4	0.801	10,000	3200	5000	0.826
4.00	0.3W	6	0.963	10,000	3000	16,700	1.253
4.00	0.3W	7	0.960	10,000	3000	18,600	1.240
4.00	0.4W	5	0.981	10,000	3000	31,700	1.640
4.00	0.4W	10	0.951	10,000	3000	33,000	1.645
4.00	0.5W	8	0.963	10,000	3000	41,200	2.019
4.00	0.5W	9	0.957	10,000	3000	42,400	2.000
4.00	0.6W	1	1.809	7,200	2200	26,500	2.434

* Thickness for all specimens was 0.085 inches.
** Specimens failed through pin hole

TABLE 2

FRACTURE TOUGHNESS DATA
OBTAINED BY THE STAINING METHOD

Specimen Width (in.)	Crack-to-Width Ratio	Specimen Number	Test Temperature (°F)	2a (in.)	$\frac{2a}{2a_o}$	Fracture Load (lbs)	q_{cl}	K_{cl} (psi $\sqrt{in.}$)
1.00	0.2W	80	78	0.550	3.14	7925	1.434	112,000
1.00	0.2W	82	78	0.525	2.52	8025	1.337	109,000
*1.00	0.3W	71	78	- -	2.50	7000	- -	- --
1.00	0.3W	72	78	0.675	2.04	6075	2.300	108,000
1.00	0.4W	73	78	0.742	1.67	5050	3.145	105,000
1.00	0.4W	76	78	0.697	1.55	4650	2.253	82,000
1.00	0.5W	77	78	0.750	1.30	3800	2.790	75,000
1.00	0.5W	78	78	0.716		4400	2.447	81,000
1.50	0.2W	61	73	0.765	2.05	8750	1.134	89,500
1.50	0.2W	62	73	0.700	2.14	9400	0.992	90,000
1.50	0.3W	63	73	0.900	1.87	8000	1.574	96,400
*1.50	0.3W	64	73	- -	- -	8575	- -	- - -
1.50	0.4W	65	73	0.980	1.41	6750	1.875	88,700
1.50	0.4W	66	73	0.925	1.44	6950	1.594	84,300
1.50	0.6W	69	73	1.183	1.21	3900	3.198	67,000
1.50	0.6W	70	73	1.186	1.28	4000	3.220	69,000
2.00	0.1W	55	77	0.625	2.73	14,950	0.586	95,200
2.00	0.2W	56	77	1.162	2.12	10,550	1.432	105,000
2.00	0.2W	57	77	1.359	2.40	11,000	2.200	136,000
*2.00	0.3W	46	77	- -	- -	10,800	- -	- - -
2.00	0.3W	47	77	1.185	1.84	10,200	1.432	103,000
2.00	0.4W	48	77	1.075	1.30	8500	1.184	77,000
2.00	0.4W	51	77	1.347	1.63	9300	2.010	110,000
2.00	0.5W	49	77	1.325	1.28	7450	1.831	83,800
2.00	0.5W	52	77	1.488	1.40	7450	2.683	102,000
2.00	0.6W	53	77	1.463	1.20	6550	2.433	85,000
2.00	0.6W	54	77	1.450	1.19	5600	2.303	70,700

* Ink Spatter

FRACTURE TOUGHNESS DATA
OBTAINED BY THE STAINING METHOD (cont.)

Specimen Width (in.)	Crack-to-Width Ratio	Specimen Number	Test Temperature (°F)	2a (in.)	$\frac{2a}{2a_o}$	Fracture Load (lbs)	q_{cl}	K_{cl} (psi $\sqrt{in.}$)
2.50	0.1W	34	76	1.175	4.80	17,000	1.023	128,000
2.50	0.1W	35	76	1.035	4.60	18,100	0.858	125,000
2.50	0.2W	36	76	1.374	2.55	13,400	1.284	113,000
2.50	0.2W	37	76	1.160	2.09	14,300	0.969	105,000
2.50	0.3W	40	76	1.824	1.91	11,050	2.651	134,000
2.50	0.3W	41	76	1.750	2.07	12,450	2.363	142,000
2.50	0.4W	39	76	1.569	1.54	10,100	1.616	95,500
2.50	0.4W	45	76	1.625	1.46	9,150	1.742	89,900
2.50	0.5W	38	76	1.812	1.43	8,600	2.387	100,000
2.50	0.5W	42	76	2.000	1.60	9,150	3.844	133,000
2.50	0.6W	43	76	1.761	1.21	7,500	2.110	81,100
2.50	0.6W	44	76	1.950	1.22	6,250	3.010	80,600
3.00	0.1W	25	75	0.738	2.35	21,050	0.433	94,100
3.00	0.2W	26	75	1.520	1.94	15,200	1.095	108,000
3.00	0.2W	27	75	1.418	2.01	16,750	0.982	113,000
3.00	0.3W	28	78	1.975	2.09	14,200	1.900	134,000
3.00	0.3W	29	78	2.144	2.30	14,750	2.557	160,000
3.00	0.4W	30	78	1.874	1.54	10,800	1,579	92,200
3.00	0.4W	31	81	1.988	1.62	12,200	1.871	113,000
3.00	0.5W	22	81	2.069	1.39	8,550	1.975	81,600
3.00	0.5W	23	82	2.302	1.52	9,450	2.923	110,000
3.00	0.6W	33	82	2.513	1.40	7,950	4.475	114,000
3.00	0.6W	32	82	2.266	1.25	8,300	2.675	92,200

* Ink spatter

FRACTURE TOUGHNESS DATA
OBTAINED BY THE STAINING METHOD (cont.)

Specimen Width (in.)	Crack-to-Width Ratio	Specimen Number	Test Temperature (°F)	2a (in.)	$\frac{2a}{2a_o}$	Fracture Load (lbs)	q_{cl}	K_{cl} (psi $\sqrt{in.}$)
3.50	0.1W	12	83	0.762	1.79	22,950	0.372	87,900
3.50	0.1W	13	84	0.824	2.14	25,050	0.413	101,000
3.50	0.2W	14	84	1.525	1.84	18,900	0.871	111,000
3.50	0.2W	15	84	1.559	2.05	19,450	0.900	116,000
3.50	0.3W	16	85	1.846	1.91	17,400	1.171	118,000
3.50	0.3W	17	85	1.571	1.66	17,550	0.912	105,000
*3.50	0.4W	18	84	- -	- -	- - -	- - -	- - -
3.50	0.4W	19	84	2.767	1.94	13,050	3.678	157,000
3.50	0.5W	20	85	2.850	1.60	12,150	4,274	158,000
3.50	0.5W	21	85	2.512	1.42	10,150	2.252	95,800
3.50	0.6W	11	85	2.382	1.15	9,000	1.890	77,800
3.50	0.6W	58	85	2.854	1.36	8,050	3.668	97,000
4.00	0.2W	3	82	1.740	2.05	20,100	0.877	111,000
4.00	0.2W	4	83	2.125	2.57	20,600	1.191	132,000
4.00	0.3W	6	84	2.650	2.11	18,850	1.929	154,000
4.00	0.3W	7	84	2.912	2.35	17,750	2.626	169,000
4.00	0.4W	5	84	2.418	1.47	14,950	1.473	107,000
4.00	0.4W	10	84	2.875	1.75	12,000	2.261	106,000
4.00	0.5W	8	84	3.100	1.53	12,500	3.050	128,000
4.00	0.5W	9	85	2.976	1.49	12,550	2.576	119,000
4.00	0.6W	1	86	3.354	1.38	11,000	4.631	139,000

*Ink Spatter

TABLE 3

FRACTURE TOUGHNESS DATA
OBTAINED BY THE FRACTURE APPEARANCE (SHEAR) METHOD

Specimen Width (in.)	Specimen Number	$2a_o$ (in.)	$2a_o/W$	Fracture Load (lb)	$\sigma_{max.}$ (psi)	P* (%)	** q_{c3}	K_{c3} (psi $\sqrt{in.}$)
1.00	80	0.175	0.175	7,925	93,235	36.0	0.538	68,300
1.00	82	0.208	0.208	8,025	94,410	40.2	0.639	75,600
1.00	71	0.290	0.290	7,000	82,353	56.5	0.984	81,700
1.00	72	0.330	0.330	6,075	71,471	29.1	0.884	67,200
1.00	73	0.445	0.445	5,550	59,412	29.4	1.278	67,200
1.00	76	0.450	0.450	4,650	54,706	29.9	1.286	62,100
1.00	77	0.570	0.570	3,800	44,706	15.1	2.015	63,500
1.50	61	0.374	0.250	8,750	68,627	33.6	0.714	71,000
1.50	62	0.328	0.219	9,400	73,725	40.6	0.665	73,700
1.50	63	0.481	0.321	8,000	62,745	41.8	0.963	75,400
1.50	64	0.471	0.314	8,575	67,255	30.2	0.873	77,000
1.50	65	0.694	0.462	6,750	52,941	27.8	1.362	75,600
1.50	66	0.641	0.428	6,950	54,510	31.3	1.257	74,800
1.50	69	0.980	0.653	3,900	30,588	33.1	2.445	58,700
1.50	70	0.925	0.617	4,000	31,373	18.6	2.023	54,600
2.00	55	0.229	0.115	14,950	87,941	78.8	0.512	88,900
2.00	56	0.550	0.275	10,500	62,059	66.3	0.940	85,100
2.00	57	0.565	0.283	11,000	64,706	94.2	0.865	85,100
2.00	46	0.629	0.314	10,800	63,529	46.5	1.068	92,800
2.00	47	0.644	0.322	10,200	60,000	37.2	0.947	82,600
2.00	48	0.826	0.413	8,500	50,000	29.1	1.205	77,500
2.00	51	0.823	0.412	9,300	54,706	27.9	1.203	84,900

*P - Shear Lip Measurement (Per cent, referred to specimen width)
**$q_{c3} = K_{c3}^2/\sigma_{max}^2 W$

Note: Specimen Thickness: 0.085 in.; Loading Rate: 3500 lb/in.; Yield Strength: 240,000 psi

FRACTURE TOUGHNESS DATA
OBTAINED BY THE FRACTURE APPEARANCE (SHEAR) METHOD (Cont.)

Specimen Width (in.)	Specimen Number	$2a_o$ (in.)	$2a_o/W$	Fracture Load (lb)	$\sigma_{max.}$ (psi)	P* (%)	** q_{c3}	K_{c3} (psi $\sqrt{in.}$)
2.00	49	1.032	0.516	7,450	43,824	30.2	1.624	78,900
2.00	52	1.060	0.530	7,450	43,824	52.3	1.879	84,800
2.00	53	1.219	0.610	6,550	38,529	38.3	2.240	81,300
2.00	54	1.216	0.608	5,600	32,941	41.9	2.221	69,400
2.50	34	0.245	0.098	17,000	80,000	62.4	0.379	77,800
2.50	35	0.225	0.090	18,100	85,176	61.6	0.358	80,400
2.50	36	0.540	0.216	13,400	63,059	61.6	0.718	84,100
2.50	37	0.555	0.222	14,300	67,294	44.7	0.688	88,300
2.50	40	0.455	0.382	11,050	52,000	48.8	1.183	74,400
2.50	41	0.845	0.338	12,450	58,588	84.9	1.310	106,000
2.50	39	1.020	0.408	10,100	46,529	33.3	1.270	84,700
2.50	45	1.115	0.446	9,150	43,059	36.0	1.361	79,500
2.50	38	1.265	0.506	8,600	40,941	33.7	1.605	81,900
2.50	42	1.250	0.500	9,150	43,059	63.5	1.740	89,700
2.50	43	1.450	0.580	7,500	35,294	45.3	2.084	80,900
2.50	44	1.600	0.640	6,250	29,412	34.9	2.454	72,700
3.00	25	0.314	0.105	21,050	82,549	47.1	0.370	87,000
3.00	26	0.783	0.261	15,200	59,608	41.9	0.776	90,900
3.00	27	0.703	0.234	16,750	65,686	83.7	0.726	97,000
3.00	28	0.945	0.315	14,200	55,686	34.9	0.919	92,400
3.00	29	0.935	0.312	14,750	57,843	62.1	0.991	99,900
3.00	30	1.220	0.407	10,800	42,353	31.4	1.203	80,600
3.00	31	1.225	0.408	12,200	47,843	27.9	1.205	90,900
3.00	22	1.490	0.497	8,550	33,529	41.9	1.577	72,900
3.00	23	1.515	0.505	9,450	37,059	47.1	1.670	82,900
3.00	33	1.801	0.600	7,950	31,176	66.3	2.381	83,300
3.00	32	1.812	0.604	8,300	32,549	59.3	2.322	88,500

*P - Shear Lip Measurement (Per cent, referred to specimen width)

**$q_{c3} = K_{c3}^2/\sigma_{max}^2 W$

FRACTURE TOUGHNESS DATA
OBTAINED BY THE FRACTURE APPEARANCE (SHEAR) METHOD (Cont.)

Specimen Width (in.)	Specimen Number	$2a_o$ (in.)	$2a_o/W$	Fracture Load (lb)	$\sigma_{max.}$ (psi)	P* (%)	** q_{c3}	K_{c3} (psi $\sqrt{in.}$)
3.50	12	0.425	0.121	22,950	77,143	67.4	0.432	94,700
3.50	13	0.384	0.110	25,050	84,202	69.4	0.463	107,000
3.50	14	0.829	0.237	18,900	63,529	65.1	0.764	104,000
3.50	15	0.760	0.217	19,450	65,378	100.0	0.781	109,000
3.50	16	0.967	0.276	17,400	58,487	100.0	0.954	107,000
3.50	17	0.945	0.270	17,550	58,992	75.2	0.885	104,000
3.50	18	1.451	0.415	13,350	44,874	72.9	1.348	97,400
3.50	19	1.425	0.407	13.050	43,866	82.5	1.352	95,400
3.50	20	1.775	0.508	12,150	40,840	61.6	1.735	100,000
3.50	21	1.764	0.505	10,150	34,118	76.7	1.762	84,700
3.50	11	2.071	0.591	9,000	30,252	63.5	2.074	81,500
3.50	58	2.090	0.598	8,050	27,059	63.5	2.625	82,100
4.00	3	0.850	0.212	20,100	59,118	53.4	0.671	96,900
4.00	4	0.826	0.206	20,600	60,588	63.8	0.670	99,000
4.00	6	1.253	0.313	18,850	55,441	100.0	1.060	112,000
4.00	7	1.240	0.310	17,750	52,206	88.2	1.024	106,000
4.00	5	1.640	0.410	14,950	43,971	61.5	1.294	100,000
4.00	10	1.645	0.411	12,000	35,294	62.6	1.290	80,000
4.00	8	2.019	0.505	12,500	36,765	62.6	1.703	96,000
4.00	9	2.000	0.500	12,550	36,912	100.0	1.875	101,000
4.00	1	3.434	0.608	11,000	32,353	74.4	2.400	97,100

*P - Shear Lip Measurement (Per cent referred to specimen width)
**$q_{c3} = K_{c3}^2/\sigma_{max}^2 W$

Note: Specimen Thickness: 0.085 in.; Loading Rate: 3500 lb/min; Yield Strength: 240,000 psi

Table #1
Fracture Toughness Data for X-200
Group #1

Specimen Number	Hardness (R/C)	Test Temperature (^{o}F)	$\frac{2a_o}{W}$	2a (in)	P_M (k)	P (%)
101	49	+150	0.358	0.984	11.95	38.4
102	50	+150	0.358	0.986	11.50	34.5
103	51	+100	0.351	0.964	8.90	27.6
104	51	+100	0.341	0.924	9.30	23.8
105	51	+ 75	0.327	0.882	8.45	17.9
106	50	+ 75	0.327	0.876	8.40	16.5
108	49	+ 25	0.361	0.940	7.20	10.7
109	50	+ 25	0.333	0.880	7.10	13.1
107	50	0	0.356	0.924	6.90	10.7
110	50	0	0.340	0.872	7.25	10.6
111	50	- 25	0.354	0.914	5.25	8.2
112	50	- 25	0.360	0.928	6.05	8.2
113	50	- 50	0.360	0.928	5.10	7.1

Table #1
Fracture Toughness Data for X-200
Group #1 (Cont.)

Specimen Number	Hardness (R/C)	Test Temperature (^{o}F)	$\frac{2a_o}{W}$	2a (in)	P_M (k)	P (%)
114	50	- 50	0.346	0.894	5.70	5.9
115	50	- 75	0.354	0.914	6.25	8.2
116	50	- 75	0.358	0.918	5.30	6.0
117	50	-100	0.356	0.990	4.85	3.6
118	51	-100	0.364	0.918	4.60	2.4
119	52	-150	0.347	0.882	3.85	0
120	51	-150	0.356	0.898	4.20	0

Table #1
Fracture Toughness Data for X-200
Group #1

Specimen Number	σ_M (ksi)	σ_{YS} (ksi)	q_{c3}	σ_N (ksi)	$\frac{\sigma_N}{\sigma_{YS}}$	K_{c3} (ksi$\sqrt{in}$)
101	70.3	215.0	1.100	138.3	0.634	104.3
102	67.6	232.5	1.073	133.4	0.574	99.0
103	52.4	220.0	1.000	101.1	0.460	74.1
104	54.7	212.5	0.953	101.7	0.479	73.5
105	49.7	237.5	0.874	88.9	0.374	65.7
106	49.4	232.5	0.867	87.9	0.378	65.1
108	42.4	207.5	0.957	79.9	0.385	57.1
109	41.8	190.0	0.877	74.6	0.393	55.3
107	40.6	208.0	0.933	75.4	0.363	55.5
110	42.6	218.0	0.855	75.6	0.347	54.1
111	30.9	213.0	0.908	56.9	0.267	41.6
112	35.6	193.0	0.934	66.4	0.344	48.6
113	30.0	225.0	0.922	56.0	0.249	40.7

Table #1
Fracture Toughness Data for X-200
Group #1

Specimen Number	σ_M (ksi)	σ_{YS} (ksi)	q_{c3}	σ_N (ksi)	$\frac{\sigma_N}{\sigma_{YS}}$	K_{c3} (ksi-$\sqrt{in}$)
114	33.5	217.5	0.876	60.6	0.279	44.3
115	36.8	220.0	0.911	67.7	0.308	49.7
116	31.2	220.0	0.912	57.6	0.262	42.1
117	28.5	215.0	1.000	56.5	0.263	40.3
118	27.1	215.0	0.911	50.0	0.233	36.5
119	22.7	220.0	0.850	40.5	0.184	29.6
120	24.7	212.5	0.877	44.8	0.211	32.7

Table #1
Fracture Toughness Data for X-200
Group #2

Specimen Number	Hardness (R/C)	Tempering Temperature (°F)	Test Temperature (°F)	$\frac{2a_o}{W}$	2a (in.)	P_M (k)	P (%)
141	57	400	83	0.348	0.948	7.800	25.5
142	56	400	83	0.353	0.962	7.350	23.5
143	56	500	80	0.364	0.998	8.450	29.4
144	56	500	80	0.380	1.028	8.650	30.5
145	57	600	81	0.342	0.962	9.650	33.7
146	56	600	81	0.345	0.954	10.255	29.8
147	57	700	81	0.345	0.938	7.900	22.9
148	56	700	82	0.354	0.958	8.400	22.0
149	54	800	82	0.367	0.972	7.750	17.6
150	54	800	82	0.363	0.966	7.450	17.6
151	49	900	82	0.354	0.960	16.650	63.4
152	49	900	82	0.353	0.954	17.175	65.0
153	48	1000	82	0.343	0.924	18.200	72.5

Table #1
Fracture Toughness Data for X-200
Group #2

Specimen Number	Hardness (R/C)	Tempering Temperature (°F)	Test Temperature (°F)	$\frac{2a_o}{W}$	2a (in.)	P_M (k)	P (%)
154	47	1000	82	0.354	0.914	18.000	63.8
155	33	1100	82	0.342	0.922	13.700	100.0
156	32	1100	82	0.345	0.936	13.600	100.0
157	26	1200	82	0.359	0.896	10.700	100.0
158	24	1200	82	0.354	0.904	10.900	100.0
159	18	1300	82	0.342	0.800	10.350	100.0
160	26	1300	82	0.360	0.832	10.100	100.0

Table #1
Fracture Toughness Data for X-200
Group #2

Specimen Number	σ_M (ksi)	σ_{YS} (ksi)	q_{c3}	σ_N (psi)	$\frac{\sigma_N}{\sigma_{YS}}$	K_{c3} (psi$\sqrt{\text{in.}}$)
141	45.9	243.0	0.961	87.2	0.359	63.6
142	43.2	237.5	0.978	83.3	0.351	60.5
143	49.7	242.5	1.042	99.2	0.409	71.7
144	50.9	243.0	1.100	104.7	0.431	75.5
145	56.8	233.0	1.000	109.4	0.470	80.3
146	60.1	222.5	1.000	115.0	0.517	85.0
147	46.5	230.0	0.952	87.5	0.380	64.1
148	49.4	230.0	0.983	94.8	0.412	69.3
149	45.6	200.0	1.008	88.7	0.444	64.8
150	43.8	210.0	0.993	84.8	0.404	61.8
151	97.9	195.0	1.312	188.3	0.966	158.3
152	101.0	197.0	1.321	193.2	0.981	162.5
153	107.1	189.0	1.400	198.9	1.052	179.2

Table #1
Fracture Toughness Data for X-200
Group #2

Specimen Number	σ_M (ksi)	σ_{YS} (ksi)	q_{c_3}	σ_N (psi)	$\frac{\sigma_N}{\sigma_{YS}}$	K_{c_3} (psi$\sqrt{\text{in.}}$)
154	105.9	190.0	1.379	195.0	1.026	165.0
155	80.6	134.0	1.627	149.5	1.116	181.7
156	80.0	135.0	1.629	150.4	1.114	144.4
157	62.9	102.0	1.570	114.0	1.118	111.4
158	64.1	102.5	1.762	117.0	1.141	120.3
159	60.9	88.0	1.700	101.5	1.153	112.3
160	59.4	88.0	1.964	101.7	1.156	117.3

Table #1
Fracture Toughness Data for X-200
Group #3

Specimen Number	Hardness (R/C)	Test Temperature (^{o}F)	$\frac{2a_o}{W}$	2a (in)	P_M (k)	P (%)
121	51	+150	0.351	0.944	12.20	28.6
122	50	+150	0.348	0.940	11.40	27.7
123	51	+100	0.340	0.932	9.40	16.9
124	51	+100	0.352	0.938	8.40	18.1
139	51	+ 50	0.359	0.936	7.75	11.8
140	51.5	+ 50	0.359	0.932	8.15	10.7
127	51	+ 25	0.333	0.872	7.85	8.2
128	50	+ 25	0.369	0.958	6.80	10.7
129	52	0	0.354	0.914	6.60	8.4
130	51	0	0.354	0.918	6.80	9.5
131	51	- 25	0.361	0.916	6.15	8.2
132	51	- 25	0.352	0.904	6.30	7.1
133	52	- 50	0.345	0.898	6.30	9.6

Table #1
Fracture Toughness Data for X-200
Group #3 (Cont)

Specimen Number	Hardness (R/C)	Test Temperature (^{o}F)	$\frac{2a_o}{W}$	2a (in)	P_M (k)	P (%)
134	52	- 50	0.330	0.868	5.85	7.1
125	51	- 75	0.362	0.922	5.75	4.7
135	52	- 75	0.368	0.944	5.20	6.1
137	50	-100	0.366	0.944	4.95	4.7
138	52.5	-100	0.358	0.910	5.00	2.4
126	51	-150	0.369	0.936	4.95	0
136	52	-150	0.360	0.906	4.30	2.4

Table #1
Fracture Toughness Data for X-200
Group #3

Specimen Number	σ_M (ksi)	σ_{YS} (ksi)	q_{c3}	σ_N (ksi)	$\frac{\sigma_N}{\sigma_{YS}}$	K_{c3} (ksi$\sqrt{in}$)
121	71.8	205.0	1.041	135.9	0.663	103.5
122	67.1	202.0	1.018	126.5	0.625	95.9
123	55.3	200.0	0.975	103.5	0.518	77.2
124	49.4	202.5	0.966	93.1	0.460	68.6
139	45.6	212.5	0.955	85.7	0.403	63.0
140	47.9	215.0	0.951	89.8	0.418	66.1
127	46.2	197.5	0.868	81.9	0.415	60.9
128	40.0	195.0	0.800	76.8	0.394	50.6
129	38.8	215.0	0.916	71.5	0.333	52.5
130	40.0	217.5	0.921	73.9	0.340	54.2
131	36.2	217.5	0.914	66.7	0.307	49.0
132	37.1	215.0	0.900	67.6	0.314	49.8
133	37.1	220.0	0.891	67.3	0.306	49.5

Table #1
Fracture Toughness Data for X-200
Group #3 (Cont)

Specimen Number	σ_M (ksi)	σ_{YS} (ksi)	q_{c3}	σ_N (ksi)	$\frac{\sigma_N}{\sigma_{YS}}$	K_{c3} (ksi-$\sqrt{in}$)
134	34.4	220.0	0.835	60.8	0.276	45.8
125	33.8	202.5	0.921	62.8	0.310	45.8
135	30.6	217.5	0.944	57.9	0.266	42.1
137	29.1	220.0	0.942	55.1	0.250	39.9
138	29.4	222.5	0.900	54.0	0.243	39.5
126	29.1	200.0	0.936	54.7	0.274	39.8
136	25.3	200.0	0.892	46.2	0.231	33.8

Table #2
Fracture Toughness Data for H-11
Group #1

Specimen Number	Hardness (R/C)	Test Temperature (^{o}F)	$\frac{2a_o}{W}$	2a (in)	P_M (k)	P (%)
17	46	+300	0.361	1.006	18.00	100
18	47	+300	0.343	0.924	19.70	100
1	44	+150	0.367	0.974	19.10	100
2	45	+150	0.360	0.952	19.75	100
3	45	+100	0.358	0.910	19.10	50.6
4	46	+100	0.358	0.980	18.50	87.8
5	45	+ 50	0.354	0.924	13.65	25.6
6	40	+ 50	0.342	0.940	13.00	37.8
19	44	+ 50	0.356	0.924	11.30	28.9
20	44	0	0.351	0.920	13.90	24.4
7	40	0	0.358	0.974	11.05	32.9
8	45	0	0.342	0.910	11.50	32.9
9	44	- 50	0.358	0.958	9.10	20.7

Table #2
Fracture Toughness Data for H-11
Group #1 (Cont)

Specimen Number	Hardness (R/C)	Test Temperature (^{o}F)	$\frac{2a_o}{W}$	2a (in)	P_M (k)	P (%)
10	47	- 50	0.346	0.928	9.20	20.7
11	51	-100	0.351	0.910	7.95	15.9
12	46	-100	0.360	0.954	7.20	15.9
13	46	-150	0.395	1.014	6.10	9.8
14	46	-150	0.342	0.976	6.80	11.0
15	43	-200	0.356	0.886	3.70	0
16	43	-200	0.366	0.920	3.80	0

Table #2
Fracture Toughness Data for H-11
Group #1

Specimen Number	σ_M (ksi)	σ_{YS} (ksi)	q_{c3}	σ_N (ksi)	$\frac{\sigma_N}{\sigma_{YS}}$	K_{c3} (ksi-$\sqrt{in}$)
17	105.9	200.0	1.619	213.0	1.065	190.6
18	115.9	193.0	1.628	215.3	1.116	210.0
1	112.4	196.5	1.741	219.0	1.114	210.2
2	116.2	198.0	1.720	221.7	1.120	215.0
3	112.4	201.5	1.306	206.0	1.022	182.1
4	108.8	202.5	1.523	213.4	1.054	190.4
5	80.3	201.0	1.053	149.2	0.742	116.4
6	76.5	205.0	1.058	144.3	0.704	111.7
19	66.5	203.0	1.050	123.5	0.608	96.4
20	81.8	203.5	1.042	151.4	0.744	117.8
7	65.0	205.0	1.069	126.7	0.618	94.9
8	67.6	211.0	1.016	124.1	0.588	96.0
9	53.5	212.0	1.000	105.1	0.496	75.4

Table #2
Fracture Toughness Data for H-11
Group #1 (Cont)

Specimen Number	σ_M (ksi)	σ_{YS} (ksi)	q_{c3}	σ_N (ksi)	$\frac{\sigma_N}{\sigma_{YS}}$	K_{c3} (ksi$\sqrt{\text{in}}$)
10	54.1	212.0	0.957	101.0	0.476	75.2
11	46.8	215.0	0.935	85.8	0.399	64.1
12	42.4	218.0	0.972	81.0	0.372	58.9
13	35.9	217.0	1.054	72.8	0.335	52.1
14	40.0	213.0	0.891	78.2	0.367	53.2
15	21.8	211.0	0.878	39.1	0.185	28.8
16	22.4	213.0	0.909	41.4	0.194	30.2

Table #2
Fracture Toughness Data for H-11
Group #2

Specimen Number	Hardness (R/C)	Tempering Temperature (°F)	Test Temperature (°F)	$\frac{2a_o}{W}$	2a (in.)	P_M (k)	P (%)
35	51	400	78	0.343	0.924	7.400	20.0
36	54	400	80	0.345	0.928	7.550	19.0
37	48	500	79	0.354	0.964	8.150	23
38	51	500	79	0.350	0.962	8.000	23
43	54	600	80	0.355	0.962	8.250	22
44	42	600	79	0.367	0.984	8.150	21
33	54	700	79	0.348	0.908	5.750	8.5
34	52	700	79	0.351	0.906	5.800	8.5
39	55	800	78	0.352	0.910	4.400	4.9
40	56	800	78	0.358	0.916	4.100	4.9
41	49	900	78	0.361	0.958	7.750	17
42	43	900	79	0.360	0.968	7.150	18
30	41	1000	78	0.372	0.894	18.750	66

Table #2
Fracture Toughness Data for H-11
Group #2

Specimen Number	Hardness (R/C)	Tempering Temperature (°F)	Test Temperature (°F)	$\frac{2a_o}{W}$	2a (in.)	P_M (k)	P (%)
49	43	1000	78	0.350	0.894	16.200	38
45	35	1100	78	0.355	0.922	13.500	100
46	39	1100	78	0.349	0.928	13.300	100
47	36	1200	78	0.351	0.894	10.000	100
48	40	1200	78	0.345	0.936	9.000	100

Table #2
Fracture Toughness Data for H-11
Group #2

Specimen Number	σ_M (ksi)	σ_{YS} (ksi)	q_{c3}	σ_N (ksi)	$\frac{\sigma_N}{\sigma_{YS}}$	K_{c3} (ksi$\sqrt{\text{in.}}$)
35	43.5	230.0	0.932	80.9	0.352	59.3
36	44.4	232.5	0.934	82.9	0.357	60.7
37	47.9	232.5	0.988	92.5	0.398	67.4
38	47.1	247.5	0.971	90.7	0.366	65.6
43	48.5	232.5	0.985	93.5	0.402	68.1
44	47.9	235.0	1.019	94.3	0.401	68.4
33	33.8	235.0	0.893	62.0	0.264	45.1
34	34.1	225.0	0.900	62.4	0.277	45.8
39	25.9	222.0	0.888	47.5	0.214	34.6
40	24.1	211.0	0.905	44.5	0.211	32.4
41	45.6	217.5	0.982	87.5	0.402	63.8
42	42.1	217.5	0.990	81.5	0.375	59.2
30	110.3	182.5	1.448	199.5	1.093	187.8

Table #2
Fracture Toughness Data for H-11
Group #2

Specimen Number	σ_M (ksi)	σ_{YS} (ksi)	q_{c_3}	σ_N (ksi)	$\frac{\sigma_N}{\sigma_{YS}}$	K_{c3} (ksi$\sqrt{\text{in.}}$)
49	95.3	175.0	1.215	172.3	0.984	176.3
45	79.4	130.0	1.737	176.9	1.360	147.7
46	78.2	130.0	1.685	146.0	1.123	143.9
47	58.8	92.5	1.762	106.4	1.150	110.5
48	52.9	90.0	1.613	99.6	1.107	95.2

Table #2
Fracture Toughness Data for H-11
Group #3

Specimen Number	Hardness (R/C)	Test Temperature (^{o}F)	$\frac{2a_o}{W}$	2a (in)	P_M (k)	P (%)
26	41	+200	0.382	0.978	16.10	54.9
27	42	+200	0.369	0.920	16.80	54.9
29	43	+100	0.351	0.890	16.80	47.6
31	41	+ 50	0.361	0.922	15.40	35.4
32	40	+ 50	0.372	0.938	15.35	32.9
50	39	0	0.353	0.894	15.30	25.9
53	43	0	0.364	0.908	14.35	32.9
52	43	- 50	0.361	0.890	7.90	0
54	41	-100	0.360	0.900	6.55	0
55	39	-100	0.360	0.900	5.80	0
56	39	-150	0.353	0.844	7.35	0
57	47	-150	0.350	0.842	7.60	0

Table #2
Fracture Toughness Data for H-11
Group #3 (cont.)

Specimen Number	Hardness (R/C)	Test Temperature (^{o}F)	$\frac{2a_o}{W}$	2a (in)	P_M (k)	P (%)
58	47	-200	0.366	0.920	5.25	0
59	46	-200	0.363	0.910	4.35	0
60	41	-300	0.364	0.914	3.15	0

Table #2
Fracture Toughness Data for H-11
Group #3

Specimen Number	σ_M (ksi)	σ_{YS} (ksi)	q_{c3}	σ_N (ksi)	$\frac{\sigma_N}{\sigma_{YS}}$	K_{c3} (ksi$\sqrt{in}$)
26	94.7	184.0	1.411	184.25	1.001	159.0
27	98.8	172.0	1.420	183.00	1.063	166.5
29	98.8	177.5	1.237	178.06	1.003	155.3
31	90.6	182.5	1.187	168.06	0.920	139.5
32	90.3	187.5	1.203	170.04	0.906	140.2
50	90.0	192.5	1.072	162.74	0.845	131.7
53	84.4	202.0	1.038	154.60	0.765	121.7
52	46.5	195.0	0.902	83.73	0.429	62.4
54	38.5	202.5	0.900	70.05	0.346	51.7
55	34.1	204.5	0.895	62.03	0.303	45.6
56	43.2	211.0	0.808	74.80	0.355	55.0
57	44.7	210.0	0.808	77.21	0.368	56.9

Table #2
Fracture Toughness Data for H-11
Group #3 (Cont)

Specimen Number	σ_M (ksi)	σ_{YS} (ksi)	q_{c3}	σ_N (ksi)	$\frac{\sigma_N}{\sigma_{YS}}$	K_{c3} (ksi$\sqrt{\text{in}}$)
58	30.9	220.0	0.914	57.18	0.260	41.8
59	25.6	227.5	0.900	46.95	0.206	34.3
60	18.5	248.5	0.900	34.12	0.137	24.8

ERRATA

Part One

1. Page 2, item (5); "fracture toughness method" should be "fracture appearance method".
2. Page 8; "stereoscope" should be "stereoscopic".
3. Page 18; "warrented" should be "warranted".
4. Page 18; "attendent" should be "attendant".
5. Figure 6b should be 6a.

Part Two

1. Page 2; "sheroidized" should be "spheroidized".
2. Page 5; "cryostatic" should be "cryostat".
3. Page 13; last paragraph; "hump to the vicinity" should be "hump in the vicinity".

APPENDIXES

1. Table 2; "Metond" should be "method".